Doctoral Dissertation

Emergence of Cooperation on Complex Networks

Hyunmo Yang

Department of Physics

Graduate School of UNIST

2019

Emergence of Cooperation on Complex Networks

Hyunmo Yang

Department of Physics

Graduate School of UNIST

Emergence of Cooperation on Complex Networks

A dissertation submitted to
the Graduate School of UNIST
in partial fulfillment of
the requirements for the degree of
Doctor of Philosophy

Hyunmo Yang

December 26th, 2018
Approved by

_____

Advisor
Cheol-Min Ghim

Emergence of Cooperation on Complex Networks

Hyunmo Yang

This certifies that the dissertation of Hyunmo Yang is approved.

December 26th, 2018

signature

_____

Advisor: Prof. Cheol-Min Ghim

signature

_____

Prof. Jaeup Kim

signature

_____

Prof. Pilwon Kim

signature

_____

Prof. Pan-Jun Kim

signature

_____

Prof. Junghyo Jo

이 논문을 저의 부모님과 할머니께 바칩니다.

Abstract

We studied the structural determinants of evolutionary dynamics on complex networks in the paradigm of social dilemma games and mathematical graph theory. Motivated by the renewed interest in the evolution of altruistic behavior in the population of rational individuals, who strive to maximize their own benefit, we qunatitatively explored the impact of the various structural characteristics on the fixation of a single cooperator in the sea of defectors. In non-complete graphs, where an individual's fitness is determined not only by the individual's strategy but also by its local neighbors' strategies, the fixation of the mutant species significantly deviates from the prediction of the traditional Moran process occurring in a well-mixed population. From the numerical experiments and analytical approximations on the ensembles of populations prescribed by a suite of structural characteristics, we map the region of facilitated altruism in the space of degree heterogeneity, clustering properties, and degree-degree correlations. Of particular interest are the attributes of the seed cooperator that leads to the fixation of cooperators with higher chance. We show that, though the degree of the seed cooperator can either positively or negatively impact the cooperation depending on the numeric details of the payoff matrix, the low average degree, degree homogeneity, and the negative degree-degree correlation is always favoured for the evolution of the social behavior. To explain these findings in a more intuitive manner, we introduced the concept of the structural reciprocity in the framework of evolutionary game theory and propose possible structural intervention strategies to promote the altruism with no centralized control. To avoid hasty generalization at all costs, however, it should be noted that the underlying population topology is not the only determinant of the fixation of cooperators. Yet another determinants are the details of the update rules and fitness-payoff relations. The interplay between these dynamical rules and the structural characteristics should be a fruitful avenue for future research.

Table of contents

List of figures

Chapter 1

Introduction

Structure and function and their interplay lies at the core of all the disciplines of science. Diversity of the scientific disciplines emerge when this fundamental scheme is combined with distinct spatial and temporal scales inherent to the system of our interest. As the patterns of condensation of atoms and molecules are related to the thermal and electromagnetic properties of condensed matter, and intrigue the chemists and material scientists, structural biologists are intrigued with the detailed combination of structural motifs producing wide range of catalytic power and specificity facilitating the biochemical reactions in a living cell.

Owing to the recent technological advance in high-throughput experiments and large-scale computation, unprecedented amount of data have been accumulated. Paradigm is rapidly changing from genes to genomes, parts to systems, and intra- to inter-disciplinary. But a bucketful of beads are not a treasure until threaded, goes an old Korean saying.

In addition to the sequence database, huge collections of protein crystal structure, protein-protein interaction, transcriptional regulation, and pathway data have been archived and keep gaining their content across the species. The wiring diagram is getting more popularity thanks to its abstraction power and, to be sure, system-wide assay and statistical analyses based on large-scale graphs have provided valuable insights into the “design” principles. However, when it comes to the efforts to manipulate cell’s metabolic capability for engineering uses, many caveats behind the abstract modeling start to override the desired outcome. Even the simplest circuit device, such as an oscillator took two years to be realized in its naive functional fidelity [1].

Networks are an abstract mathematical construct of all the interacting systems, regardless of the nature of their “nodes”. The local and overall structure can be evolving over time, reflecting the dynamics in both the nodes and links. The macroscopic behavior of large and complex biological systems as an outcome of accumulated or majority of microscopic actions from system components. Those microscopic

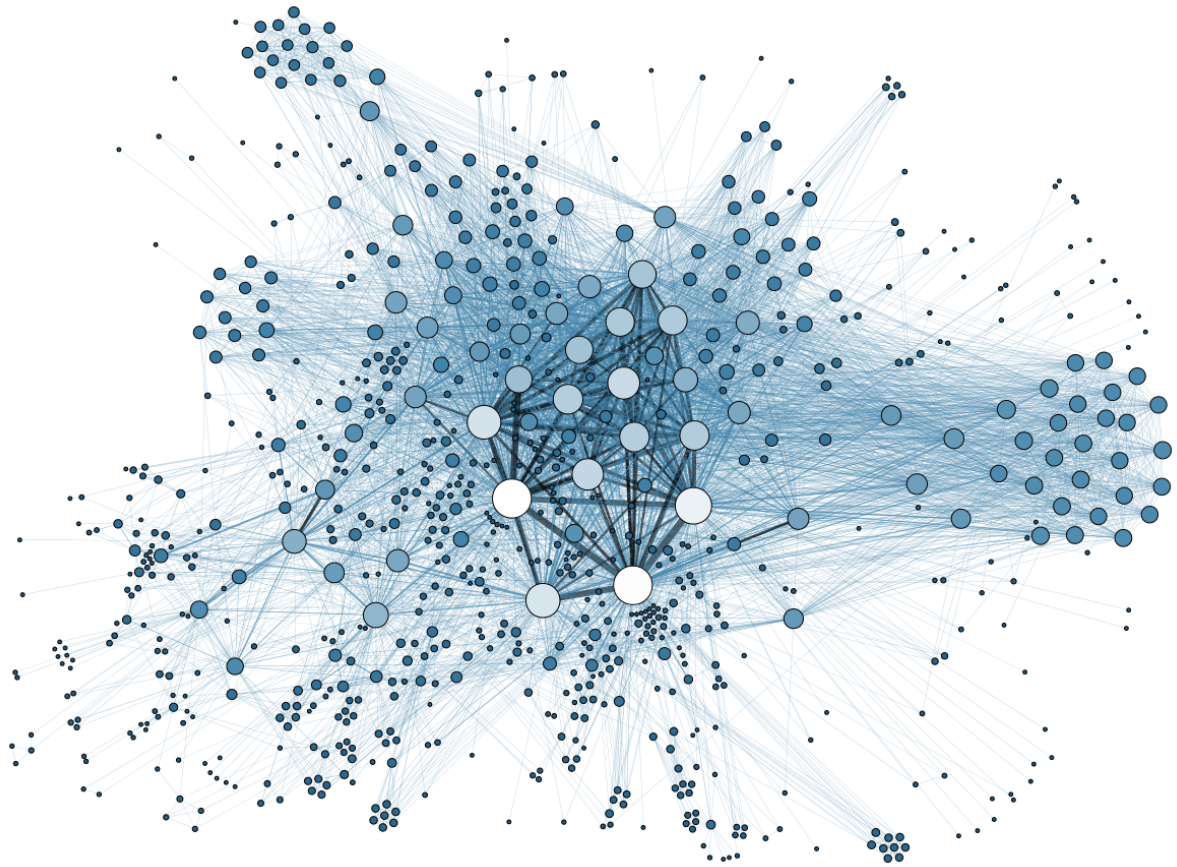

Fig. 1.1 Example of complex network. Any of complex systems can be described in from of networks. A node of network represent a consisting component and a link indicating interaction between a pair of parts. For example, a social network represent interaction patterns among consisting of individuals. The macroscopic behavior of the system depends on the interplay between microscopic dynamics through the links and the pattern of interactions. Figure adopted from [2].

actions propagate and stimulate through interacting path ways under the governing dynamics and thus the pattern of interactions across system components determines overall behavior. Hence finding the structural determinants of a functional network is crucial to the understanding of biological networks responsible for genetic regulation, cellular metabolism, and intra-cellular signal transduction. The evolutionary rationale behind these evolved structures allows us to reverse-engineer the complex biological systems for various engineering applications [3].

Likewise, the topological structure of a population, which is itself a manifestation of social and ecological interactions, may well have significant impact on the spreading of, say, epidemics, innovations, and social influence [4–6]. Accordingly, any public health strategies or regulatory measures aimed to control the spread of diseases should consider the population structure in which the interacting agents are embedded. This is particularly so because the social networks are known to be far from uniform or completely random in the connectivity patterns [7].

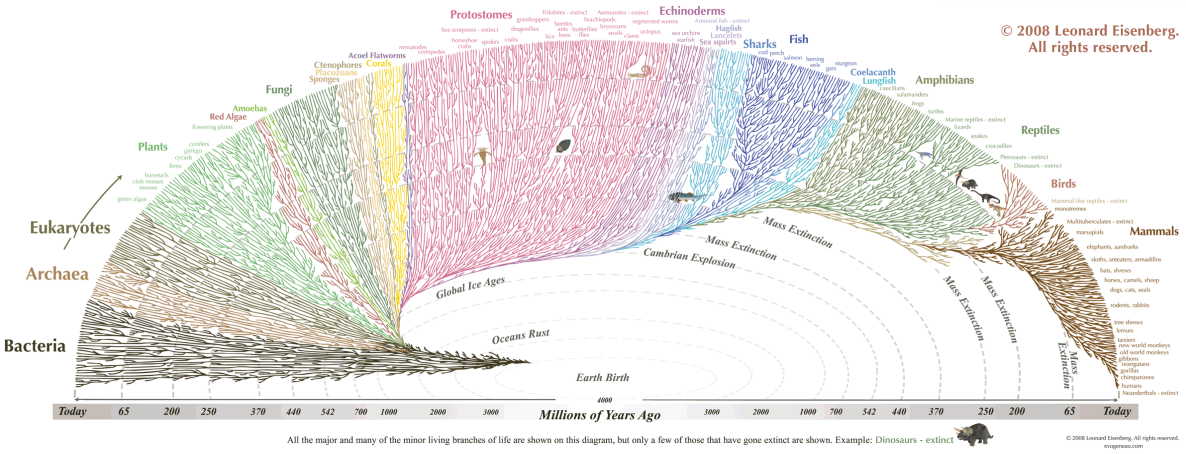

Fig. 1.2 Tree of life. Form of the life have been evolved through the evolutionary processes over the billions of years. Every branches in the tree of life representing the emergence of new kind. The emergence of new kind at each stage of the era, survived in fitter form of the life under the natural selection. However, many of evolved creatures cooperate each other, even build up the eusociality that requires the sacrifice of individuals for the common goods that leads reducing the fitness of individual. How the cooperation can survive under the natural selection is the largest question in evolutionary biology. Figure is used under the permission. The copyright © Leonard Eisenberg 2008, 2017 (https://www.evogeneao.com/)

Meanwhile, across all fascinating researches about biological systems the evolution is at the center of scientific mind. Every living organism evolve over the time. We don't know yet what is the origin of life on the mother Earth, but at least we dimly know how the form of life has been changed through the history of the earth. From the prokaryotes to the multicellular organism, evolutionary processes repeated again and again over the billions of years and derived changing the form of life and the diversity. Regardless the type of biological system, the actual form of reactions or interactions in ecosystem, the evolution conceptually summarized three main processes which are replication, selection, and mutation.

The main property of evolutionary process lies on the emergence and the extinction. Throughout an eternity of time millions of thousands form of life appeared and disappeared. Since the Earth is dynamic system at each stage of the era the environment of the Earth have been changed. Under the dynamic changes of environment living organisms were drifted by the natural selection. The natural selection simply favours the fitter and the fittest, which leads "the survival of fitter" [8]. However, the life is also dynamic system. Throughout uncountable number of mutations let the life evolve into another forms. That unwilling 'mistakes' is the source of the diversity in life.

At the same time, the life start being 'strategic' for survival under the selection. From a single cell to multi-cell, from an individual to a group, and from a group to a society, the life start cooperate to each other. However, the cooperation is risky behavior since it requires sacrifice oneself to provide goods for others. In terms of the fitness cooperation is an action reducing the fitness of oneself. The natural selection,

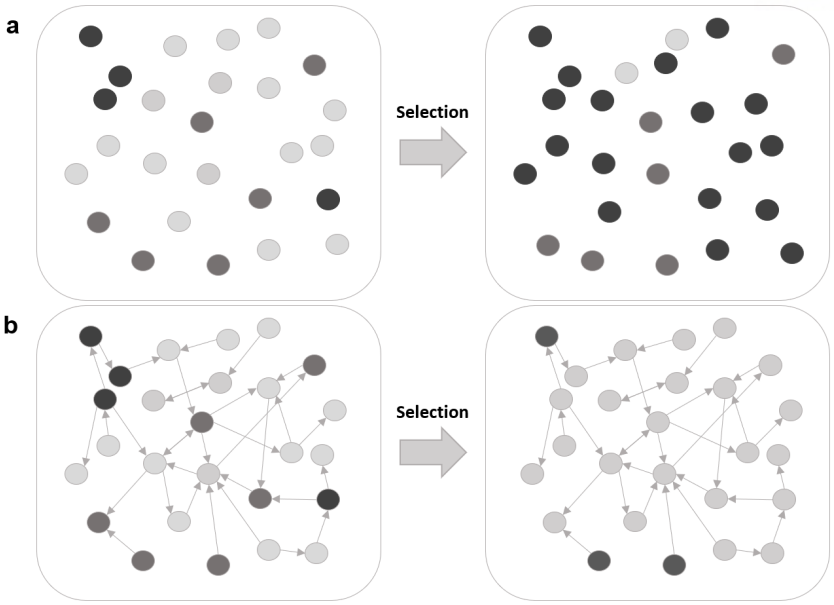

Fig. 1.3 Schematic representation of evolutionary process in (a) in well-mixed population and (b) in structured population. Contrast of an individual represent the fitness. The natural selection favours fitter type of individuals. However, interplay between the dynamics and structure may lead different destination of evolutionary processes. In this dissertation we mainly focus on how such interplay effect on the emergent phenomenon.

therefore, dose not favour the cooperation. One may wonder 'when' the cooperation of life started, 'how' cooperating individual can survive compensation, 'what' initiated the evolution of cooperation.

The evolution of cooperation out of natural selection is an emergent phenomenon that cannot be reduced to the understanding of pairwise two-body interactions. How could economically rational agents pursuing their own interest achieve the common good of cooperation with no centralized coordination? How do individual cells in multicellular organisms choose to cooperate at its own cost instead of proliferating autonomously? [9] The mathematical abstraction of these questions laid the foundation of evolutionary game theory [10–12], which now provides a paradigm for the dynamics of competing strategies not only in biology but also in social and behavioral sciences.

Both empirical evidence and theoretical analysis for the social dilemma games highlight that cooperation emerges when a certain type of "assortment" is at work that allows the benefits of altruistic acts to be preferentially channeled to other altruists and/or partly fed back to the original altruists [13, 14]. Leaving out the strategic complexity [15, 16], the direct and indirect reciprocity [17–19] formed by iterated social interactions is one of the dominant mechanisms for the evolution of altruism. Assortment by virtue of kinship [20–24] or group selection [25–38], though being at the center of the heated controversy between schools of thoughts [39, 40], have also been widely accepted mechanisms. Other factors that can potentially play a significant role include the voluntary interaction [41, 42] and mobility-assisted mechanism [43, 44].

A fundamental, yet largely unanswered question is the role of the spatial reciprocity [45–48], which stems from the physical limitations in the range of social interactions or population dispersal. Unlike the other mechanisms, spatial reciprocity does not require actors' cognitive abilities for discriminating among interaction partners. Earlier studies showed a general tendency that the restricted interaction range or increased social viscosity promotes cooperation [45, 49]. Moreover, heterogeneity in degree distribution, as in most real-world networks, has been attributed to either increased or decreased level of cooperation[50–56]. Other studies tried to relate the topological properties of social network such as degree-degree correlation and clustering coefficient to the degree of cooperation. However, despite the volume of research from a wide range of perspectives [57], it still remains largely unanswered which structural characteristics are responsible for enhanced or suppressed cooperation.

Based on above curious we are motivated to explore the emergence of cooperation on structured populations. To investigate how structural characteristics effect on the selection of cooperation we employ the evolutionary graph theory which synthetic approach of the complex networks and the traditional evolutionary population dynamics. Interestingly it had been shown the structural characteristics of populations can changes the drift of selection [58]. In addition to the evolutionary graph theory we apply the game between individuals and tried to expand recent understanding of the network reciprocity based on the selection dynamics.

The structure of this thesis is following: In chapter 2, we briefly overview definitions and concepts of the complex networks which describing topological characteristics in interest to discuss how structural properties of population influence on the evolutionary process and the evolution of cooperation. Methods for generating a desired graph also discussed. In chapter 3, we will review essentials in the evolutionary dynamics from the differential equation that describing replication, selection and mutation to the stochastic dynamics in finite and fixed sized populations. Based on the evolutionary graph theory the interplay between dynamics and interaction patterns will be discussed. In chapter 4, we will discuss the evolution of cooperation based on the game theory with the 2×2 payoff matrix. After looking over known mechanisms which allows the selection of cooperation, we will explore the effect of the degree-heterogeneity and the degree-mixing on the emergence of cooperation. In chapter 5, we will summarize discussions.

Chapter 2

Complex Networks

Throughout this dissertation, individuals and social interactions thereof, such as given in social dilemma games, are represented as a mathematical graph composed of nodes and links among them. Intensive and extensive research effort has been poured for the last decade to the structure of social networks. In his seminal book [59], based on his own experiments, Steven Milgram proposed the hypothesis of "six degrees of separation'', claiming any individual is connected by any other individual by six steps of an acquaintance network on average.

Another milestone observation from the classic quantitative sociology was the so-called "strength of weak ties''. Unlike the late structures, social networks are not uniform in a sense that individuals' connection is not more or less the same. They contain the nodes of relatively loose connections as well as densely connected subnetworks which constitute an almost complete graph in a local neighborhood.

2.1 Introduction

A complex network is a graph representing the topological feature of a given complex system that composed of individual parts and connections among them. During the past decades researchers investigated many of real systems with huge spectrum of interests. Representative of examples are the internet, the world wide web, the power grid networks, the metabolic networks, the protein-protein interactions, the functional brain networks, the social networks based on the social media and in personal relation, the coauthor ships, and the transportation networks [60–68]. As the consequence of empirical explore the variety of systems across the fields, soon after it had been discovered that complex systems sharing the topological feature in their pattern of connections which is the heavy-tailed distribution of the number of connections among the individual parts. In other words, the degree distribution follows the power law such as, where the k is the degree, i.e. the number of connections of a component has. From the most of

empirical studies it had been found that the value γ, the degree-exponent, in the range of $2 < \gamma < 3$. Such networks are so-called the scale-free networks [61].

The "Scale-free network" means that there is no "scale" characterizing a given network. Compare to the classical random networks which the degree distribution follows the Poisson distribution introduced by Eldos and Renyi, the average degree cannot explain well the scale-free networks. This "scale-freeness" characteristics were attracted to statistical physicists because the power-law appears in the critical behavior in a physical system in terms of phase transition. For example, the correlation length in the paramagnetic system follows the power-law at the critical temperature. This leaded the theoretical approach to study complex networks in the physical and the mathematical society and the hundreds of papers were published.

Population in biological and social systems have a spatial structure meaning limited interaction patterns. This spatial stricture can be described in context of complex network based on the graph theory. An individual of population can be represented as a node and interaction patterns between any two individuals can be represented as a link. The number of link, a node have is the degree of node. Then any given structured population can be represented as a complex network.

2.2 Definitions and concepts

Formal definition of a graph is a set G consisting of two sets, the set of vertexes or nodes, V, where an element, i, is a single part of consisting components and the set of links, or edges, L, which consists of pair of vertexes, (i, j) that have connection between them.

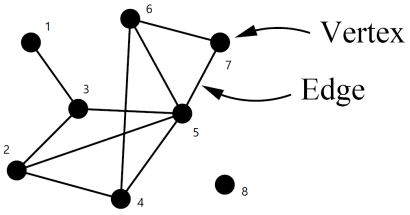

$$A = \begin{pmatrix} 0 & 0 & 1 & 0 & 0 & 0 & 0 & 0 \\ 0 & 0 & 1 & 1 & 1 & 0 & 0 & 0 \\ 1 & 1 & 0 & 0 & 1 & 0 & 0 & 0 \\ 0 & 1 & 0 & 0 & 1 & 1 & 0 & 0 \\ 0 & 1 & 1 & 1 & 0 & 1 & 1 & 0 \\ 0 & 1 & 1 & 0 & 1 & 1 & 0 & 0 \\ 0 & 0 & 0 & 1 & 1 & 0 & 1 & 0 \\ 0 & 0 & 0 & 0 & 0 & 0 & 0 & 0 \end{pmatrix}$$

Fig. 2.1 Simple graph and its corresponding adjacency matrix, A.

Adjacency matrix

All information of a given network can be stored in a matrix. The matrix is, so called, the adjacency matrix, A, where each element of the adjacency matrix, a_{ij}, is given by

$$a_{ij} = \begin{cases} 1 & \text{if } (i,j) \text{ is connected,} \\ 0 & \text{otherwise} \end{cases} \tag{2.1}$$

For undirected graphs, the adjacency matrix is symmetric, $a_{ij} = a_{ji}$, in which the direction of a link is ignored or considered as bidirectional for a given pair. The elements of adjacency matrix, a_{ij} can be a real number to represent weighted edges, for example the strength of interaction between a pair of nodes.

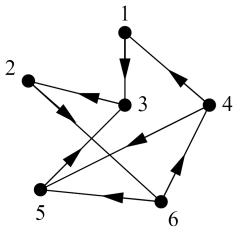

$$A = \begin{pmatrix} 0 & 0 & 1 & 0 & 0 & 0 \\ 0 & 0 & 0 & 0 & 0 & 1 \\ 0 & 1 & 0 & 0 & 0 & 0 \\ 1 & 0 & 0 & 0 & 1 & 0 \\ 0 & 0 & 1 & 0 & 0 & 0 \\ 0 & 0 & 0 & 1 & 1 & 0 \end{pmatrix}$$

Fig. 2.2 In this figure, the element of adjacency matrix, a_{ij}, represent connection *from i to j*.

Structural characteristics of a given network can be measured as numbers by manipulating of the adjacency matrix. Following concepts and definitions are used to represent structural characteristics in interest throughout in this dessirtation.

Degree

The number of connections that a node i has is the degree of node i, denoted by k_i. In terms of a_{ij},

$$k_i = \sum_j A_{ij} \tag{2.2}$$

The average degree $\langle k \rangle$ of a graph is the arithmetic mean of k_i over all nodes,

$$\overline{k} = \frac{1}{N} \sum_{i=1}^{N} k_i \tag{2.3}$$

Degree distribution

The degree distribution, $P(k)$, of a given graph is the frequency distribution of node degrees.

$$P(k) = \frac{1}{N} \sum_i \delta(k, k_i) \tag{2.4}$$

The probabilistic interpretation of the degree distribution, $P(k)$, is the probability that a node of degree k is choosen by random chose. The degree sequence is another construct of the same information as the degree distribution. The degree sequence is the set $\{k_1, k_2, k_3, \dots\}$ of degrees for all nodes. The degree

distribution, or the degree sequence of a given graph tell us information that how connectivity of the graph is distributed, however, it does not tell us complete structure of a network.

Assortativity

The assortativity, usually denoted by r in network science community, is the Pearson-correlation coefficient of degrees between a pair of connected nodes, (i, j). The formal definition of the assortativity is given by [69],

$$r = \frac{\langle k_l k'_l \rangle - \langle (k_l + k'_l)/2 \rangle^2}{\langle k_l^2 + k_l'^2 \rangle + \langle (k_l + k'_l)/2 \rangle^2} \tag{2.5}$$

where k_l and k'_l are the degrees of two end-nodes of a link, l, respectively and the average $\langle \ldots \rangle$ is over the set of all links. Roughly speaking, if $r > 0$, the pattern of connections between nodes of the given graph has a tendency that nodes with similar degrees are linked each other, such networks are called assortative networks, or assortatively degree-mixed, whereas $r < 0$, reveal the opposite trend, and called disassortative. When $r = 0$, it is called neutral [70].

Clustering coefficient

The clustering coefficient of a single node of degree k_i, c_i, is defined by

$$C_i = \frac{2\Delta_i}{k_i(k_i - 1)} = \frac{\text{number of pairs that connected among neighbors of i}}{\text{number of possible links among neighbors of i}} \tag{2.6}$$

The local clustering coefficient of node i reflects the tendency of friends of i are also friends to each other. If the local clustering of node i, C_i For a given network, the average clustering coefficient is the mean of local clusterings taken over the set of all nodes,

$$\overline{C} = \frac{1}{N} \sum_i C_i. \tag{2.7}$$

Similarity

The similarity is the concept that represents the structural equivalence between a pair of nodes. Consider two nodes, say i and j, that are sharing many of common neighbors but are not connected. In this case, i and j are structurally equivalent or structurally similar in a sense that interactions or influence from neigbors that i and j would feel or information about neighbors that i and j would know will be similar because they both know many of same neighbors commonly, even not directly connected [7]. For the

quantitative measure for similarity we will use the cosine similarity [71], defined by,

$$\sigma_{ij} = \frac{\sum_k A_{ik}A_{kj}}{\sqrt{\sum_k A^2{}_{ik}}\sqrt{\sum_k A^2{}_{kj}}} = \frac{n_{ij}}{\sqrt{k_i k_j}} \tag{2.8}$$

2.3 Structural characteristics of complex networks

Degree heterogeneity

In crude terms, The degree has a role of importance, or influence of a node in many studies. We may wonder how the degree is distributed. The degree distribution, $P(k)$ give us the answer. Depends on the distribution broadness, the feature of network can be classified into one of two catagolies. The homogenous networks, in which the distribution sufficiently narrow near to the mean degree, or, the heterogenous networks, where the distribution is broad enough so that the average degree is far away as the representative. Especially, if the degree distribution follows a power low for large k, such that,

$$P(k) \sim k^{-\gamma} \tag{2.9}$$

the network is called the scale-free network [72]. The exponent, γ, usually called the degree-exponent and used to indicate the degree heterogeneity. It had been discovered that many of real networks of systems in biology, engennering, internet, and social interactions have the scale-freeness in common and the degree exponents of such networks laid on the range, $2 < \gamma < 3$ [73].

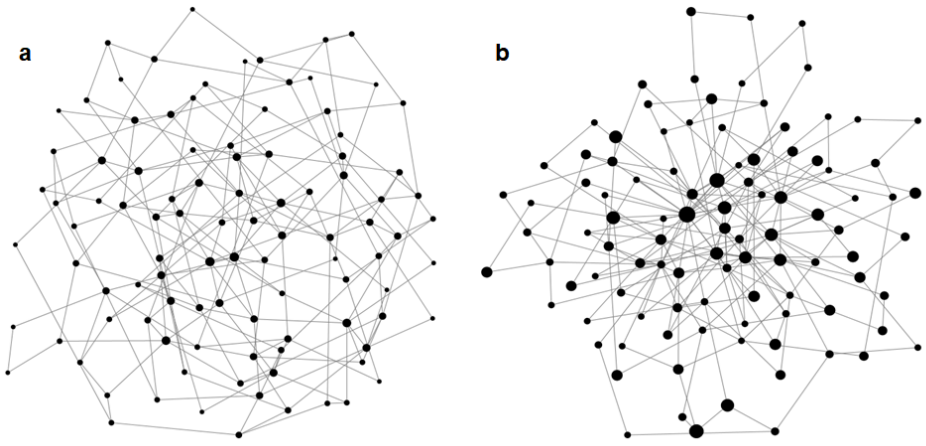

Fig. 2.3 Visualized (a) Erdős-Rényi (ER) and (b) Barabáshi-Albert (BA) networks. ER is representative the degree-homogeneous structure which the degree distribution has form of the Poisson distribution, $P(k) = \lambda^k/k!e^{-\lambda}, \lambda = \overline{k}$ and BA representative as the degree-heterogeneous structure with $P(k) \sim k^{-\gamma}$, where $\gamma \sim 3$.

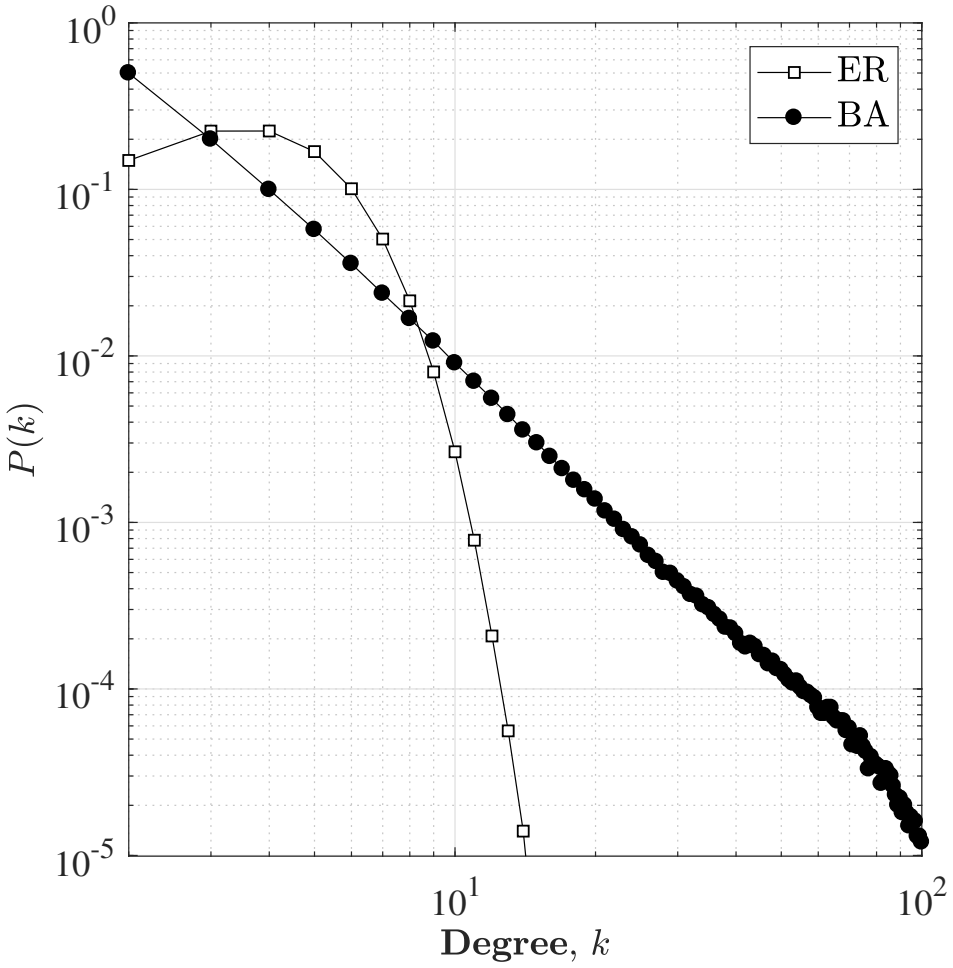

Fig. 2.4 The degree distribution, $P(k)$, of the Erdős-Rényi (ER) and the Barabáshi-Albert (BA) networks. Each network is the representative of the degree-homogeneous (ER), and the degree-heterogeneous (BA) structure. Figure obtained from independently generated 5,000 networks size of 1,000, $\overline{k} = 4$ using each model.

Degree-mixing

The joint distribution, $P(k,k')$, defined by the probability that a randomly selected link has two end nodes with degrees k and k' respectively, provide more detailed information compare to the degree distribution, $P(k)$. It encodes the two point correlation in the simplest from [74]. The factorizability of $P(k,k')$,

$$P(k,k') = \frac{kk'P(k)P(k')}{\langle k \rangle^2} \tag{2.10}$$

reveals the lack of two point correlation, and deviation from it represents the existence of the degree-degree correlation.

Alternative way to show the degree-mixing is measuring the average neighbor degree as a function of 'centered' or 'ego' node k, $\langle k_{nn} \rangle (k)$ [75].

$$\langle k_{nn} \rangle (k) = \sum_{k'} k' P(k'|k) = \sum_{k'} k' \frac{P(k',k)}{kP(k)} \langle k \rangle , \tag{2.11}$$

where the conditional probability, $P(k'|k)$ corresponds to the probability that the degree of randomly chosen neighbor of node with degree k is k'. In general, increasing $\langle k_{nn} \rangle$ corresponds to the assortative mixing, decreasing corresponds to the disassortative mixing. In some cases, it turns out $\langle k_{nn} \rangle$ can be represented by another power law [75, 76],

$$\langle k_{nn} \rangle (k) \sim k^{\mu}. \tag{2.12}$$

In case of neutral, or non-correlated configuration, 2.11 is reduced to $\langle k_{nn} \rangle (k) = \langle k^2 \rangle / \langle k \rangle$, which independent of k.

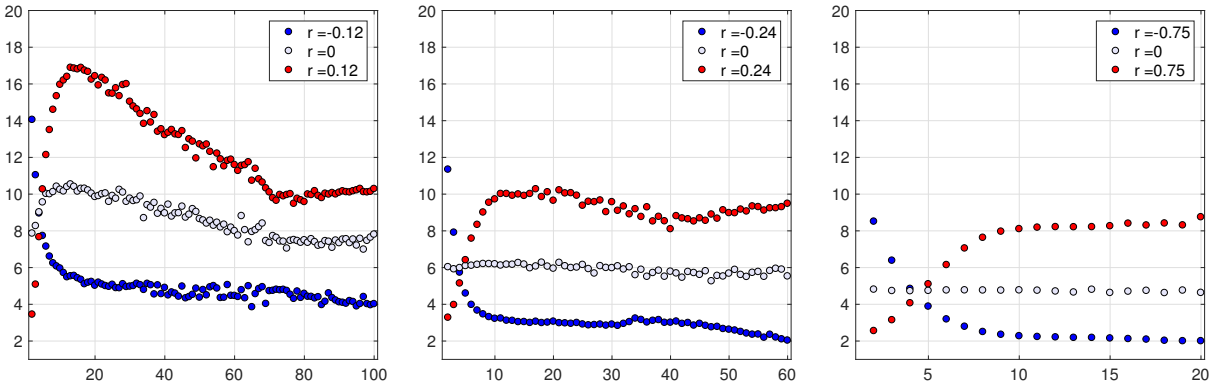

Fig. 2.5 The averaged degree of nearest neighbors, $\overline{k_{nn}}(k)$, as function of the degree of 'ego' node for each level of the degree-heterogeneity (left, $\gamma = 2,5$, middle, $\gamma = 3.0$, right,$\gamma = 5.0$) and the assortativity (see the legend). The cross point placed at the average degree of the networks, $\overline{k} = 4$. Based on definition, $\overline{k}_{nn}(k) \propto k$, however, in case of the most heterogeneous structure (left), $\overline{k}_{nn}$ is decreasing as k increasing for high degree nodes which represent minority of massively connected hubs.

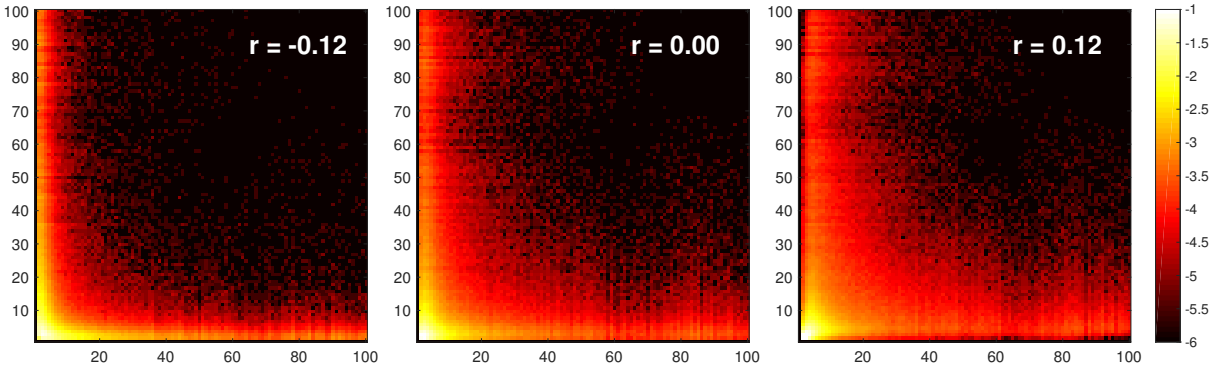

(a) $\gamma = 2.5$

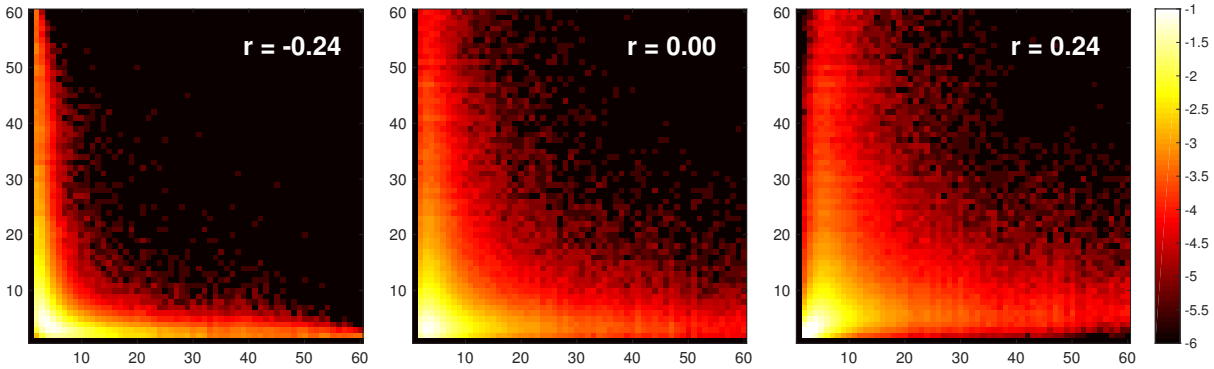

(b) $\gamma = 3.0$

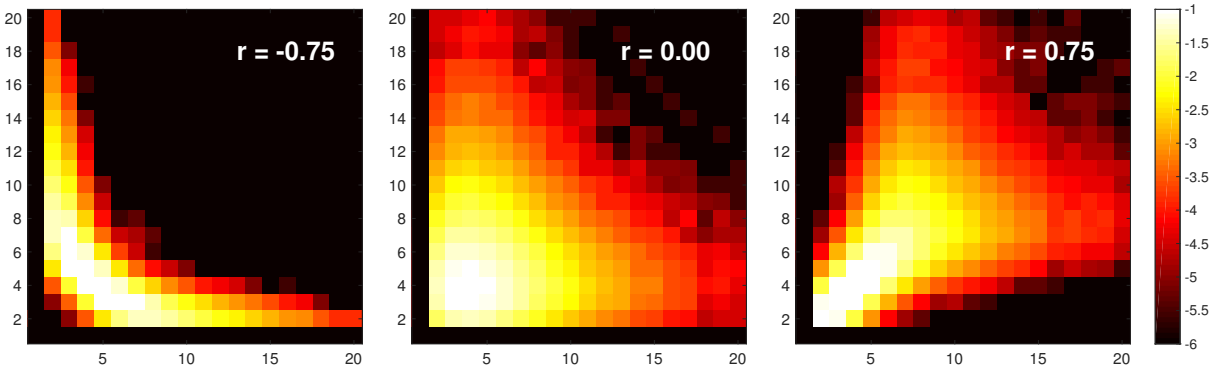

(c) $\gamma = 5.0$

Fig. 2.6 Log-scaled joint distribution, $P(k,k')$, from different level of the degree heterogeneity, (a) $\gamma = 2.5$, (b) $\gamma = 3.0$, (c) $\gamma = 5.0$, and different level of degree-mixing. The joint probability obtained from the ensemble of 200 independently generated network samples size of $N = 1000$, with the average degree, $\overline{k} = 4$.

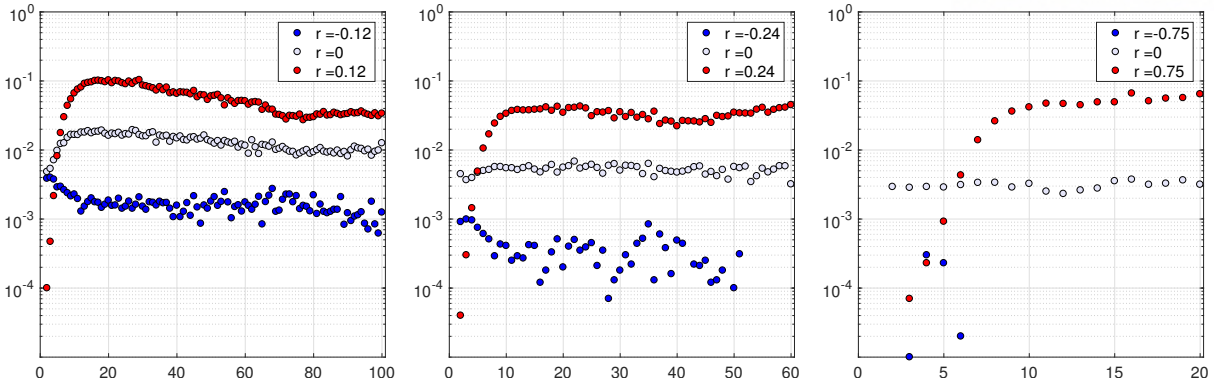

Fig. 2.7 Clustering distribution, $C(k)$, of each characterized networks. From left to right the corresponding degree-exponents are $\gamma = 2.5, 3.0,$ and 5.0 and the averaged clustering coefficient $\overline{C} \sim 0$. The distribution of clustering depends on the level of degree-mixing. Assortative configuration, $r > 0$, have the distribution that very low clustering around low degree nodes while relatively high clustering around high degree nodes. Disassortative mixing have opposite form compare to assortative and neutral mixing is in between. Relatively high clustering distribution among highly connected nodes in assortative mixing contributed viscous connection pattern among them.

Clustering

Based on definition of clustering coefficient [77] many of previous studies on real network reported that real networks showing high clustering compare to the prediction of random graph theory [77–80], however, the mechanism explaining collective forming of interaction is not well understood yet. It is also reported that in many real world networks the local clustering distribution, $C(k)$, defined by the average local clustering coefficient of nodes of degree k, shows a scaling, [80–83]

$$C(k) \quad \sim \quad k^{-\beta}. \tag{2.13}$$

In many cases the exponent fit to $\beta \sim 1$ [81], and termed the hiearachical clustering [83].

Relation between structural characteristics

Definitions discribed in previous section try to capture a certain structural characteristics in large scale networks. In fact, however, there are relations between definitions and also each defnition has the limitation. For example, the clustering coefficient and the degree-mixing. It had been reported that the clustering drives the assortativity in the model study [84], in which high clustering coefficient among the highly connected node naturally contribute to the positive degree-degree correlation as shown in Fig. 2.7. On the other hand, the positive and negative degree-mixing decrease or increase structural similarity between a pair of nodes as shown in Fig. 2.8.

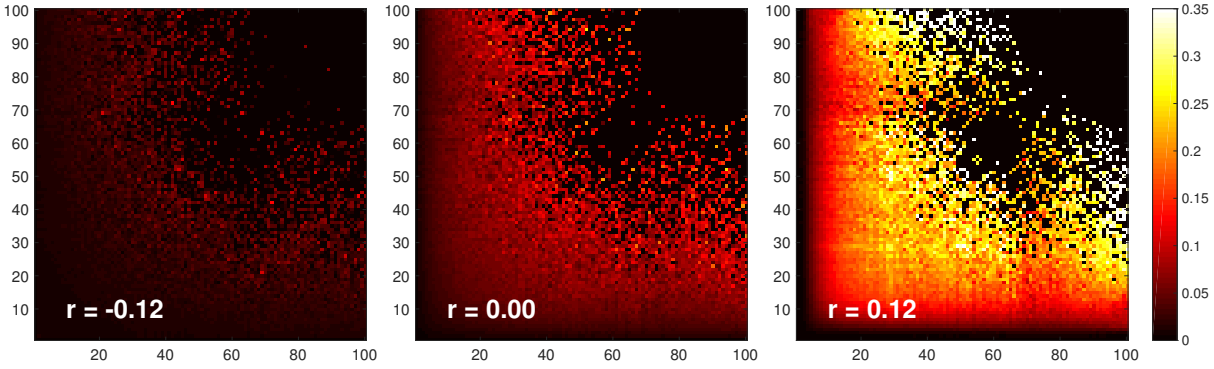

(a) $\gamma = 2.5$

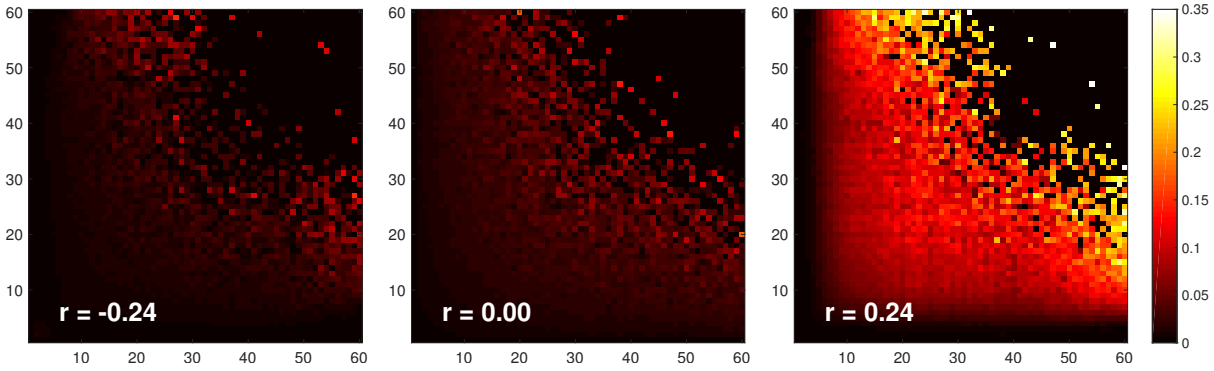

(b) $\gamma = 3.0$

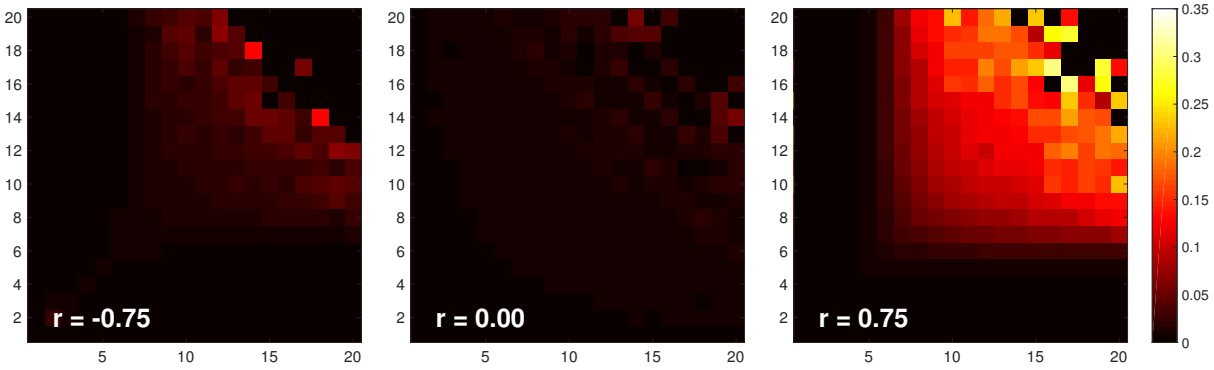

(c) $\gamma = 5.0$

Fig. 2.8 Averaged cosine similarity between pair of nodes with degree k_i and k_j for various degree heterogeneity, (a) $\gamma = 2.5$, (b) $\gamma = 3.0$, (c) $\gamma = 5.0$, and different level of degree-mixing. The ensemble of networks used to obtain figure is same that were used for Fig. 2.6. Figure shows that very high level of similarity in the assortative configuraton compare to the disassortative, especially between high degree nodes.

2.4 Generation of networks

Through out this dissertation we are going to focus on the effect of the degree-heterogeneity and the degree-degree correlation on the evolutionary dynamics and the emergence of cooperation. For numerical simulation on variously characterized networks as the combination of the degree-heterogeneity and the degree-mixing, we employed following methods for generating desired complex networks. Generation of a network consist of generating the degree-sequence , which controlling the level of degree-heterogeneity and tuning detailed characteristics. Finite sized un-directed and un-weighted network size of, N, with average connectivity, $\bar{k}$ will have N nodes and $L = N\bar{k}/2$ links and corresponding information of network will be stored in the adjacency matrix size of $N \times N$ with components. Technically what we do is, therefore, generating the adjacency matrix.

2.4.1 Generation of degree sequence

Random graph

Erdős-Rényi introduced the random graph model in 1959 [85, 86] and studied is a statistical ensemble whose members are all possible labelled graphs of given number of nodes N and links L, and all these members have equal statistical weight. To generate ensemble of networks size of N and the average degree of $\bar{k}$ or $L = N\bar{k}/2$ links, we simply iterate random linking between randomly chosen two nodes, until the total number of link reached L. As the results, the degree-distribution of random graph will follows the Poisson distribution,

$$P(k) = \lambda^k / k! e^{-\lambda}, \tag{2.14}$$

where, $\lambda = \bar{k}$.

Barabáshi-Albert model

The Barabási-Albert (BA) model or scale-free network model is the model which reproduce power-law degree distribution based the algorithm, called *the preferential attachment* [73]. The model is growing model in which starting from small number of initial configuration, at each step we add a node, say i, and build links from i to already existing node. The node i choose its neighbor, say j, with the probability proportional to the degree, k_j, such that

$$\Pi(k_j) = \frac{k_j}{\sum_l k_l} \tag{2.15}$$

Using the BA model, one can generate the degree sequence which follows the power-law degree distribution, $P(k) \sim k^{-\gamma}$, with the degree exponent $\gamma \sim 3.0$.

Static model

For a configurational model, each of the N nodes is assigned an index $n \in \{1,2,\cdots,N\}$ and the corresponding weight $n^{-\alpha}$, where $\alpha \in [0,1)$. Then selecting a pair of nodes u and v according to the normalized weight $u^{-\alpha}/\sum_{n=1}^{N} n^{-\alpha}$ and $v^{-\alpha}/\sum_{n=1}^{N} n^{-\alpha}$ and connect the two half-edges unless one already exists. By repeating this pairing process up until mN edges are formed, we obtained a scale-free network of degree distribution $P_D(k) \propto k^{-\gamma}$ with the mean degree $2m$. From the analytic relation between α and γ [87], we could modulate the degree exponent $\gamma = 1 + 1/\alpha \in (2,\infty)$ by tuning the weighting parameter α.

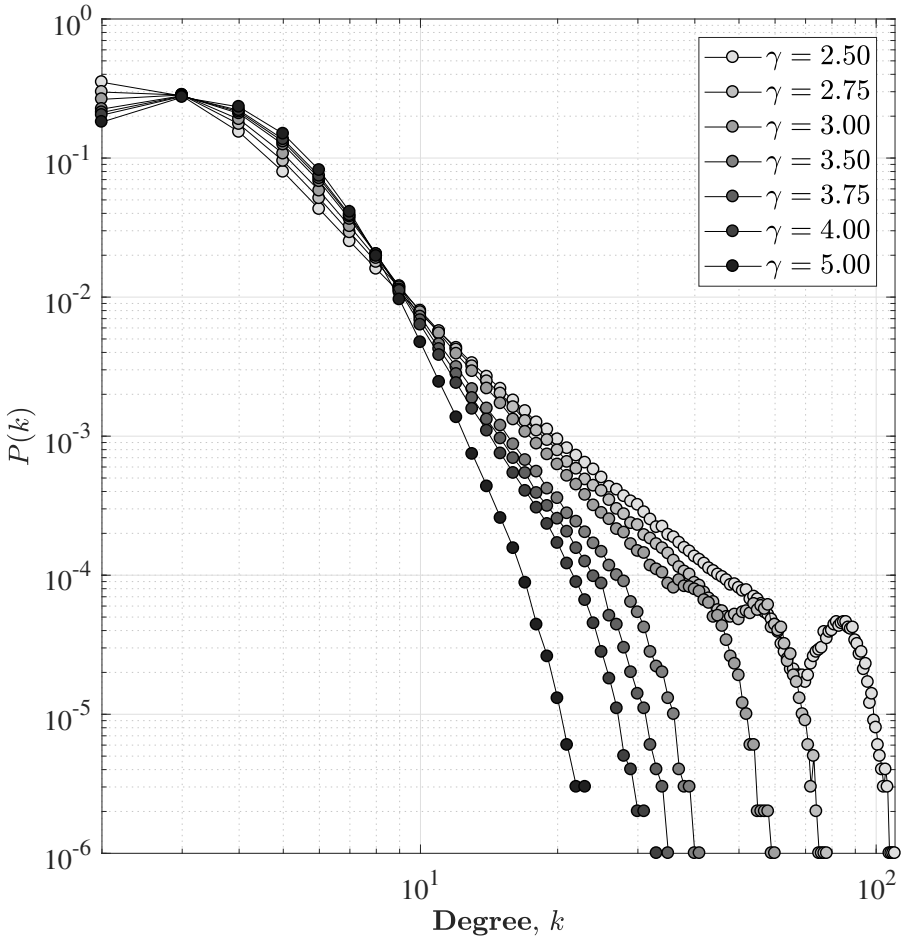

Fig. 2.9 The degree distribution $P(k)$ of generated scale-free networks with desired degree-exponents using the static model. Figure obtained from the ensemble of 5,000 independently generated network samples, size of 1000, and the average degree, $\overline{k} = 4$. As the degree-exponent, γ, decreases the degree-distribution more fat-tailed.

2.4.2 Tuning topological characteristics

Degree-preserved rewiring

Tuning detailed characteristics of network can be achieved by rewiring process. To obtain various levels of degree-degree correlation, we introduce random rewiring of edges in a degree-preserving manner [76], through which the desired sign and magnitude of assortativity of a graph can be asymptotically tuned. More specifically, we try to construct an ensemble of graphs that have the maximum entropy (or maximal information) among all the graphs specified by a value of assortativity, and degree distribution. In analogy with the canonical NVT ensemble for a thermodynamic system, we consider the network "Hamiltonian" $\mathscr{H}(G)$ such that the probability distribution over a set of graphs is given by [88, 89]

$$P(G) = Z^{-1} e^{-\mathscr{H}(G)} , \tag{2.16}$$

where Z is the normalization constant and the Hamiltonian is directly proportional to the assortativity.

- **Degree-mixing Hamiltonian** Since the only term allowed to vary in Eq. 2.5 for a given degree distribution is $\langle kk' \rangle$, the Hamiltonian should be of the form

$$\mathscr{H}(G) = -J \sum_{i>j}^{N} a_{ij} k_i k_j , \tag{2.17}$$

  where J modulates the sign and magnitude of the degree-mixing pattern. As the magnitude of J increases in a positive (negative) direction, the degree-degree correlation of the "equilibrium" or maximum entropy graph becomes more assortative (disassortative) and eventually saturates to the maximal (minimal) value allowed for a given degree sequence.

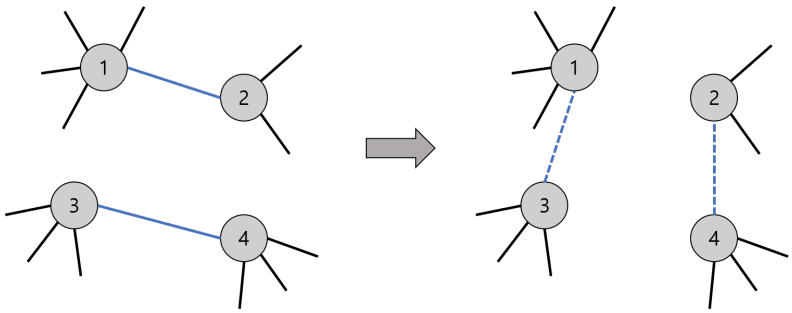

Fig. 2.10 Schematic description of degree preserving rewiring. Randomly chosen two pairs of nodes, $(1,2)$ and $(3,4)$ are going to be rewired as $(1,3)$, $(2,4)$ depend on the difference between Hamiltonians, $\Delta\mathscr{H} = \mathscr{H}(G') - \mathscr{H}(G)$.

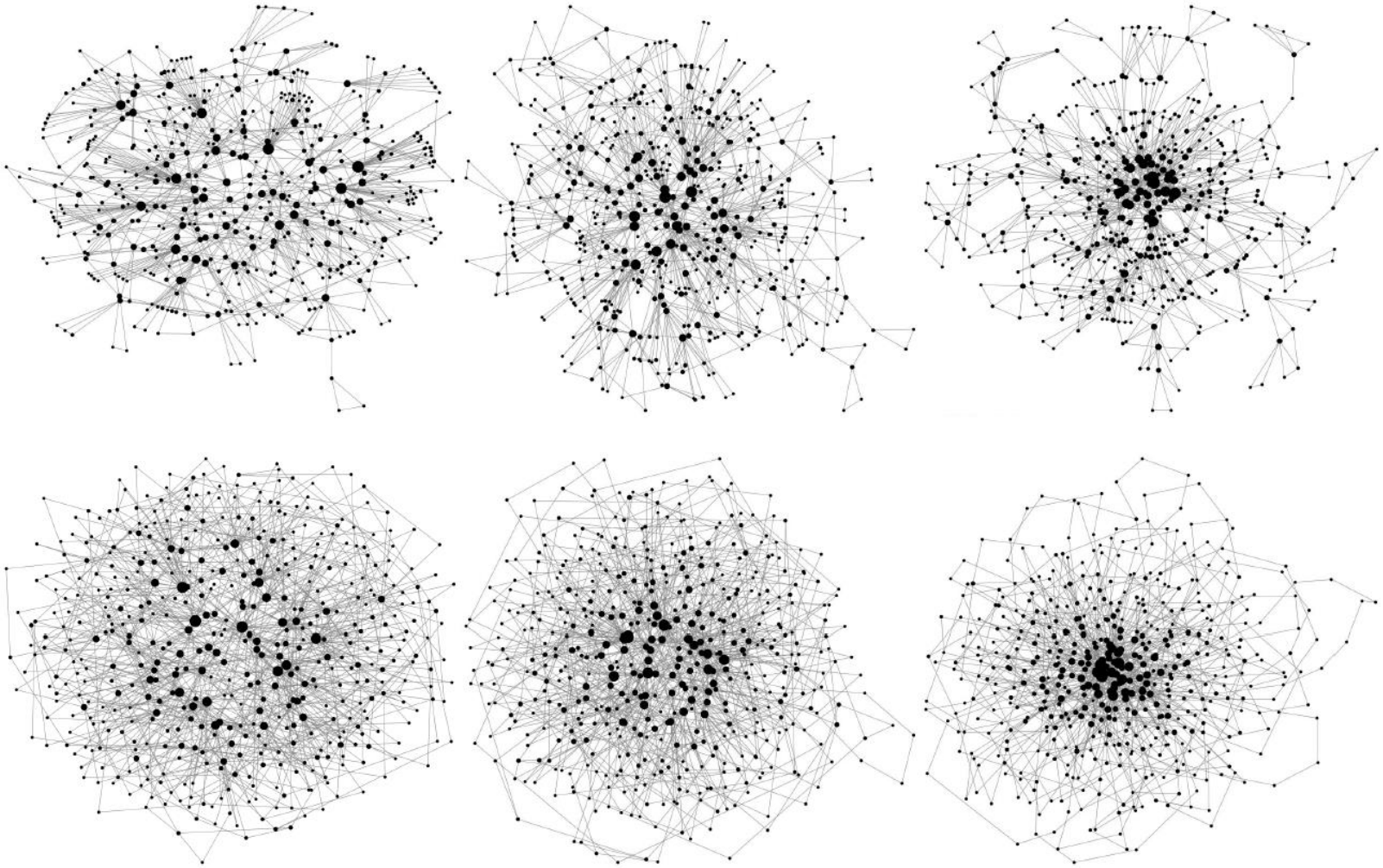

Fig. 2.11 Example view of rewired Scale-free networks with degree-exponent, $\gamma = 2.5$, size, $N = 1000$, and the average connectivity, $\overline{k} = 4$. In this diagram the size of node proportional to its degree, k_i. Desired assortative, r and mean clustering coefficient $\overline{c}$ are following, left-disassortative($r = -0.12$), middle-neutral($r = 0.0$), right-assortative($r = 0.12$), top-highly clustered($\overline{c} = 0.3$) and bottom-barely clustered($\overline{c} \sim 0.0$). All rewired configurations share the degree-sequence, $P(k)$. The figure generated using the NodeXL software (https://nodexl.com/).

Chapter 3

Evolutionary Dynamics on Graphs

In this chapter, we review the basic concepts of population dynamics and the mathematical framework for capturing the evolutionary processes occurring on structured populations. We model the structure or pattern of social interactions as mathematical graphs, where the nodes represent individuals and the (un)directed links interactions among individuals. We consider a variety of dynamical processes taking place in a general population and try to seek the correlations between the dynamical processes and the underlying population structure.

3.1 Introduction

Evolution in population is a dynamical process which consists of replication, selection, and mutation [90]. Individuals in population reproduce their offsprings by giving same genetic information or identity. Based on what identity or genetic information an individual has, its fitness is given, which describes individual the rate of reproduction. In such a process the selection comes naturally as a domination of population by a specific identity or species, which may have the highest fitness among all kinds in the whole population. Such an emergence phenomenon is understood as main mechanism of evolution in nature.

The evolutionary dynamics is the mathematical tool to describe the evolutionary process. It has the form of the coupled differential equations or the form of the stochastic processes. The deterministic equations mostly used to describe behavior and to understand of evolutionary systems of large size, which large enough to describe the consists of a population with continuous variables. In this case we focus on the domination of population by a certain type, which have the fittest fitness among composition. On the other hand, the stochastic version of evolutionary system, in which closely related to interest of this thesis, is very powerful tool to understand the emergent properties in the population of finite size.

3.1.1 Evolutionary process

Evolutionary system evolve based on three processes, replication, selection, and mutation. Subject of replication in evolutionary theory mainly a genotype which delivered from a parent to its offspring as form of giving birth. In consequence of an error during replication, mutation occur and it derives the biological diversity. During the processes the selection only allows the survival of fitter, since the resources in environment is limited. In this subsection we review above evolutionary processes in large sized and unstructured population system with deterministic equations to understand the logic governing nature.

Replication

Suppose we have population that growing with a rate, α, and die out with a rate, δ. Dynamics of this population is given by,

$$\dot{x} = (\alpha - \delta)x \tag{3.1}$$

and thus, equation of population growth is,

$$x(t) = x_0 e^{(\alpha-\delta)t} \tag{3.2}$$

The equation tells the population will grow indefinitely as long as $\alpha > \delta$. However, in real world there are limitations due to the competition for finite resources allowed by environment. This is captured by the carrying capacity, K, quantifying the maximum population level that can be sustained by the given environment. Then, the population dynamics is modified to,

$$\dot{x} = rx(1 - x/K) \tag{3.3}$$

The equation of population growth with carrying capacity is given by,

$$x(t) = \frac{Kx_0 e^{\alpha t}}{K + x_0(e^{\alpha t} - 1)} \tag{3.4}$$

In the limit of infinite time, $t \to \infty$, the population size converges to the limit, $x^* = K$.

Selection

Selection functions whenever more than two types of individuals reproduce at different rates. Suppose we have population consists of two types, say x, and y with corresponding rate of reproduction, α for x, and

β for y. The rate of reproduction is interpreted as *fitness*. We have,

$$\begin{aligned} \dot{x} &= \alpha x \\ \dot{y} &= \beta y \end{aligned} \tag{3.5}$$

and thus,

$$\begin{aligned} x(t) &= x_0 e^{\alpha t} \\ y(t) &= y_0 e^{\beta t} \end{aligned} \tag{3.6}$$

Denote by $\rho(t) = x(t)/y(t)$ the ratio of x over y at time t, we have,

$$\dot{\rho} = \frac{\dot{x}y - x\dot{y}}{y^2} = (\alpha - \beta)\rho \tag{3.7}$$

$$\rho(t) = \rho_0 e^{(\alpha-\beta)t} \tag{3.8}$$

If $\alpha > \beta$, ρ will exponentially increase, meaning x will out compete y over time.

Let consider a situation that the total population is constant. For the fixed sized population, say, $x+y=1$, and now x, and y represent the relative abundance of each kinds.

$$\begin{aligned} \dot{x} &= x(\alpha - \phi) \\ \dot{y} &= y(\beta - \phi) \end{aligned} \tag{3.9}$$

where, $\phi = \alpha x + \beta y$ ensures $x+y=1$. ϕ is the average fitness of the population. Now, let $y=(1-x)$, we obtain,

$$\dot{x} = x(1-x)(\alpha - \beta). \tag{3.10}$$

The equation has two stable points, at $x=0$ and $x=1$. At these points, $\dot{x}=0$. If $x=1$, the population consists only of x type and if $x=0$, the population consists only of y.

- **Selection - the survival of the fitter**: From Eq. 3.10 we can observe that if $\alpha > \beta$, then $\dot{x} > 0$ for all values of x, between 0 and 1, $0 < x < 1$. It means that for any of mixed population, consisting of x and y with certain fraction of each, the relative abundance of x will increase if the fitness of x is greater than the fitness of y. At the end the fraction of x will converge to 1, while the fraction of y will converge to 0, *"the survival of fitter"*.

Mutation

During the process of reproduction errors can occur, and those errors are called *mutation*. Consider again a population consists of two types, x and y. Let assume that x and y have same reproduction rate. Denote by u_{xy} the mutation rate from x to y, and u_{yx} the mutation rate from y to x. u_{xy} is the probability that the reproduction of x result in y. The population system evolve following equations,

$$\begin{aligned} \dot{x} &= x(1-u_{xy}) + yu_{yx} - \phi x \\ \dot{y} &= y(1-u_{yx}) + xu_{xy} - \phi y \end{aligned} \tag{3.11}$$

Since x and y have same fitness, the average fitness of the population is constant as $\phi = 1$. Using $x+y=1$, the equation reduced to,

$$\dot{x} = u_{yx} - x(u_{xy} + u_{yx}). \tag{3.12}$$

Therefore, the relative abundance of x converges to the stable point,

$$x^* = \frac{u_{yx}}{u_{xy} + u_{yx}}. \tag{3.13}$$

As the consequence of mutation, the population become mixed state of x and y. At stable point, the ratio between x and y is given by $x^*/y^* = u_{yx}/u_{xy}$.

In some cases the mutation rate in one direction is much higher than in the other direction. If mutation from x to y is much higher than mutation from y to x, type x will keep decreasing and finally y will take over the population. As the result, different mutation rates can lead selection even without differences of fitness.

In general, we can consider population with n different types. Denote by u_{ij} the mutation rate from type i to j, we have the mutation matrix, $U = [u_{ij}]$. Since each type reproduce itself or other type, $\sum_{j=1}^{n} u_{ij} = 1$, thus, U is a $n \times n$ stochastic matrix. The generalized mutation dynamics can be written as,

$$\dot{x}_i = \sum_{j=1}^{n} x_j u_{ji} - \phi x_i \qquad i = 1, 2, \ldots, n \tag{3.14}$$

using vector notation,

$$\dot{\vec{x}} = \vec{x}U - \phi\vec{x} \tag{3.15}$$

Again the average fitness, $\phi = 1$, the equilibrium, $\vec{x}^*$, is given by the eigenvector associated to the eigenvalue 1:

$$\vec{x}^* U = \vec{x}^*. \tag{3.16}$$

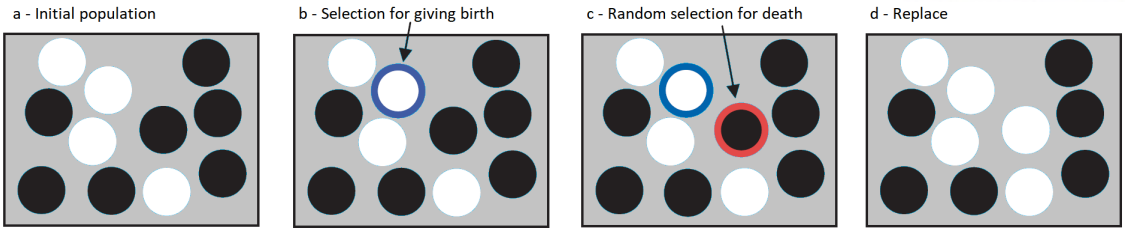

Fig. 3.1 Schematic discription of the Moran process

3.1.2 Evolutionary processes in finite population

So far we have looked the overview of evolutionary processes in terms of differential equations with continuous variables. In this subsection we consider evolutionary process in a population of fixed size. in finite populations, the scheme based on continuous variable, which described the fraction of a certain type of individuals, is no longer suits since we will count each type of individuals as integers. For finite sized population we consider the dynamics in terms of stochastic processes. That is the Moran process, invented by the population geneticsit P.A.P. Moran in 1958 [91].

Moran process

In Moran process, the size of population, N, is fixed. It consist of two random processes, the birth and the death. At each time step one individual randomly selected with probability proportional to its fitness and reproduces its offspring which the identical type, and another one randomly chosen for being replaced by the offspring from the one who chosen for reproduction so that the size of population is fixed.

Fixation probability

Consider a population size of N. At certain time point mutation has occurred, and now we have $N-1$ of the wild type, say W, and 1 of the mutated type, M. The mutated type has the relative fitness, r, compare to the wild type. We may wonder the probability of the whole population is going be conquered by a single mutated type. This probability is called the fixation probability.

The Moran process of this case can be formulated by the transition matrix, T, with elements T_{ij}. T_{ij} is the probability that the state of the system is going be changed from state i to state j. The process laid on the states space, $m = 0, 1, 2, ..., N$, where m represents the number of mutated type, M. From the definition of the Moran process allowing increasing or decreasing one mutated type at each step, the corresponding the transition matrix is given as follows:

$$T^{N+1\times N+1} = \begin{pmatrix} 1 & 0 & 0 & \dots & 0 & 0 & 0 \\ T_1^- & 1-T_1^+-T_1^- & T_1^+ & \dots & 0 & 0 & 1 \\ \vdots & \vdots & \vdots & \ddots & \vdots & \vdots & \vdots \\ 0 & 0 & 0 & \dots & T_{N-1}^- & 1-T_{N-1}^+-T_{N-1}^- & T_{N-1}^+ \\ 0 & 0 & 0 & \dots & 0 & 0 & 1 \end{pmatrix} \tag{3.17}$$

where, $T_m^{\pm}$ is the probability that mutant, M, increased$(+)$ or decreased$(-)$ from the state m. Denote by ρ_m the probability of reaching state N starting from the state m. We have,

$$\begin{aligned} &\rho_0 = 0 \\ &\rho_m = T_m^-\rho_{m-1} + (1-T_m^- - T_m^+)\rho_m + T_m^+\rho_{m+1} \qquad i = 1,2,\dots,N-1 \\ &\rho_N = 1 \end{aligned} \tag{3.18}$$

Note that the states, $m = 0$ and $m = N$ are *absorbing state*, because once the system has reached one of two states, it will stay there. Therefore, the population will be taken over by the mutant or the mutant will be wiped out at the end. Let the variable ϕ_m such that

$$\phi_m = \rho_m - \rho_{m-1} \qquad m = 1,2,\dots,N, \tag{3.19}$$

using ϕ_m rearrange Eq. 3.18 to

$$\phi_{m+1} = \frac{T_m^-}{T_m^+}\phi_m. \tag{3.20}$$

Denote by $\gamma_m = T_m^-/T_m^+$ the ratio between transitions for decreasing and increasing from the state m. From the iterative relation,

$$\begin{aligned} \phi_2 &= \rho_1 - \rho_0 = \rho_1 \\ \phi_1 &= \rho_2 - \rho_1 = \gamma_1\rho_1 \\ &\vdots \\ \phi_k &= \rho_k - \rho_{k-1} = \rho_1\prod_{m=1}^{k-1}\gamma_m \\ &\vdots \\ \phi_N &= \phi_N - \phi_{N-1} = \rho_1\prod_{m=1}^{N-1}\gamma_m \end{aligned} \tag{3.21}$$

The sum over all ϕ_m is,

$$\sum_{k=1}^{N} \phi_k = \rho_1 - \rho_0 + \rho_2 - \rho_1 + \rho_3 - \rho_2 + \cdots + \rho_N - \rho_{N-1} = 1. \tag{3.22}$$

Finally, we have,

$$1 = \sum_{k=1}^{N} \phi_k = \sum_{k=1}^{N} \rho_1 \prod_{m=1}^{k-1} \gamma_m = \rho_1 \left(1 + \sum_{k=1}^{N-1} \prod_{m=1}^{k} \gamma_m \right) \tag{3.23}$$

Therefore, the fixation probability of a single mutant, ρ_1, is given by

$$\rho_1 = \frac{1}{1 + \sum_{k=1}^{N-1} \prod_{m=1}^{k} \gamma_m}. \tag{3.24}$$

In general, the fixation from m mutants, ρ_m is given by,

$$\rho_m = \sum_{k=1}^{m} \phi_k = \rho_1 \sum_{k=1}^{i} \prod_{m=1}^{k-1} \gamma_m = \rho_1 \left(1 + \sum_{k=1}^{m-1} \prod_{m'=1}^{k} \gamma_{m'} \right) = \frac{1 + \sum_{k=1}^{m-1} \prod_{m'=1}^{k} \gamma_{m'}}{1 + \sum_{k=1}^{N-1} \prod_{m=1}^{k} \gamma_m}. \tag{3.25}$$

Hereafter we denote the fixation probability of the wild type by $\rho_{W,1}$ and the fixation probability of the mutant type by $\rho_{M,1}$. Note that the fixation probability for a single individual of the wild type is equal to the probability that $N-1$ of mutant failed take over the population pool, $\rho_{M,N-1}$, therefore, the fixation probability of the wild, $\rho_{W,1}$ is given by,

$$\begin{aligned}
\rho_{W,1} &= 1 - \rho_{M,N-1} \\
&= 1 - \frac{1 + \sum_{k=1}^{N-2} \prod_{m=1}^{k} \gamma_m}{1 + \sum_{k=1}^{N-1} \prod_{m=1}^{k} \gamma_m} \\
&= \frac{1 + \sum_{k=1}^{N-1} \prod_{m=1}^{k} \gamma_m}{1 + \sum_{k=1}^{N-1} \prod_{m=1}^{k} \gamma_m} - \frac{1 + \sum_{k=1}^{N-2} \prod_{m=1}^{k} \gamma_m}{1 + \sum_{k=1}^{N-1} \prod_{m=1}^{k} \gamma_m} \\
&= \frac{\prod_{m=1}^{N-1} \gamma_m}{1 + \sum_{k=1}^{N-1} \prod_{m=1}^{k} \gamma_m} \\
&= \rho_{M,1} \prod_{m=1}^{N-1} \gamma_m.
\end{aligned} \tag{3.26}$$

Hence, the ratio of the fixation probabilities is $\rho_W / \rho_M = \prod_{m=1}^{N-1} \gamma_m$. If the product smaller than 1, $\rho_W < \rho_M$, meaning a single the mutant type more likely take over the population of the wild type compare to the contrary case. In general, the ratio between type A and B, ρ_A / ρ_B is the indicator of the time spend that the population is governed by whether type A or type B [92].

Drift and selection

Consider the case when the mutant arise with the constant relative fitness, r, compare to the wild type. The transition probabilities of increasing or decreasing the number of mutant population when the system in the state m are given by,

$$\begin{aligned} T_m^+ &= \text{Birth of mutant} \times \text{Death of wild} &&= \frac{mr}{rm+N-m} \times \frac{N-m}{N}, \\ T_m^- &= \text{Birth of wild} \times \text{Death of mutant} &&= \frac{N-m}{rm+N-m} \times \frac{m}{N} \end{aligned} \tag{3.27}$$

therefore, $T_m^-/T_m^+ = \gamma_m = 1/r$ for all m, and the sum of products in denominator reduces to the sum of geometric sequence with common ratio $1/r$, thus, the fixation probability is given by,

$$\rho_M(r) = \frac{1-1/r}{1-1/r^N}. \tag{3.28}$$

One can notice that the chance of extinction for the advantageous mutant always remains, compare to the deterministic models of evolution in which regardless how small r, as long as $r > 1$ the mutant take over the population. As the result of the stochastic process, the fixation probability identifies a balance between natural selection and the random drift [58, 8].

In this case the relative fitness of the mutant, $r = 1$, the fixation occurs with the probability $1/N$. It is called the *neutral drift*, meaning the probability that the population become a lineage of a certain individual is one over the size of the population. Since all individual have the same rate of reproduction and death, the chance leave a pedigree to the whole population is $1/N$. If the population contain i of certain type, the fixation of the type will be i/N.

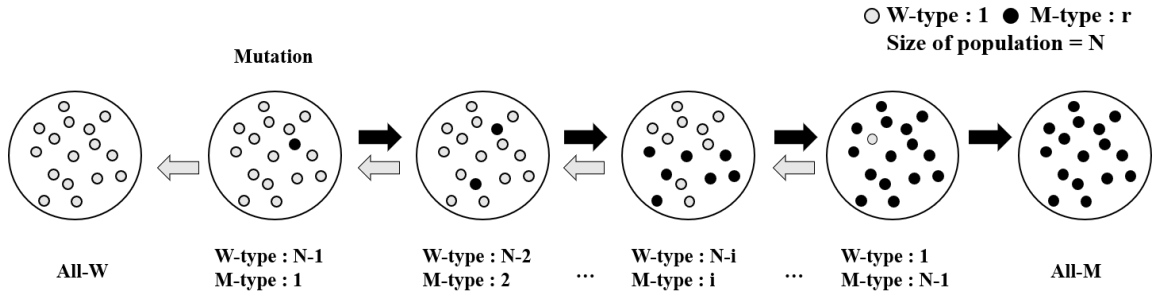

Fig. 3.2 Evolutionary process in a finite population size of N. The initial population were identical until sudden mutation appear with relative fitness r. Through the stochastic drift and selection, population evolve until it reach one of two absorbing states; all-W or all-M. Fixation of mutant occur with the probability, $\rho_M(r,N)$.

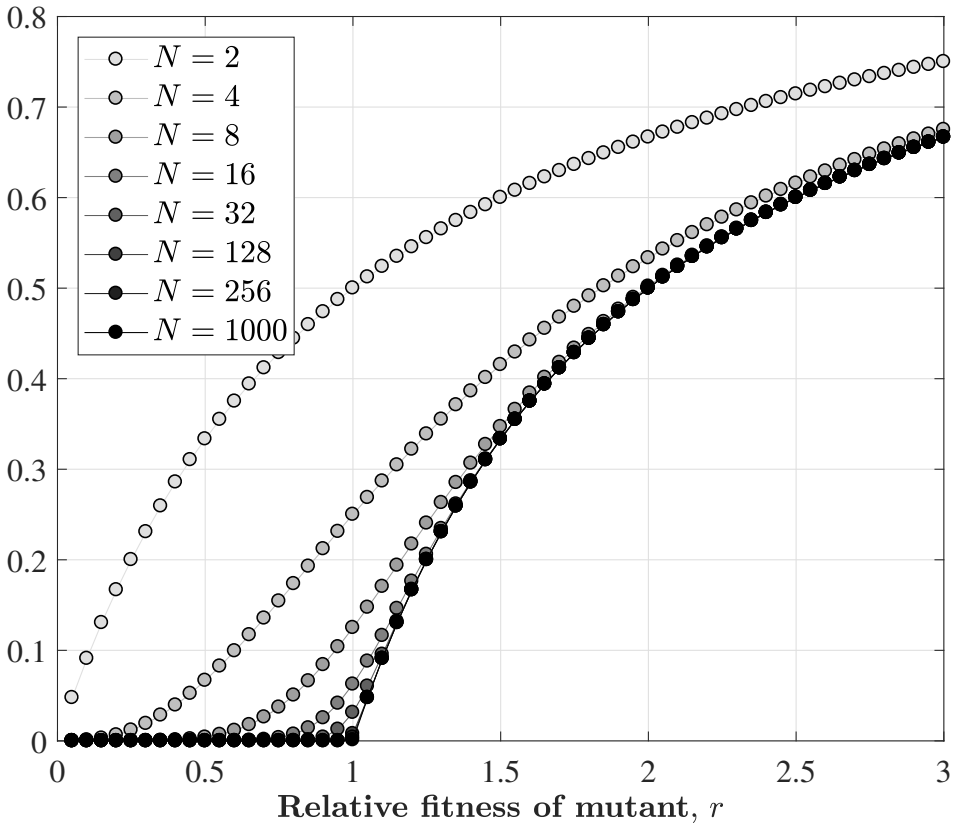

Fig. 3.3 The Moran fixation probability, $\rho_M(r,N)$, as the function of the relative fitness of mutant for each size of population. The Moran fixation probability measure the probability that population taken over by a single mutant of relative fitness r introduced to initial wild-type population. Unlike the deterministic system described by differential equation, the stochastic evolutionary process in finite sized population has the extinction probability for fitter as $1-\rho_M(r,N)$ for $r>1$ and also the fixation probability of inferior for $r<1$. The balance between drift and selection depends on the size of population and the fitness of invader. As the size of population increases, the selection become stronger.

Fixation time

One may wonder how long does the stochastic process take time until the system reach to one of absorbing states. The time is called a *fixation time*. For the case of Moran process, we have three different fixation times. τ_m: The average time until the population system reaches to one of two absorbing states, all-M or all-W from the state m. τ_m^M: The average time until the population system reaches to all-M state from the state m. τ_m^W: The average time until the population system reaches to all-W state from the state m. τ_m is the unconditional fixation time that doesn't consider the final state, while τ_m^M and τ_m^W are the conditional fixation times corresponding final states. Notice that usually the distribution of fixation times broad, depending on the size of population and the relative fitness of mutant type. $\tau_m, \tau_m^M,$ and τ_m^W represent the mean of the broad distributions.

Unconditional fixation time, τ_m: Analogous to the fixation probability, the fixation time have the recurrence relation and the boundary values,

$$\begin{aligned} &\tau_0 = 0 \\ &\tau_m = 1 + T_m^- \tau_{m-1} + (1 - T_m^- - T_m^+)\tau_m + T_m^+ \tau_{m+1} \\ &\tau_N = 0 \end{aligned} \tag{3.29}$$

Introducing the variable, $\zeta_m = \tau_m - \tau_{m-1}$, the recurrence relation can be rewritten as,

$$\zeta_{m+1} = \gamma_m \zeta_m - \frac{1}{T_m^+} \tag{3.30}$$

where $\gamma_m = T_m^-/T_m^+$ again. From the iteration one may yields,

$$\begin{aligned} \zeta_1 &= \tau_1 - \tau_0 = \tau_1 \\ \zeta_2 &= \tau_2 - \tau_1 = \gamma_1 \tau_1 - \frac{1}{T_1^+} \\ \zeta_3 &= \tau_3 - \tau_2 = \gamma_2 \gamma_1 \tau_1 - \frac{\gamma_2}{T_1^+}\frac{1}{T_2^+} \\ &\vdots \\ \zeta_k &= \tau_k - \tau_{k-1} = \tau_1 \prod_{m=1}^{k-1} \gamma_m - \sum_{l=1}^{k-1} \frac{1}{T_l^+} \prod_{m=l+1}^{k-1} \gamma_m \end{aligned} \tag{3.31}$$

Sum over ζ_m, we have,

$$\sum_{k=j+1}^{N} \zeta_k = \tau_{j+1} - \tau_j + \tau_{j+2} - \tau_{j+1} + \cdots + \tau_N - \tau_{N-1} = -\tau_m \tag{3.32}$$

For $m = 1$, we find,

$$\tau_1 = -\sum_{k=2}^{N} \zeta_k = -\tau_1 \sum_{k=1}^{N-1} \prod_{m=1}^{k} \gamma_m + \sum_{k=1}^{N-1} \sum_{l=1}^{k} \frac{1}{T_l^+} \prod_{m=l+1}^{k} \gamma_m \tag{3.33}$$

and thus we have,

$$\begin{aligned} \tau_1 &= \frac{1}{1+\sum_{k=1}^{N-1} \prod_{m=1}^{k} \gamma_m} \sum_{k=1}^{N-1} \sum_{l=1}^{k} \frac{1}{T_l^+} \prod_{m=l+1}^{k} \gamma_m \\ &= \rho_1 \sum_{k=1}^{N-1} \sum_{l=1}^{k} \frac{1}{T_l^+} \prod_{m=l+1}^{k} \gamma_m \end{aligned} \tag{3.34}$$

where, ρ_1 is the fixation probability given by Eq. 3.24. Therefore, the average unconditional fixation time from the state m is given by,

$$\tau_m = -\sum_{k=j+1}^{N} \zeta_k = -\tau_1 \sum_{k=1}^{N-1} \prod_{m=1}^{k} \gamma_m + \sum_{k=1}^{N-1} \sum_{l=1}^{k} \frac{1}{T_l^+} \prod_{m=l+1}^{k} \gamma_m \tag{3.35}$$

Conditional fixation time, τ_m^M: Following Ref. [93], for the conditional fixation time that the population system reach to all-M from the state m start from,

$$\begin{aligned} &\rho_0 \tau_0^M = 0 \times \tau_0^M = 0 \\ &\rho_m \tau_m^M = \rho_{m-1} T_m^- (\tau_{m-1}^M + 1) + \rho_m (1 - T_m^- - T_m^+)(\tau_m^M + 1) + \rho_{m+1} T_m^+ (\tau_{m+1}^M + 1) \\ &\rho_N \tau_N^M = 1 \times 0 = 0 \end{aligned} \tag{3.36}$$

where ρ_m is the fixation probability of m mutant individuals. Denote by $\eta_m^M = \rho_m \tau_m^M$, rearrange above equation, we have,

$$\eta_{m+1}^M - \eta_m^M = \eta_m^M - \eta_{m-1}^M \frac{T_m^-}{T_m^+} - \frac{\rho_m}{T_m^+} \tag{3.37}$$

One can notice that Eq. 3.37 has the identical structure compare to Eq. 3.30. Therefore, using similar iteration as above and using the boundary values, $\eta_0 = 0$ and $\eta_N = 0$, we obtain,

$$\eta_k^M - \eta_{k-1}^M = \eta_m^M \prod_{m=1}^{k-1} \gamma_m - \sum_{l=1}^{k-1} \frac{\rho_l}{T_l^+} \prod_{m=l+1}^{k-1} \gamma_m \quad \text{and} \quad \sum_{k=m+1}^{N} \eta_k^M - \eta_{k-1}^M = -\eta_m^M \tag{3.38}$$

Now we have, for $m = 1$,

$$\tau_1^M = \sum_{k=1}^{N-1} \sum_{l=1}^{k} \frac{\rho_l}{T_l^+} \prod_{m=l+1}^{k} \gamma_m, \tag{3.39}$$

and for general m,

$$\tau_m^M = -\tau_1^M \frac{\rho_1}{\rho_m} \sum_{k=m}^{N-1} \prod_{m=1}^{k} \gamma_m + \sum_{k=m}^{N-1} \sum_{l=1}^{k} \frac{\rho_l}{\rho_m} \frac{1}{T_l^+} \prod_{m=l+1}^{k} \gamma_m. \tag{3.40}$$

Conditional fixation time, τ_m^W: For the conditional fixation time that the population system reach to all-W from the state m, we can obtain from the symmetry argument, in which τ_m^W count the time opposite direction against τ_m^M, from the state $m = N-1$ the fixation time of a single W type,

$$\tau_{N-1}^W = \sum_{k=1}^{N-1} \sum_{l=1}^{k} \frac{\tilde{\rho}_{N-l}}{T_{N-l}^-} \prod_{m=l+1}^{k} \frac{1}{\gamma_{N-m}}, \tag{3.41}$$

where $\tilde{\rho}_{N-l} = 1 - \rho_{N-1}$ and for the general case,

$$\tau_m^W = -\tau_{N-1}^W \frac{\tilde{\rho}_{N-1}}{\tilde{\rho}_m} \sum_{k=(N-m)}^{N-1} \prod_{m=1}^{k} \gamma_{N-m} + \sum_{k=(N-m)}^{N-1} \sum_{l=1}^{k} \frac{\tilde{\rho}_{N-l}}{\tilde{\rho}_m} \frac{1}{T_{N-l}^-} \prod_{m=l+1}^{k} \gamma_{N-m}. \tag{3.42}$$

Rate of evolution

Suppose we have a population size of N. At initial stage the population in equilibrium that all individuals are identical type, W, thus, producing offspring with the same rate. All of a sudden with very rare chance a mutation occur during reproduction. The mutation rate, u, represents the probability that an individual of type W reproduce its offspring as M. What is the required time that this population system totally replaced by a newly introduced mutant type, M? The average rate of mutant appearing from the reproduction of population is Nu, thus the time of mutant occurrence exponentially distributed with the average $1/(Nu)$.

Assume that the newly introduced mutant type M has a relative fitness r compare to the initial population type W. The Moran fixation tells the probability that whole population taken over by the mutant is

$$\rho_M = \frac{1 - 1/r}{1 - 1/r^N}. \tag{3.43}$$

The rate in which a mutation occur is Nu, and the probability that mutant take over the population is ρ. Therefore, the rate of evolution from all-W to all-M is given by,

$$R = Nu\rho \tag{3.44}$$

If introduced mutation is neutral, the fixation reduced to $\rho = 1/N$, and the rate of neutral evolution is given by, $R = u$, where the rate of neutral evolution is simply equals the mutation rate, independent of the population size. This result was derived by Mooto Kimura and is at the center of the neutral theory of evolution. The neutral theory address that the majority of mutations should be neutral. Since advantageous mutations in genes are extremely rare which optimized throughout thousand of thousand generations, pernicious mutations are not able to observe because those have high probability of elimination. Therefore, the majority of mutations in any phylogeny should be neutral [94, 95].

3.2 Evolutionary processes on graphs

Traditional approaches assume that the population is well-mixed, meaning all individuals are in equivalent environment and have identical interaction among them. However, In many of real world observation suggests the importance of interaction patterns which can be captured as a network. Interpretation of a local interaction could be geometrical formation of population, such as the architecture of cells in a multi cellular organism, or geographical distribution of habitation for animal species. Human society is also far from well-mixed population. Such localized interaction limit the competition range of birth and death processes. Our main interest is how the interplay between evolutionary dynamics and the population structure will make differ the outcome of evolutionary processes.

3.2.1 Evolutionary graph theory

Evolutionary graph

To describe the evolutionary process on structured population, we introduce the stochastic matrix, W, which the element of the matrix, w_{ij}, is representing the probability that the offspring of i take over the site of j, with labeling all individuals in the populations as $i = 1,2,\ldots,N$. The matrix, W, is stochastic with following properties:

$$\begin{aligned} 0 \leq w_{ij} \leq 1, \\ \sum_i w_{ij} = 1. \end{aligned} \tag{3.45}$$

The matrix, W, defines a weighted and directed graph and it is called the evolutionary graph [58]. If $w_{ij} > 0$, there is and directed link from node i to j, while if $w_{ij} = 0$, there is no link from i to j. The evolutionary process is now depends on the $N \times N$ matrix $W = w_{ij}$. We can generalize the Moran process in finite sized population as the special case of the complete graph with identical weights, $w_{ij} = 1/N$, for all i, and j.

Temperature of node

A node i in an evolutionary graph has the property, the temperature, T_i, defined by,

$$T_i = \sum_{j=1}^{N} w_{ji}. \tag{3.46}$$

The temperature of node i represents the sum of incoming probability flow of offsprings from its neighbors. If a node, i has a high temperature, it will be changed or updated more offten compare to a node has a low temperature.

Isothermal theorem

If all nodes in the evolutionary graph have identical temperature, then a graph is isothermal, in the sense that all nodes in a graph equally likely 'hot' likewise the concept of isothermal state of an object at the thermal equilibrium in the thermodynamics. The isothermal graph have the property that the fixation probability of the evolutionary dynamics on it same as the fixation probability of the Moran process of the same size [58].

Theorem: "a graph is fixation equivalent to the Moran process if and only if it is isothermal"

Let describe the configuration of a population using a binary vector, $\vec{s} = (s_1, s_2, \ldots, s_N)$, where s_i denote the type of population as $s_i = 0$ for the wild type, and $s_i = 1$ for the mutant type. Then the number of mutant type is given by $m = \sum_i s_i$. The probability of increasing one and decreasing one mutant type from the state m is given by,

$$\begin{aligned} T_m^+ &= \frac{r\sum_i s_i}{rm+N-m}\sum_j w_{ij}(1-s_j) = \frac{r\sum_i\sum_j w_{ij}s_i(1-s_j)}{rm+N-m} \\ T_m^+ &= \frac{\sum_i(1-s_i)}{rm+N-m}\sum_j w_{ij}s_j = \frac{\sum_i\sum_j w_{ij}(1-s_i)s_j}{rm+N-m} \end{aligned} \tag{3.47}$$

If the ratio, $\gamma_m = T_m^-/T_m^+$ on a given evolutionary graph is identical to the ratio from the Moran process, $\gamma_m = 1/r$, the fixation probability of the mutant with the relative fitness r on the graph will be the Moran fixation. The condition is satisfied, if,

$$\sum_i\sum_j w_{ij}s_i(1-s_j) = \sum_i\sum_j w_{ij}(1-s_i)s_j \tag{3.48}$$

for any configuration of $\vec{s}$. Especially, for all configuration with, $s_k = 1$, $s_i = 0$, $i \neq k$ the equality in Eq. 3.48 must be held. In such cases,

$$\sum_j w_{kj} = \sum_j w_{jk}, \quad \text{for all} \quad k \tag{3.49}$$

By definition, $\sum_j w_{kj} = 1$, and we have, $\sum_j w_{jk} = 1$. Therefore, if the matrix of evolutionary graph, W, is doubly stochastic, the graph is isothermal and the fixation probability on that graph identical to the Moran fixation. Examples of isothermal graphs are represented in Fig. 3.4. In particular, a symmetric graph, where $w_{ij} = w_{ji}$ for all i, and j is isothermal. A circulating graph, where $\sum_{j=1}^N w_{kj} = \sum_{j=1}^N w_{jk}$ for all k meaning that the incoming and outgoing weight is identical for all nodes, is also isothermal graph.

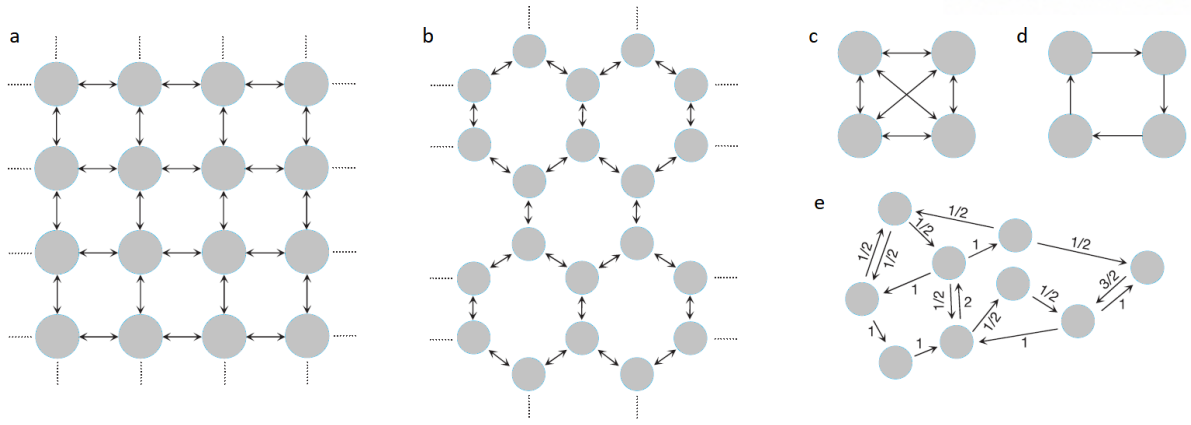

Fig. 3.4 Examples description of the isothermal graphs. (a) and (b) the lattice of k=4 and k=3. (c) Well-mixed graph size of $N = 4$ (d) and (e) are examples of the circulation graphs, where the graph such that the inflow and outflow of the directed replication rate is same at all vertexes. Figure adopted from ref [58].

3.2.2 Selection amplifier, suppressor

Moreover, of particular interest are two specific classes of graphs, namely selection amplifiers and selection suppressors. A graph, G, is called an amplifier of selection, if superior mutants $(r > 1)$ have a higher fixation, $\rho_M^G(r) > \rho_M^{Moran}(r)$ and mutants with lower fitness $(r < 1)$ have a lower fixation, $\rho_M^G(r) < \rho_M^{Moran}(r)$ compared to the Moran fixation, on this graph. Some examples for amplifiers of selection are given in [58], e.g. the star, the superstar or the funnel.

The mechanism of selection amplifier could be understood as follows. Let consider a star graph. In case of star graph, most of the seed mutant appear one of leaf node. At the beginning the mutant-type has very low probability for giving birth but the death-probability is much lower than that. Since the death of the seed mutant requires two event at the same time which are the birth of the wild-type at the center and chosen for being replaced. Therefore, the seed mutant survive with high probability and when it chosen for giving birth it send its offspring to the center. The spread of mutant to other leaf node happens if luckily when the center node chosen for the birth with the mutant type. As increasing the number of mutant among the leafs the probability that the center has the mutant type will be higher. So finally the mutant type takeover the population. Superstar is double layered star graph, so the amplification of selection get stronger. However, If the seed placed at the center node, it will more likely replaced by wild-type offspring since the center is "hot" spot but the chance that the seed mutant appear at the center is very low.

Conversely, a graph, G, is called a selection suppressor, if, compared to the Moran fixation probability, advantageous mutants $(r > 1)$ have a lower fixation $\rho_M^G(r) < \rho_M^{Moran}(r)$ and disadvantageous mutants $(r < 1)$ have a higher fixation probability $\rho_M^G(r) > \rho_M^{Moran}(r)$ on this graph. Examples for suppressors of selection are mostly source and sink populations, such as one-rooted graphs or hierarchical tissues. In

such cases there is no chance that the seed takeover the population unless it appear the root. Therefore, regardless the relative fitness, selection is suppressed.

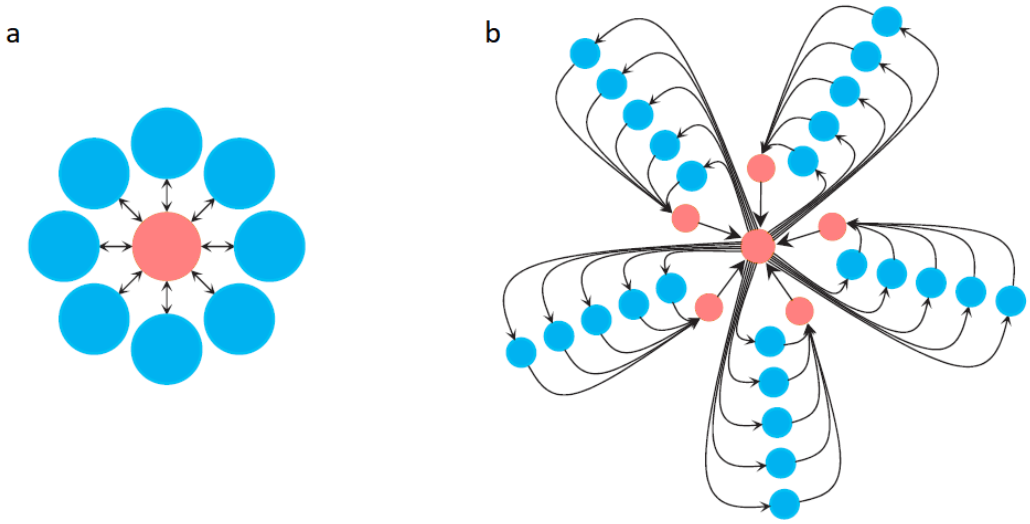

Fig. 3.5 Examples the selection amplifier. (a) Star and (b) the super-star. On the star graph, most of the seed mutant appear one of leaf node. At the beginning the mutant-type has very low probability for giving birth but the death-probability is much lower than that. Since the death of the seed mutant requires two event at the same time which are the birth of the wild-type at the center and chosen for being replaced. Therefore, the seed mutant survive with high probability and send its offspring to the center when the chance has come. The spread of mutant to other leaf node happens if luckily when the center node chosen for the birth with the mutant type. As increasing the number of mutant among the leafs the probability that the center has the mutant type will be higher. So finally the mutant type takeover the population. Superstar is double layered star graph, so the amplification of selection get stronger. Figure adopted from [58].

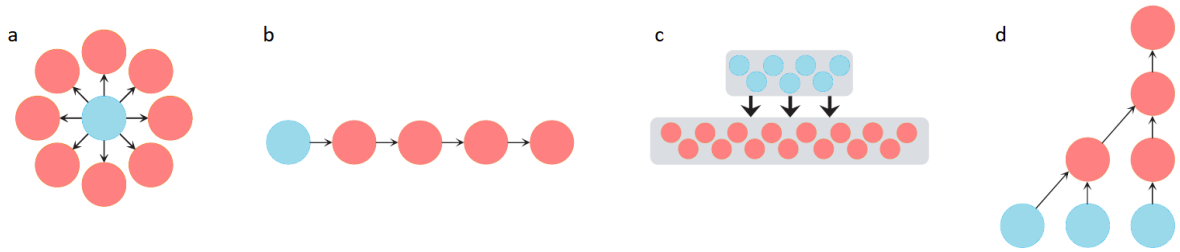

Fig. 3.6 Examples the selection suppressors. From (a) to (d) there is the 'frozen' node that never be replaced by others in terms of the temperature. Unless the invasion started at those spot the population never be taken over by newly introduced mutant. Figure adopted from [58].

3.3 Interplay between evolutionary dynamics and population structure

So far we have looked the overview of the evolutionary graph theory which classifying structured populations into three categories, the isothermal graph, the selection amplifier and the selection suppressor. Introducing limited interaction pattern among individuals in a population changed the possibilities that by whom an individual will be replaced from every one can be replaced by anyone. The theory, however, is valid only for the Moran process in which the sequence of the update rule is "birth-death" and the limited interaction localized the death part. We investigated the interplay between flipped order dynamics, which is the death-birth, and structured population. In this case, the competition for giving birth is localized.

3.3.1 Birth-death vs. Death-birth

Compare to the birth-death, in the death-birth process we choose one of individual among a population in random for the death and the next we choose another individual proportional to its fitness for the birth. In the well-mixed population flipping order of the dynamics doesn't change the ratio of transition probabilities, $\gamma_m = T_m^- / T_m^+$. Since, we have,

$$\begin{aligned} T_m^+ &= \text{Death of wild} \times \text{Birth of mutant} &&= \frac{N-m}{N} \times \frac{mr}{rm+N-m}, \\ T_m^- &= \text{Death of mutant} \times \text{Birth of wild} &&= \frac{m}{N} \times \frac{N-m}{rm+N-m}. \end{aligned} \tag{3.50}$$

However, if we restrict the self replacement which the dead individual cannot chosen for the birth, the transition probabilities are,

$$\begin{aligned} T_m^+ &= \frac{N-m}{N} \frac{mr}{rm+N-m-1}, \\ T_m^- &= \frac{m}{N} \frac{N-m}{r(m-1)+N-m}. \\ \gamma_m^{DB} &= \frac{1}{r} \frac{mr+N-m-1}{(m-1)r+N-m} \end{aligned} \tag{3.51}$$

The corresponding fixation probability of the death-birth process is given by,

$$\rho_M^{DB} = \frac{1}{1+\sum_{k=1}^{N-1} \prod_{m=1}^{k} \gamma_m^{DB}} = \frac{N-1}{N} \frac{1-1/r}{1-1/r^{N-1}}. \tag{3.52}$$

As we can see if the size of the population get larger, $N \to \infty$, the fixation probability of the death-birth will converge to the fixation probability of the Moran process, $\rho_m^{DB} \to \rho_m^{Moran}$. However, when the size of the population is small the difference is not ignorable.

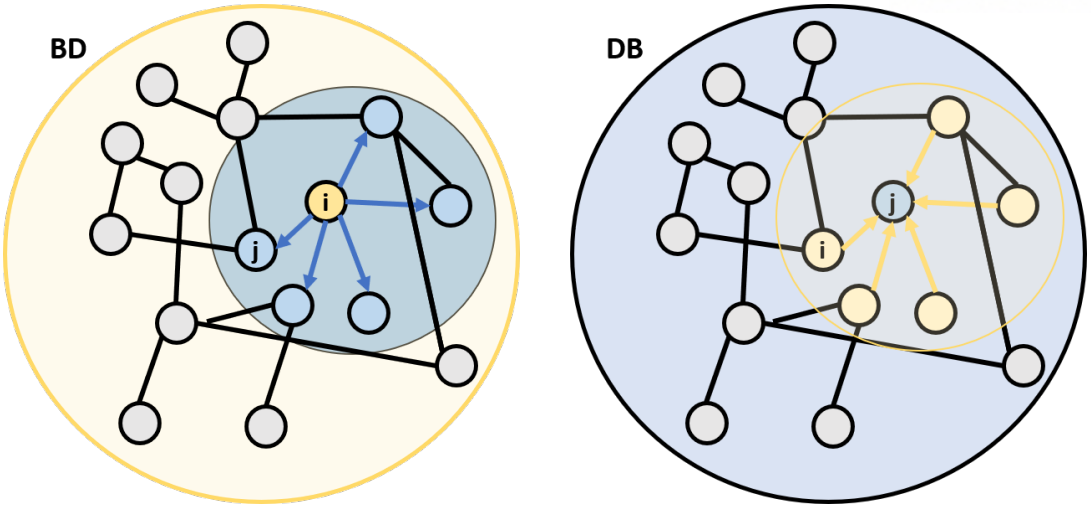

Fig. 3.7 Schematic representation of the global and the local competition under the birth-death (left) and the death-birth (right). The domain of yellow and blue represent the competition pool for the reproduction and the death, respectively. Under the birth-death i send its offspring to j with the probability, w_{ij}, when it chosen for reproduction. In case of the death-birth, the probability that i achieve the evolutionary success for the node j is proportional to its fitness, f_i when individual at node j is chosen for the death.

3.3.2 Results

Fixation probabilities

To confirm how the flipping order of the dynamics changes the behavior of selection on the structured population we performed the numerical simulations of the selection dynamics on the set of structured populations. First, Fig. 3.8 and shows the fixation probabilities on simple graphs. As we confirmed from the analytic form of the fixation probability of death-birth (DB), ρ_m^{DB} is lower than the fixation of birth-death (BD), ρ_m^{BD} even in the well-mixed. The gap between the fixation probabilities are independent from the size of the population that we used, which are $N = 25, 49, 100$. The set of isothermal graphs, the well-mixed, the ring, and the lattice return the Moran fixation under the BD while under the DB the selection of mutant suppressed relatively. Especially in case of the star structure, which is the selection amplifier under the BD, totally suppressed the selection of mutant even with high relative fitness $r \sim 2.5$.

In case of the generalized structures with the degree-heterogeneity and the degree-mixing also the selection is suppressed under the DB as shown in Fig. 3.10 (a),(c), and (e). The effect of the degree-heterogeneity under the DB turned out as the more heterogeneous, the more suppressed. Interestingly, the effect of the degree-mixing is not significant, but under the BD negatively degree-mixed structures enhance the selection of mutant while under the DB the effect is opposite. Why under the death-birth dynamics the selection is suppressed on structured populations and why the effect of the degree-mixing is not aligned?

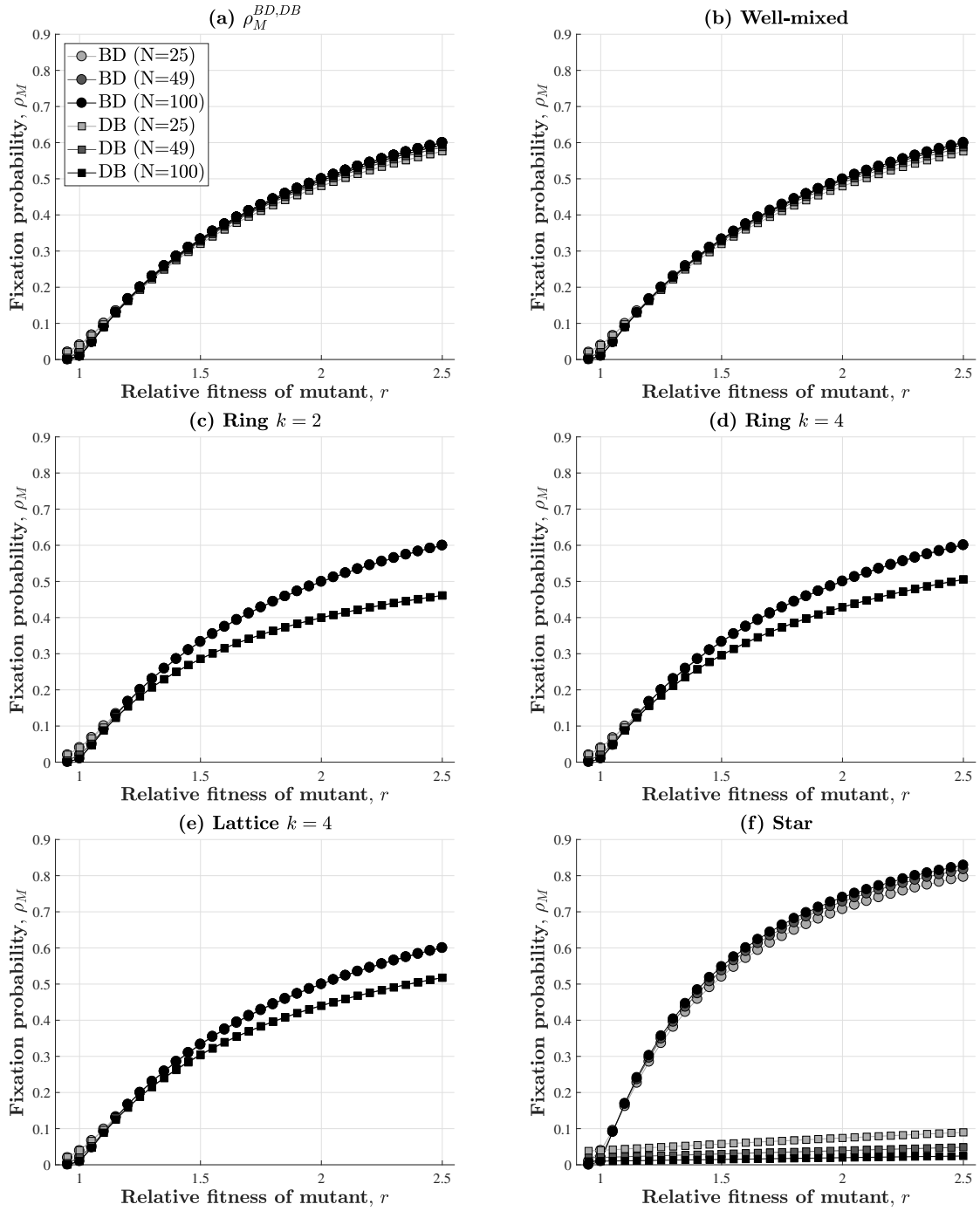

Fig. 3.8 The fixation probability of single mutant on simple graphs under the birth-death (BD) and the death-birth (DB) dynamics as a function of the relative fitness of invading mutant, r. As increasing r, the gap between ρ_M^{BD} and ρ_M^{DB} increases from all tested structures. The isothermal graphs under the Moran processes no longer have same fixation probability compare to well-mixed population. Of particular interests, the star graph, (f) the amplifier under the BD become the suppressor under the DB.

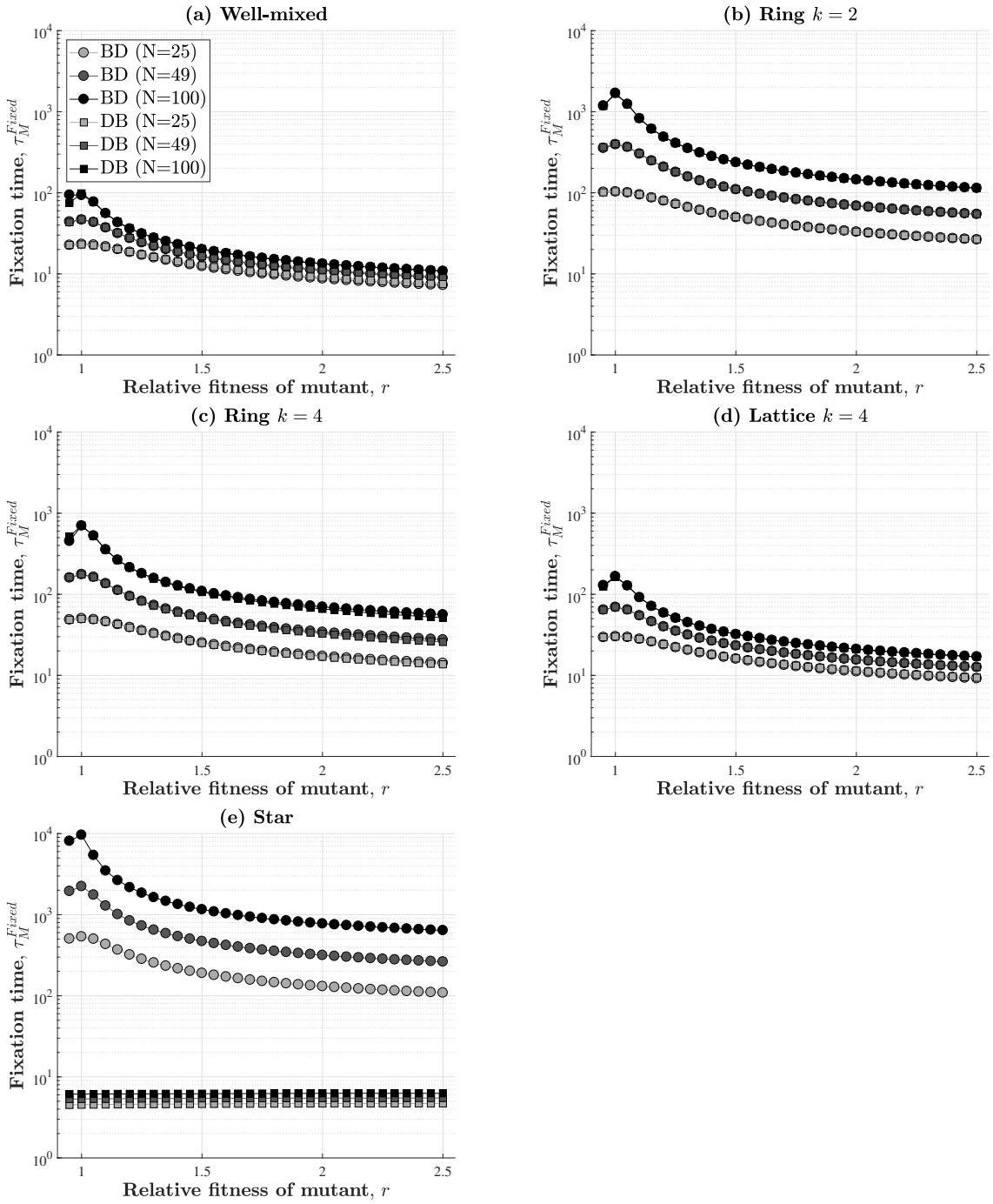

Fig. 3.9 The conditional fixation time, τ_M^{Fixed}, on simple graphs from the birth-death (BD) and the death-birth (DB) dynamics as a function of the relative fitness of invading mutant. The time represented in the scale of the Monte-Carlo step(τ_M/N). The fixation time is size dependent. Results represent that the difference in τ_M under the BD and DB on structured population are ignorable except the star graph. In case of the star the fixation time very long under the BD while very short under the DB.

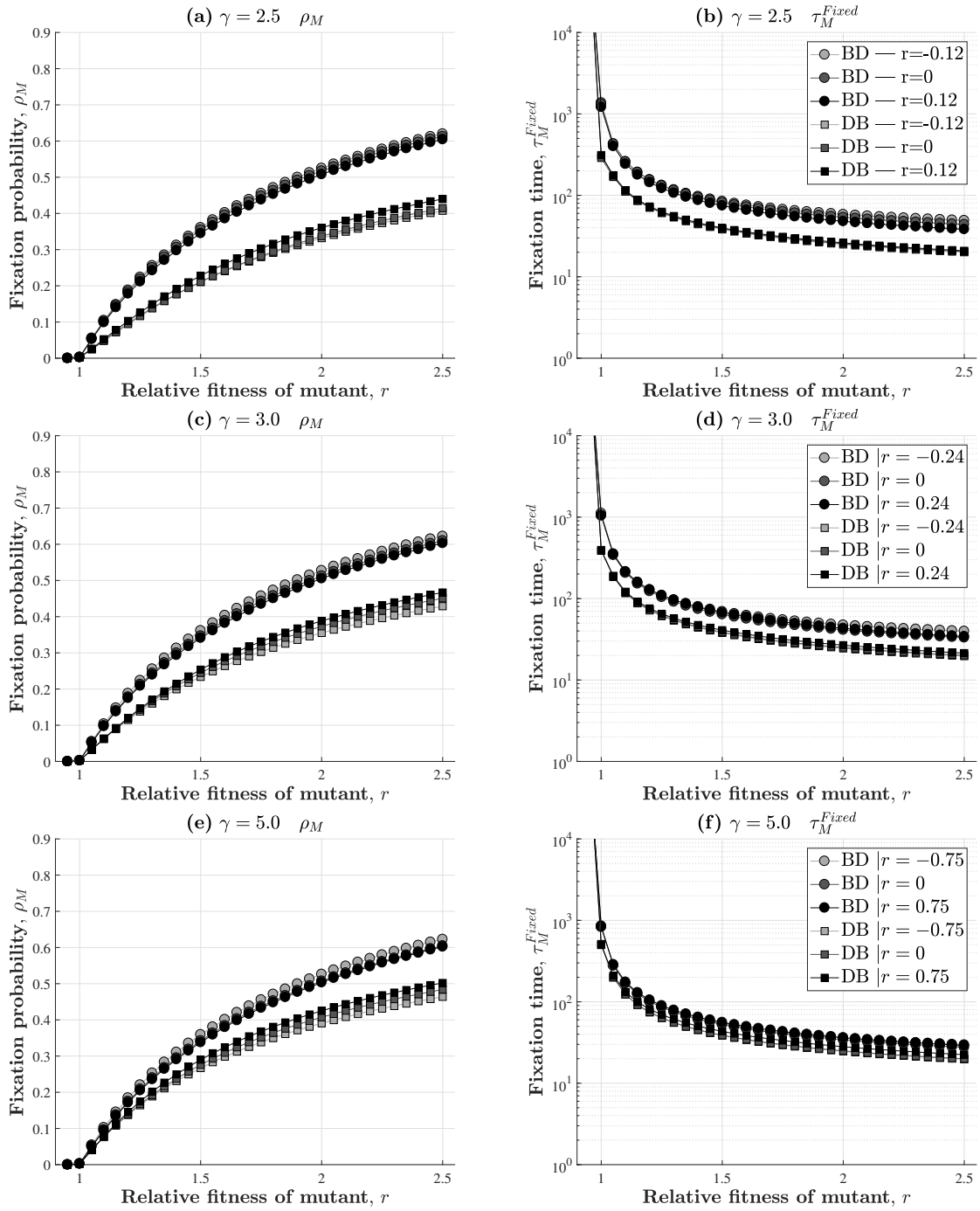

Fig. 3.10 The fixation probability, ρ_M and the conditional fixation time, τ_M^{Fixed} from a single mutant under the BD and the DB on structured populations of each level of the degree-heterogeneity and the degree-mixing. The gap between ρ_M^{BD} and ρ_M^{DB} is slightly increased as the degree-heterogeneity increased. The degree-mixing affect on the fixation as following. Under the BD, the negatively degree-mixed pattern slightly increases the selection of mutant while the positively correlated pattern suppresses. Under the DB the effect is opposite.

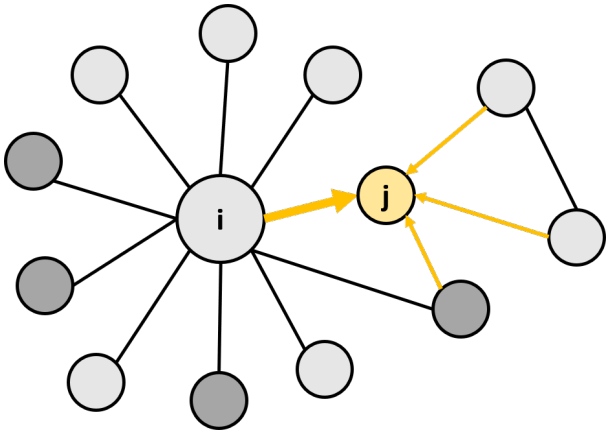

Fig. 3.11 The diagram of influence of node. When individual j is death its neighbors join the competition for giving birth. The evolutionary success of individual i is proportional to the fitness. The sum over the potential probability that the individual i achieve the evolutionary success for spots of its neighbors at each time step defined as the influence of i.

Flipped order of the dynamics changed the scale of the competition in each time step as shown in Fig. 3.7. Under the brith-death, The competition pool for the reproduction is global but the death of an individual only possible when one of its neighbor selected for reproduction, in which it is localized. The temperature of a node, T_i, defined as Eq. 3.46, captures which node is more often being replaced by its neighbors. If the temperature of a node is high, the spot will be chosen more often for the death. However, in case of the death-birth process, the chance of the death is equivalent to every individuals as $1/N$. Therefore, there is no more "hot" or "cold" spot.

Influence of node

Instead, the globalized pool of death utilized as the structural advantage of reproduction for a highly connected individual while it is disadvantage for a less connected individual. That is because, a highly connected individual will have more chance to join a competition for reproduction, since, a competition for reproduction happens when one of its neighbor is dead, and the probability that one of neighbor is selected for the death proportional to the degree, k. At the same time, a competition for reproduction is limited only for the nearest neighbors of the empty site.

To capture this structural inequality we defined the *influence of a node* for the death-birth dynamics. Contrary to the temperature of a node from the evolutionary graph theory, the influence of a node measure the capability of evolutionary success at each time step. The evolutionary success of an individual i occur when i is selected for reproduction at that local competition. Therefore, the influence of an individual i can be formulated as the sum of the probabilities that i become a winner at each local competition, which i potentially participating.

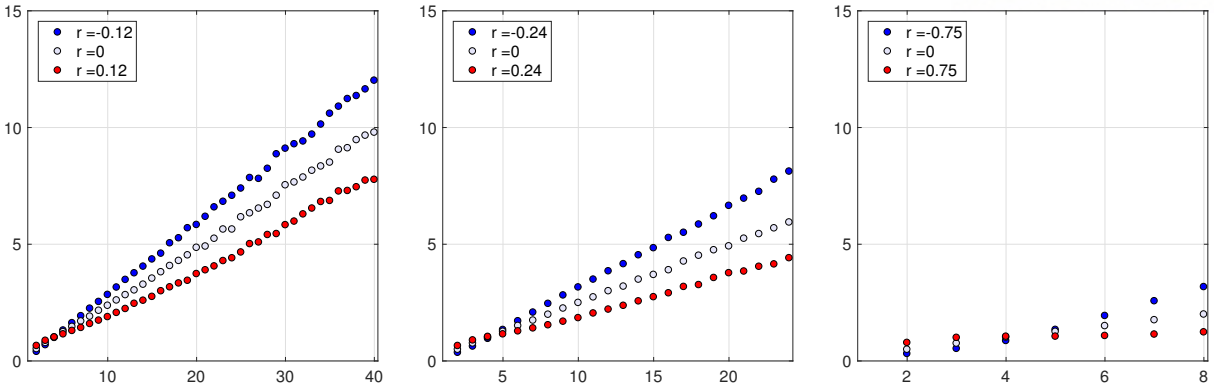

Fig. 3.12 Averaged influence for the neutral selection as function of the degree of node, $\langle I(k)\rangle$ from each level of the degree-heterogeneity (from left to right, $\gamma = 2.5, 3.0, 5.0$) and the degree-mixing. $\langle I(k)\rangle$ is identical to $\langle T(k)\rangle$ under the neutral selection. Figure obtained from the network ensemble of $N = 400$, $\overline{k} = 4$ independently generated 200 samples.

Denote by f_i the fitness of i, and $\mathbf{N_i}$ the neighbors of i, we define the influence of a node i as,

$$I_i = \sum_{j \in \mathbf{N_i}} \frac{f_i}{\sum_{l \in \mathbf{N_j}} f_l} \tag{3.53}$$

In case of the neutral selection, the influence of node i reduced to,

$$I_i = \sum_{j \in \mathbf{N_i}} \frac{1}{k_j} = \frac{k_i}{H_{k_j \in N_i}} \tag{3.54}$$

where, $H_{k_j \in N_i}$ is the harmonic mean over degrees of i's neighbors. Interesting point is that the temperature of node defined in Eq. 3.46 also reduced to the identical form when we consider undirected and unweighted graphs.

$$T_i = \sum_{j \in \mathbf{N_i}} w_{ij} = \sum_{j \in \mathbf{N_i}} \frac{1}{k_j} = \frac{k_i}{H_{k_j \in N_i}} \tag{3.55}$$

Fig. 3.12 is showing the influence of structured population under the neutral selection. We can notice that the influencer under the DB process is the hot spot under the BD process from the relation between the temperature and the influence of node.

Based on understanding of the influence of node, now we can argue about the results from the star graph. In case of the star the center node is hot spot under the BD, meaning that it is influencer under the DB. Unless the seed mutant placed at the center node the evolutionary success of mutant is very difficult under the DB, since, the center node monopolize reproduction whenever its neighbor is dead and even the competition for the center spot occur, the evolutionary success of mutant at leaf is very rare, because the scale of competition for the center is global $(N-2)$. Therefore, the star structure is the selection suppressor under the DB.

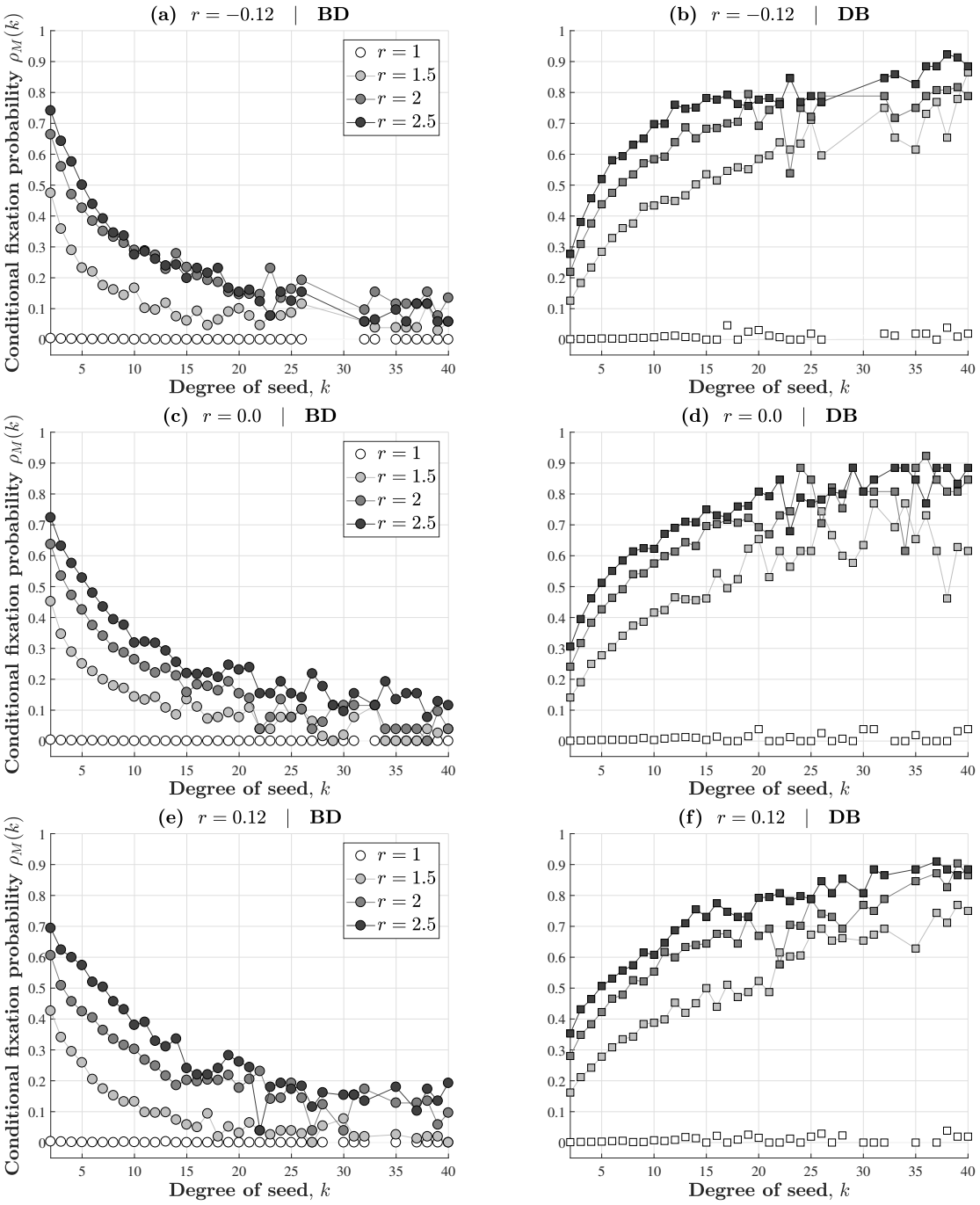

Fig. 3.13 The conditional fixation probability as the function of the degree of seed, k_{seed}, $\rho_M(k)$ on structured populations with $\gamma = 2.5$, and each level of degree-mixing. Under the BD the fixation probability inversely proportional to the degree of seed, $\rho_M(k)^{BD} \propto 1/k$ while under the DB, $\rho_M(k)^{BD} \propto k$. Figure obtained from 10^5 of simulations on 10 independently generated network samples, size of $N = 400$, with $\overline{k} = 4$.

The star graph is the typical extreme case. Expanding similar logic to the results from the degree-heterogeneous and the degree-mixed populations, we can observe the seed effect. Fig. 3.13 represent the conditional fixation probability, $\rho_M(k)$, when the degree of seed mutant was k under the BD and DB for networks of each level of degree-mixing with the degree-exponent $\gamma = 2.5$. Under the BD process the fixation of mutant more likely to occur when the seed placed lower degree nodes. Since the temperature of node is proportional to the degree, we could expect the survival of invading mutant is easier with lower degree in the degree-heterogeneous structure. Contrarily, under the DB the evolutionary success of mutant proportional to the degree of seed. We could confirm from the results that the utilized structural advantage of reproduction to highly connected individual outperform other causes. Consequently, the inequality between fixation probabilities on structured populations, $\rho_M^{BD} > \rho_M^{DB}$, is because of the majority of low-degree nodes in the degree-heterogeneous structures.

Fixation times

Of particular interest we also examined the fixation time on the structured populations. Fig. 3.9 and 3.10 (b),(d), and (f) shows the averaged conditional fixation time, τ_M^{Fixed}, on each characterized structures. Structures in the class of isothermal graphs the fixation times were longer commonly compare to the well-mixed population. Under the DB the fixation times are same. In case of the star graph, the fixation time is longest under the BD and shortest under the DB. The set of population structure characterized with the degree-heterogeneity and the degree-mixing represent not much differences across the structural character, however the fixation take longer under the BD than under the DB.

How does the fixation time has meaning in the evolutionary dynamics? If the fixation time is longer than the rate of mutation the rate of evolution no more same as the rate of mutation as we discussed in previous section. Since the rate of evolution assumes that the scale of the fixation time is much smaller than the scale of the inverse rate of mutation. In our simulation, we restricted situation that no mutation occur during the dynamics but if the fixation take longer than the time of mutant appearance, during the selection dynamics one can expect the other mutation. Therefore, further investigation on the effect of structured population on the fixation time and the rate of evolution could be worth.

3.4 Summary

In summary, we have looked the overview of the evolutionary dynamics from the traditional perspective to the interplay between the microscopic dynamics and the limited interaction of populations.

Compare to the Moran process as the standard of the selection dynamics, the structured population can be classified into three classes, the isothermal graph, the selection amplifier, and the selection suppressors. Isothermal theorem provide the analytic tool to distinguish a population structure whether the fixation probability of a given graph will be identical to the Moran fixation or not. The temperature of node identifies the spot which more likely to be replaced of a given graph. Significantly, the selection amplifiers commonly have the hot spots and the selection suppressors have the node of zero temperature.

We examined the death-birth dynamics which has the opposite sequence compare to the traditional Moran process. Flipped order of the dynamics changed the domain of competition at each step, the death and the birth, in return, under the DB isothermal graphs have suppressed fixation probability than the well-mixed. As the special example, in case of the star graph, one of the selection amplifier, became the selection suppressor under the DB. From the set of characterized populations in terms of the degree-heterogeneity and the degree-mixing, also the fixation of mutant suppressed by the flipped Moran process.

Under the DB the temperature of node is meaningless. Instead the influence of node measure the potential capability of an individual's reproduction success under the DB. Interplay between the DB and limited interaction in return the structural advantage of reproduction for highly connected individuals. Consequently under the DB the evolutionary success of mutant more likely happens when the seed has higher degree while under the BD it is inversely proportional to the degree of seed.

Chapter 4

Evolution of Cooperation on Structured Populations

4.1 Introduction

Game Theory was formulated to study human behavior and economic decision making by J. von Neumann and O. Morgenstern [96]. It is a suit of mathematical models of strategic interaction between rational decision makers and has been applied not only to the subfields of social science but also to logic and computer science. The traditional game theory concerns the behavior of two game players who try to maximize their payoff in a game by choosing either cooperation or defection without knowing the counterpart's strategy.

The evolutionary game dynamics, combination of the evolutionary dynamics and the game theory, was developed to address the seeming paradox of the ubiquity of cooperation in the biosphere [10]. In the evolutionary game theory, we considers a population of individuals interacting via a game with fixed strategies rather than reasonable choice. An individual in a population plays a game with another individual at a time and gets payoffs from the games witheach of the neighbors. The accumulated payoff of an individual determines the *fitness*, a measure of success in reproducing the offsprings. One who has higher payoff will reproduce more offsprings compared to the one with a lower payoff. Therefore, success in the game represents the success of reproduction.

Cooperation or altruism is, however, a behavior that provides benefits to others at his/her own cost. On the other hand, a defector dose not provide any benefit to the counterpart but seeks a chance of exploitation. Thus, it is trivial that cooperation is not favored in the natural selection since cooperators always have lower fitness than defectors [90]. However, cooperation exists in nature and human society in various forms [97–99, 15, 100].

4.1.1 Frequency-dependent selection

Unlike in the evolutionary dynamics, in this situation the fitness of an individual is not a constant, but depends on the fraction of individuals playing game with one of two strategies. Let consider we have population consists of individuals playing one of two strategies, say A and B. The strategy of an individual is fixed. Individuals interact each other equaly likely, meaning population is well-mixed. Fitness of an individual is given by the sum of all payoffs from games played with others.

Corresponding payoff given by the *payoff matrix* Eq. 4.1. For the simplest game with two strategies, we have 4 combinations of strategies, thus payoff matrix is 2×2 matrix. If A meets A, both get a. If B meets B, both get b. If A meets B, A gets b and B gets c.

$$\begin{array}{c} \\ \mathrm{A} \\ \mathrm{B} \end{array} \begin{array}{c} \begin{array}{cc} \mathrm{A} & \mathrm{B} \end{array} \\ \begin{pmatrix} a & b \\ c & d \end{pmatrix} \end{array}. \tag{4.1}$$

When the fraction of A individuals in population is x_A and for B is x_B, the expected fitness for type A, f_A and B, f_B is given by,

$$\begin{aligned} f_A &= ax_A + bx_B \\ f_B &= cx_A + dx_B \end{aligned} \tag{4.2}$$

Now we have the selection dynamics for the population of A and B which is given by,

$$\begin{aligned} \dot{x_A} &= x_A[f_A(\vec{x}) - \phi] \\ \dot{x_B} &= x_B[f_B(\vec{x}) - \phi], \end{aligned} \tag{4.3}$$

where $\vec{x} = (x_A, x_B)$ and $\phi = x_A f_A(\vec{x}) + x_B f_B(\vec{x})$, the average fitness. Since $x_A + x_B = 1$, represeting $x = x_A$ system reduced to,

$$\dot{x} = x(1-x)[f_A(x) - f_B(x)] \tag{4.4}$$

Plug the fitness function into the Eq. 4.4, we have,

$$\dot{x} = x(1-x)[(a-b-c+d)x + b - d]. \tag{4.5}$$

The behavior of the system can be classified into five catagories depending on the order relation of the elements in the payoff matrix.

- **A dominates B**: If $a > c$ and $b > d$, the average fitness of A always surpass that of B for any composition of the population. Selection will guide the system to the state the whole population consist of A.

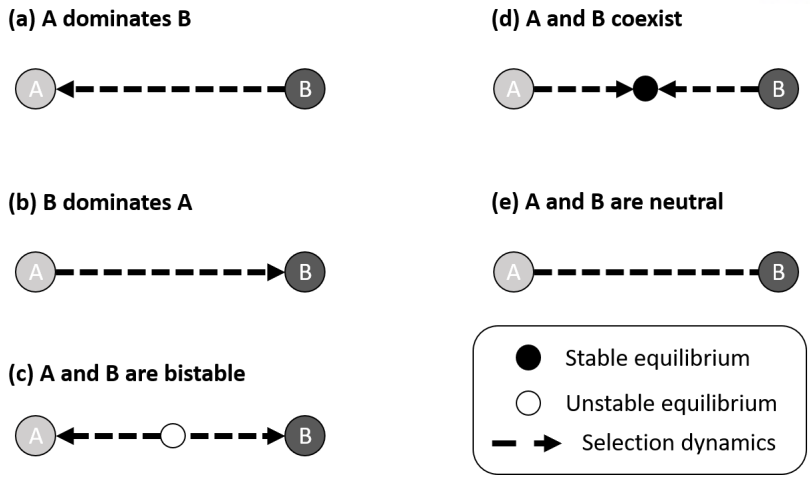

Fig. 4.1 Five possibilities of frequency dependent selection with two strategies. The ranking of entries in payoff matrix decide behaviors of the given system.

- **B dominates A**: As the opposite case to above, If $a < c$ and $b < d$, B will dominates A.
- **A and B are bistable**: In case of $a > c$ and $b < d$, A is the best against A and B is the best against B. The unstable equilibrium point, x^* is given by,

$$x^* = \frac{d-b}{a-b-c+d} \tag{4.6}$$

  The destiny of the system depends on the initial condition, if $x(0) < x^*$, system will converge to all-B, and if $x(0) > x^*$ it will converge to all-A.

- **A and B coexist**: If $a < c$ and $b > d$, the best strategy for an individual always the opposite strategy against partner. In this case the system will converge to the stable equilibrium, x^*, given by Eq. 4.6.
- **A and B are neutral**: If there is no difference between playing A or B, the system simply reduced to the neutral. Whatever the initial composition was, it will be not changed, therefore, any mixture of A and B can be an equilibrium.

The dynamics, Eq. 4.3, that we used to describe behavior of population with a game is called *the replicator dynamics* [101–103]. In general we can expand the dynamics with n strategy game.

4.1.2 Evolutionary stable state

The evolutionary stable strategy an important concept liked with the replicator dynamics, invented by J. Maynard Smith [11]. Suppose we have a large population of individuals with strategy A. At certain time point a single mutant with strategy B introduced. Then the game between A and B is given by the payoff matrix (4.1). We may ask the condition for selection to oppose the invasion of B into the population of A.

A single mutant of B in a large population considered as infinitesimally small, express the fraction of B as ε. The fraction of A then $1-\varepsilon$. The Fitness for each A and B is given by,

$$\begin{aligned} f_A &= a(1-\varepsilon)+b\varepsilon \\ f_B &= c(1-\varepsilon)+d\varepsilon \end{aligned} \tag{4.7}$$

Therefore A outcompete B if the fitness of A is greater than the fitness of B, $f_A > f_B$ and we have,

$$a(1-\varepsilon)+b\varepsilon > c(1-\varepsilon)+d\varepsilon \tag{4.8}$$

cancelling ε inequality reduced to,

$$a > c \tag{4.9}$$

However, if $a = c$, inequality leads to,

$$b > d. \tag{4.10}$$

Therefore, strategy A is ESS if either (i) $a > c$ or (ii) $a = c$ and $b > d$. The definition ensures that selection will block the invasion of B into the population of A.

Nash Equilibrium

For any given game, or technically for a corresponding payoff matrix, there is an equilibrium point as the result of reasonable choice of players, that is the *Nash equilibrium*, the concept of the Nobel prize winner, J.F. Nash [104]. Suppose we have two individual and each individual can take one of two strategies. Again, employ the general 2×2 payoff matrix (4.1), the Nash equilibrium defined by following criteria:

- A is a strict Nash equilibrium if $a > c$.
- A is a Nash equilibrium if $a \geq c$.
- B is a strict Nash equilibrium if $d > b$.
- B is a Nash equilibrium if $d \geq b$.

If both players play a strategy correspond to a Nash equilibrium, any of two cannot escape from that strategy and increase payoff. Suppose the strategy A is a strict Nash equilibrium. Then the strategy is also ESS. In case of $a = c$ and $b > d$, the second criteria that the strategy A is ESS, A is a Nash equilibrium.

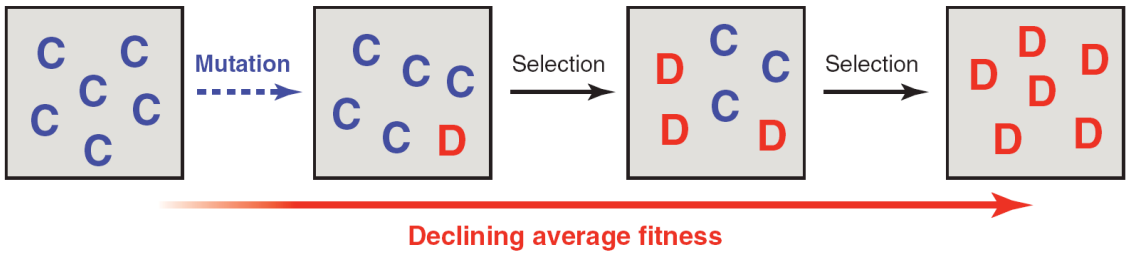

Fig. 4.2 Defectors are favored in natural selection. In a mixed population, defectors, D, always have a higher payoff than cooperators, C. Therefore, the population of Cs are reduced continuously until they are extinct. Figure adopted from [8].

4.1.3 Prisoner's dilemma

The game mostly employed for studying evolution of cooperation is the Prisoner's dilemma game. The payoff matrix for the Prisoner's dilemma is given by,

$$\begin{array}{cc} & \begin{array}{cc} \mathrm{C} & \mathrm{D} \end{array} \\ \begin{array}{c} \mathrm{C} \\ \mathrm{D} \end{array} & \begin{pmatrix} b-c & -c \\ b & 0 \end{pmatrix}. \end{array} \tag{4.11}$$

For each game, a cooperator pays a cost, c. Playing against cooperator earn a benefit, b. Thus, a cooperator playing against a cooperator earn $b-c$, a defector playing against a cooperator earn b and mutual defection earn nothing. In the Prisoner's dilemma, defection is a strict Nash equilibrium.

The Prisoner's dilemma game captures the essential problem of cooperation. Mutual cooperation will earn higher payoff compare to mutual defection, however, defection against cooperation can have the highest payoff. Therefore cooperation is not rational which is the dilemma.

4.1.4 Five mechanisms for the evolution of cooperation

If we plug in the Prisoner's dilemma game into the evolutionary game dynamics the selection always favour defection rather than cooperation, therefore, without any mechanism cooperation cannot survive. However, there are five known rules that cooperation can be favoured [90], which are the kin selection, the direct reciprocity, the indirect reciprocity, the group reciprocity, and the network reciprocity. About the network reciprocity, we will discuss in the next section.

Kin selection

Idea of kin selection is that cooperation can be favored if the two individual of a cooperative act are genetic relatives. Assume a population where the average of relatedness among individuals is r, which representing the probability of sharing the same gene. From the concept of inclusive fitness there is

additional payoff to relatives which the payoff for its donner multiplied by r. Based on the idea we have the modified payoff matrix

$$\begin{array}{c} \\ \mathrm{C} \\ \mathrm{D} \end{array} \begin{array}{c} \begin{array}{cc} \mathrm{C} & \mathrm{D} \end{array} \\ \begin{pmatrix} (b-c)(1+r) & br-c \\ b-rc & 0 \end{pmatrix} \end{array}. \tag{4.12}$$

Now, the condition for evolution of cooperation is $b/c > 1/r$, which is the Hamilton's rule [20].

Direct reciprocity

In case of repeated Prisoner's dilemma game it had been asked "what is the best strategy?" by Axelrod [15]. Studies discovered that the answer is the "Tit-for-tat(TFT)", where cooperation for cooperators and defection for defectors [105–107]. Consider we have population playing "TFT" and "All-defection(ALLD)". TFT will cooperate at the first game for ALLD, but from the second playing it will defect against ALLD. Therefore, the payoff for cooperators using TFT is $b-c$, and for defectors, $-c$ only for the first game, and 0 for both. Denote by w the probability of playing another round between two same individuals, the average number of games is given by, $1/(1-w)$. The payoff matrix reduced to,

$$\begin{array}{c} \\ \mathrm{C} \\ \mathrm{D} \end{array} \begin{array}{c} \begin{array}{cc} \mathrm{C} & \mathrm{D} \end{array} \\ \begin{pmatrix} (b-c)/(1-w) & -c \\ b & 0 \end{pmatrix} \end{array}. \tag{4.13}$$

The condition that cooperation to be ESS is given by, $b/c > 1/w$.

Indirect reciprocity

Indirect reciprocity have been developed to address the cooperation behind human society. Individual decide to cooperate the other or not based on one's reputation [18]. The basic idea is that cooperation increases the reputation of cooperator while defection decreases. In this frame, we have defectors and cooperators who cooperate based on reputation of the individual to indicate a defector. With the probability of knowing one's reputation, q, a cooperator always cooperating to other cooperators, and helps defector with probability $1-q$. The concept leads the payoff matrix to,

$$\begin{array}{c} \\ \mathrm{C} \\ \mathrm{D} \end{array} \begin{array}{c} \begin{array}{cc} \mathrm{C} & \mathrm{D} \end{array} \\ \begin{pmatrix} b-c & -c(1-q) \\ b(1-q) & 0 \end{pmatrix} \end{array}. \tag{4.14}$$

Thus, if $b/c > 1/q$, cooperation is ESS.

Group reciprocity

Expanding the scope of selection from the individual level to the group level, the group reciprocity arise [26]. The model describing group selection is following.

A population split into m groups. Each group can have n individuals at maximum. Individuals interact each other among group members. Cooperators pay a cost c at each interaction and earn benefit b from each interaction with other cooperators within the group. Defectors pay nothing and earn benefits. The fitness of an individual is given by $1-w+wP$, where P is the payoff and w is the selection strength. At each time step an individual from the whole population selected for giving birth proportional to its fitness and its offspring added to its group. If the group reaches the maximum capacity, n, with probability p, that group divided and one random group erased to keep the total population is less than nm. If the group is not divided with probability $1-p$, one random individual from whole population selected for death. The fixation probability from a single cooperator take over the whole population is the fixation probability for take over a group times the fixation probability of the group which a seed cooperator included.

The fixation probability of single cooperator among $n-1$ defectors to take over its group is given by

$$\phi_C = [1/n][1-(b+cn-c)w/2] \tag{4.15}$$

and the fixation probability of single cooperator group among $m-1$ defector groups is given by

$$\Phi_C = [1/m][1+(b-c)(m-1)w/2] \tag{4.16}$$

under the weak selection, $w \ll 1$. The criteria, the selection favours cooperation is $\rho_C > 1/nm$, and since $\rho_C = \phi_C \Phi_C$, we arrive to

$$b/c > 1+[n/(m-2)]. \tag{4.17}$$

Since the fitness of group of cooperative individuals is higher than the fitness of selfish one the group of cooperative one will be selected.

4.2 Evolutionary game dynamics on graphs

So far we have looked the overview the evolutionary game theory. Our main interest is how structure of population affects on the evolution of cooperation. The limited interaction among individuals can cooperators coexist with or outcompete defectors without any complexity of strategy. The effect called the spatial reciprocity [45]. The spacial reciprocity usually indicate the effect of symmetric structures such as lattice. The generalized version of spacial reciprocity is the network reciprocity.

4.2.1 Network reciprocity

The network reciprocity was introduced by Ohtsuki based on the pair approximation on regular graph [49]. The core finding from the pair approximation is that if a structure of population has the average degree of k, the average number of cooperators around a cooperator is one more than that of defectors. To outcompete defector with higher fitness, therefore, the benefit from extra cooperator must exceed the total cost. The condition is,

$$b/c > k. \tag{4.18}$$

The network reciprocity based on the death-birth update rule. In case of the birth-death update, which is the traditional Moran process, cooperation never be favoured. Noteworthy that the condition exactly indicate the threshold benefit cost ratio, b/c^*, for the degree-homogeneous networks, in which the fixation probability of randomly placed a single cooperator overcome the neutral selection, $\rho_C > 1/N$.

Further studies on the degree heterogeneous networks discussed that the heterogeneity actually suppresses the selection of cooperation. According to the study, since the competition occurs between the nodes that are two steps away, it was pointed out that based on the pair approximation should be modified to the mean neighbor degree instead of the mean degree [108]. Based on conjecture the condition for evolution of cooperation is given by,

$$b/c > \langle k_{nn} \rangle = \frac{\langle k^2 \rangle}{\langle k \rangle} = \langle k \rangle + \frac{\sigma_k^2}{\langle k \rangle} \tag{4.19}$$

where, $\langle k_{nn} \rangle$ is the average degree of nearest neighbors, and $\sigma_k^2 = \langle k^2 \rangle - \langle k \rangle^2$ is the variance of the distribution $P(k)$. Hence, the heterogeneity becomes extra burden for population-wide cooperation. In "scale-free" networks characterized by $P(k) \propto k^{-\gamma}$ with a fixed mean degree $\langle k \rangle$, σ_k^2 in Eq. 4.19 sharply increases with decreasing γ. Notice that $\sigma_k^2 \sim (\gamma - 2)^{-2}$ as γ approaches 2. That is, the more heterogeneous in degree distribution, the rarer the fixation events. However, above discussion only holds when we use the death-birth update rule.

4.2.2 Imitation update

The main stream in studies of evolutionary game dynamics on structured population divided into two groups. One use the asynchronous death-birth update, which update one individual at one time step, and measure the fixation probability under the weak selection. The other one use the synchronous update scheme, which update whole population together for each time step without the weak selection and measure the fraction of cooperators in steady state. For the later case several update functions were suggested and representative is *the imitate the best*. The concrete scheme is in following way,

- At initial stage, cooperators and defectors are randomly distributed with same probability.
- At each time step, all individuals play game with their neighbors and get payoff, P_i. With that payoff update their strategy as following,
- individual i choose one of its neighbor, j, in random and i imitate strategy of j with the probability,

$$P_{ij} = \begin{cases} (P_j - P_i)/\max\{k_i, k_j\}b & \text{if } P_i < P_j, \\ 0 & \text{otherwise} \end{cases} \tag{4.20}$$

- Repeat until the population reach to the steady state.

Interestingly based on synchronous update, the scale-free networks were much better than other kinds to sustain the high level of cooperation under the high temptation to defect [51, 50, 53, 52, 109, 110]. The high level of cooperation in the scale-free population were maintained by high degree nodes, the hubs. Since a hub is highly exposed to population it has higher chance to meet cooperators. If a hub defects its payoff will instantaneously increased but soon it will lose its cooperating neighbors. As consequence the payoff of defector hub will be decreased and later it will imitate again cooperation. Once the hub became a cooperator, its payoff will be keep increased by neighbors which imitating cooperation from the hub and therefore the level of cooperation maintained. Thus, cooperation take successfully hubs.

The difference between update rule can be interpreted as different perspective. In case of synchronous imitation update scheme, scholars were trying to describe the human behavior in which try to maximize one's payoff from comparison with others. However, in this case a node have higher payoff than all of its neighbor never update its strategy. When the population structure is degree-mixed, neither assortative nor disassortative mixing shows higher level of cooperation compare to neutral mixing (Fig. 4.3). In case of assortative mixing one observed sudden drop of cooperation fraction when temptation to defect increased. In assirtative mixing hubs compare payoff and imitate more likely from other hubs, therefore, if defector hub appeared with relatively high payoff the cooperating cluster of hubs can be break down easily. In case of disassortative mixing, since a hub is isolated from other hubs there is very rare chance that the payoff of hub is lower than its neighbors. Meaning in disassortative mixing the initial strategy become the final strategy for most of high degree individuals (Fig. 4.4).

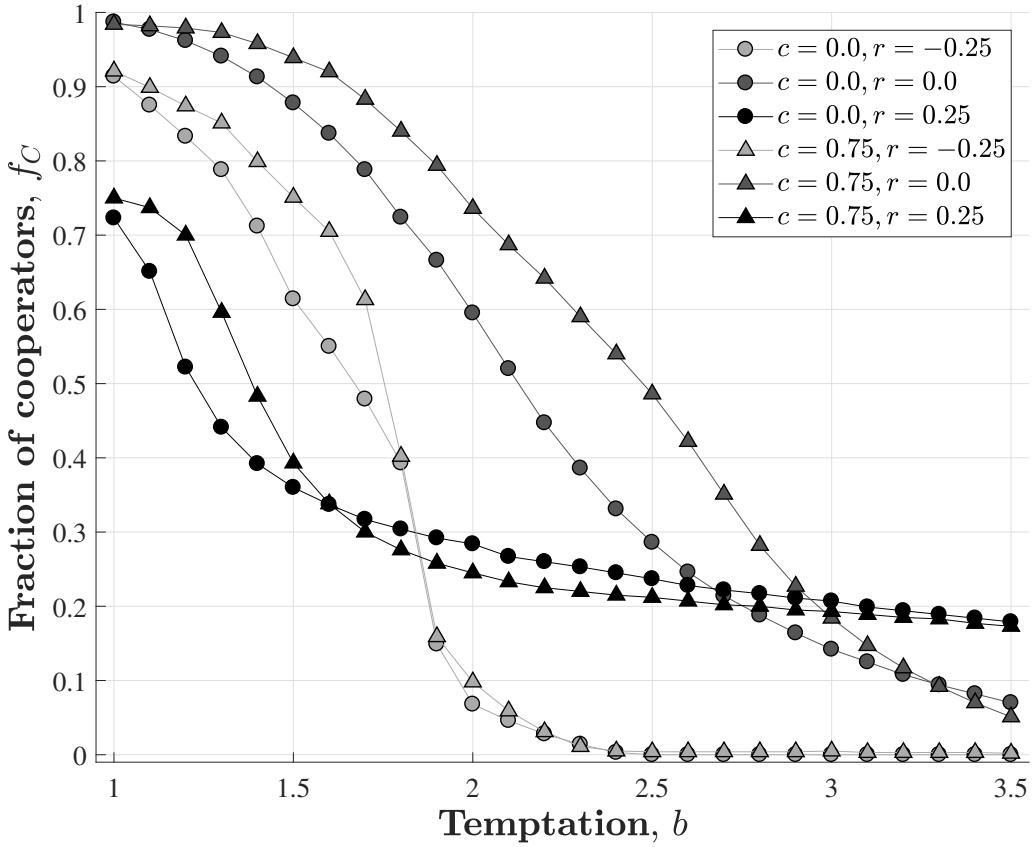

Fig. 4.3 Averaged fraction of cooperators as function of temptation to defect, b based on imitation update on scale-free networks. Each network were tuned for desired degree-mixing and clustering. We used BA algorithm to generate population size of, $N = 5000$, and the average connectivity, $\overline{k} = 6$. 10 networks were independently generated for each configuration. The level of cooperation averaged over 100 generation after 5000 of incubation periods.

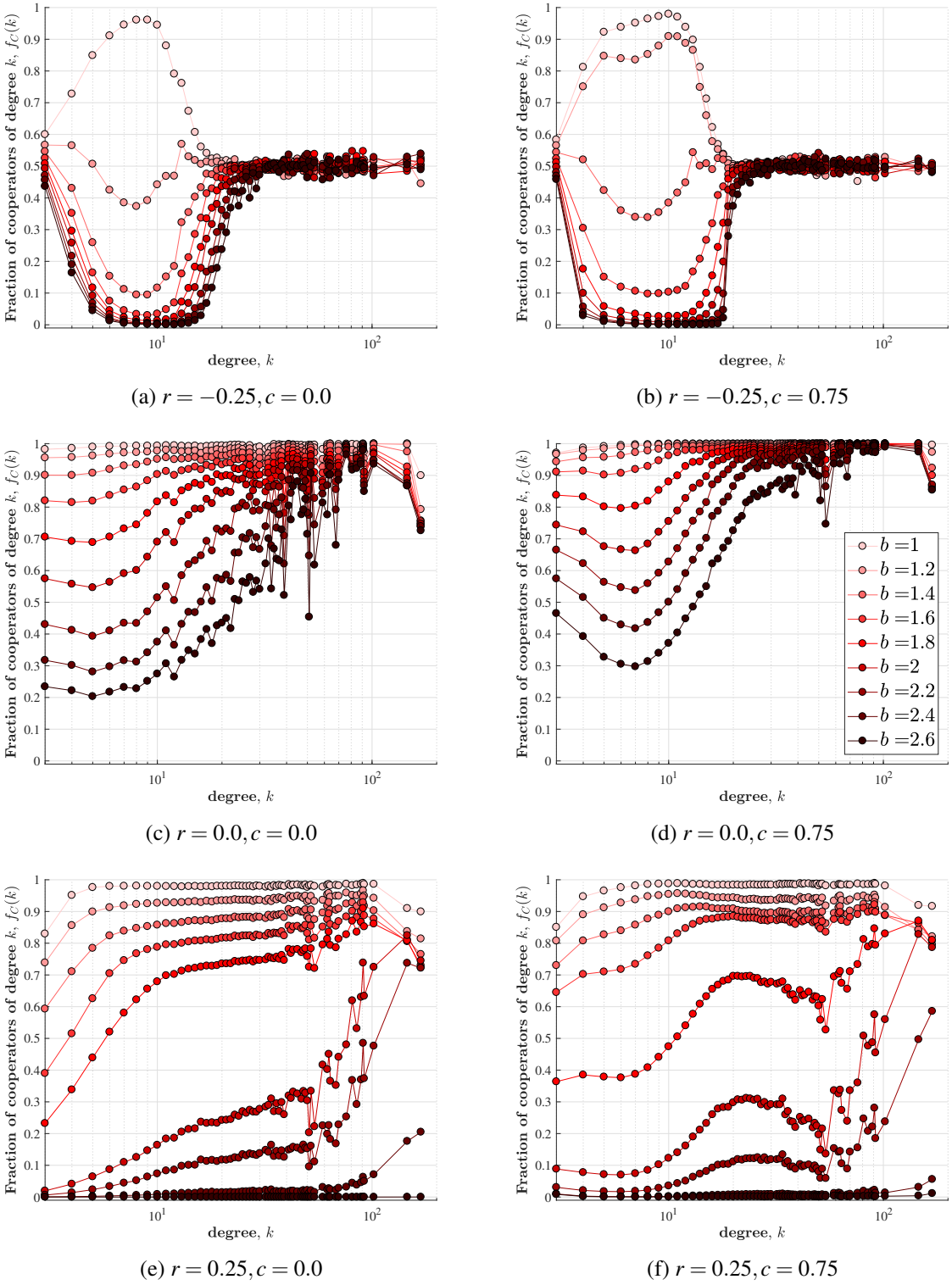

(a) $r = -0.25, c = 0.0$ (b) $r = -0.25, c = 0.75$

(c) $r = 0.0, c = 0.0$ (d) $r = 0.0, c = 0.75$

(e) $r = 0.25, c = 0.0$ (f) $r = 0.25, c = 0.75$

Fig. 4.4 Averaged fraction of cooperators among nodes of degree, k at each level of temptation, b for characterized structures. In disassortative mixing, the fraction of cooperators in high degree class, $k > 20$, is remained as initial strategy. The majority of low degree nodes are mostly connected to hubs, the total fraction at high temptation can be sustained (a), (b). In case of assortative mixing, temptation leads breaking of reciprocal relation in hub community and thus losing cooperator clusters as shown in (e) and (f). The clustering doesn't have critical impact but little bit helpful to maintain higher level of cooperation due to tightly clustered reciprocal links.

4.2.3 Death-birth update

Despite many of discussions about the effect of structured population on maintaining the level of cooperation, it is still unclear that how the degree-heterogeneity and the degree-degree correlation affect on the evolution of cooperation. To address that point we explored the selection dynamics on complex population structures based on following scheme. Results and discussions will be presented in following section.

Simulation scheme

To understand more precisely we simulated the death-birth dynamics on the set of generated networks based on the Prisoner's Dilemma game under the weak selection. To adjust a single parameter for the game, we used modified payoff matrix which rescaled original Prisoner's dilemma (4.11) by the cost as,

$$\begin{array}{c} \\ \mathrm{C} \\ \mathrm{D} \end{array} \begin{array}{c} \begin{array}{cc} \mathrm{C} & \mathrm{D} \end{array} \\ \begin{pmatrix} b/c-1 & -1 \\ b/c & 0 \end{pmatrix} \end{array} \equiv \Pi \,. \tag{4.21}$$

Each individual on a given network is assigned an accrued payoff from the interaction with the neighbors. The fitness of an individual i, F_i, is proportional to its payoff, P_i,

$$F_i = (1-w) + wP_i \qquad P_i = \sum_{j=1}^{N} a_{ij} \left\langle s_i | \Pi | s_j \right\rangle \tag{4.22}$$

where, w is the selection strength in range of $0 \leq w \leq 1$. The weak selection means w is much smaller than 1. So under the weak selection the payoff contribute on the fitness only a small portion. Again, in the death-birth dynamics on a graph at each step randomly chosen individual dies and around neighbors compete to take over the empty site proportional to its fitness.

Criteria of selection

To justify whether cooperation is favoured in selection or not we measure the fixation probability of randomly placed a single cooperator, ρ_C. If $\rho_C > 1/N$, we say the cooperation is favoured. We also measured the threshold benefit cost ratio of a given network, b/c^*, which the point cooperation started being favoured. It is a indicator to show a given network is facilitative or not for the evolution of cooperation.

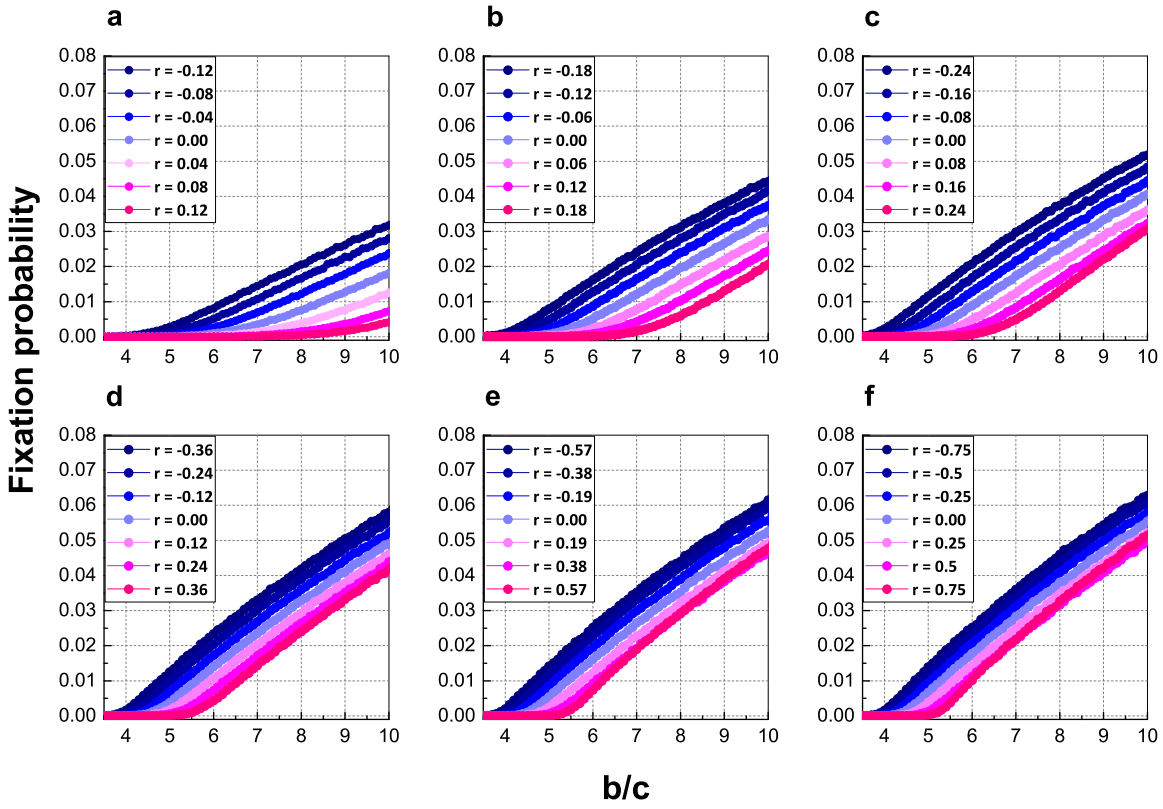

Fig. 4.5 Fixation probability of cooperator, ρ_C, as a function of b/c on structured populations. The corresponding degree exponent to each window is γ = (a) 2.5, (b) 2.75, (c) 3.0, (d) 3.5, (e) 4.0,and (f) 5.0. The fixation probability, $\rho_C(b/c)$, were measured from 10^6 trials at each b/c in range of $3.5 \leq b/c \leq 10.0$ with interval 0.1 for each configuration, $G(\gamma, r)$, that independently generated 200 network samples under the weak selection, $w = 0.0095$.

4.3 Emergence of cooperation on complex population structures

We have simulated the discrete selection dynamics on the set of population structures that controlled the degree-heterogeneity and the degree-degree correlation. To avoid the bias from the clustering we controlled the structure to have low clustering coefficient. We have found several points that were not discussed in the community so far especially the effect of degree-mixing on the selection of cooperation.

4.3.1 Main observation

As shown in Fig. 4.5, regardless the level of heterogeneity and degree-mixing the fixation probability, ρ_C, increasing as the benefit cost ratio, b/c, increased. Differences appeared in the slop of ρ_C, where we observed smoothest from the most heterogeneous with the degree exponent, $\gamma = 2.5$, while the steepest from the most homogeneous with the degree exponent, $\gamma = 5.0$. We observed also the effect of the degree-mixing appeared as the tendency that the highest ρ_C from the most disassortative mixing while

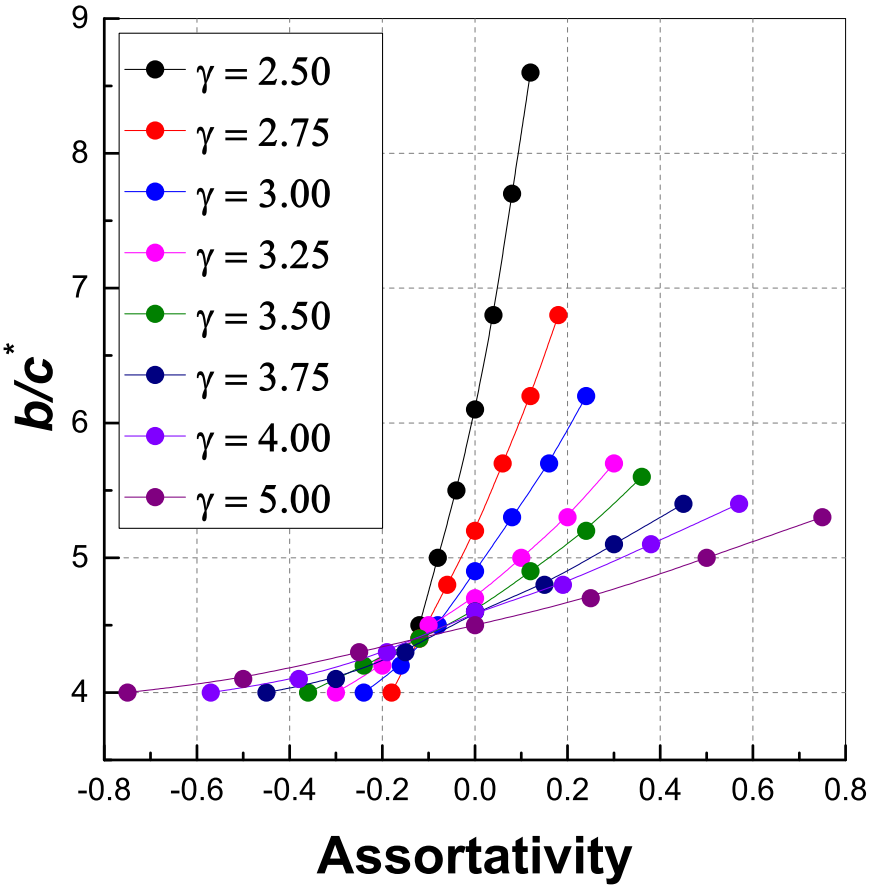

Fig. 4.6 Threshold b/c^* for varying degree distributions of the form $P \sim k^{-\gamma}$ and degree-degree correlations. Throughout the data points the average degree is constrained at $\bar{k} = 4$. Disassortative degree mixing promotes altruism, sometimes overcompensating for the negative effects of heterogeneous degree distribution.

the lowest ρ_C from the most assortative mixing from each level of the degree-heterogeneity, however the gap between ρ_C from assortative and disassortative is much bigger in heterogeneous networks.

The threshold b/c^* from each configuration shows more clearly how the degree-heterogeneity and the degree-mixing enhance or suppresses the evolution of cooperation. Our results agrees with the previous discussions on the average degree [49] as shown in Fig. 4.6 that from all configuration $b/c^* > \bar{k}$. It is also agrees with the discussion that the degree-heterogeneity suppresses cooperation [108] as higher b/c^* for the more degree-heterogeneous structure in neutral mixing ($r = 0$). The effect of degree-mixing is shown as b/c^* decreased as the level of degree-mixing varies from assortative to disassortative and the effect amplified by the degree-heterogeneity.

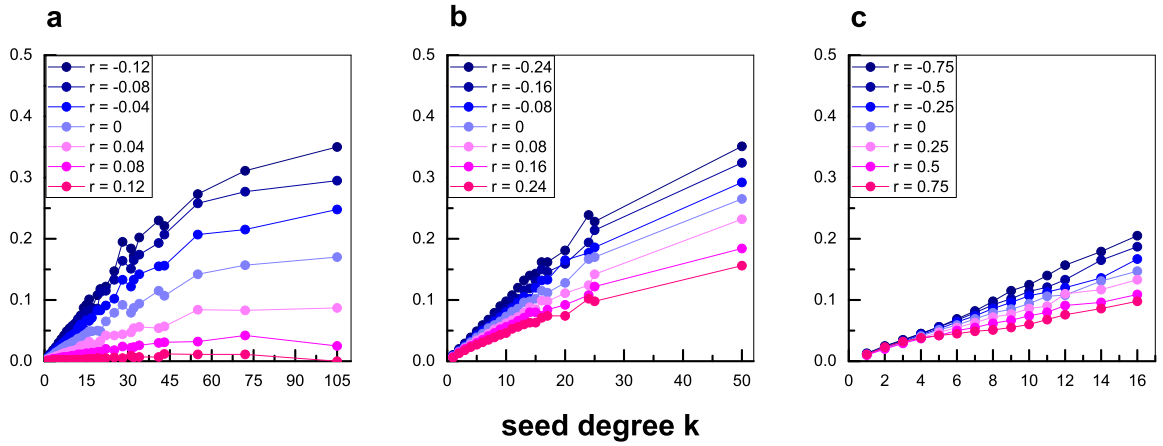

Fig. 4.7 Degree of the seed cooperator positively correlates with the fixation probability in the weak selection strength. $\gamma =$ (a) 2.5, (b) 3.0, and (c) 5.0 . This tendency, however, becomes saturated for highly heterogenous and highly assortative networks (lower plots in a). **d.** The probability of arival when the cooperation starts from a node whose degree is less than the mean degree, i.e. $k_{\text{seed}} < \bar{k}$. (d) aw. **e.** Higher-degree seeds proceed farther that the lower-degree seeds.

4.3.2 Seed effect

Let us begin discussions from the seed effect. As we saw that in previous chapter under the death-birth update a node with higher degree has better chance to spread its offspring compare to lower one due to the influence. However, in the evolutionary game dynamics the fitness is not a constant. Since a seed cooperator doesn't have any cooperating neighbor at the beginning, it must endure paying the cost until it achieve the evolutionary success. The cost paying from the seed proportional to its degree, therefore, rational guess suggest that starting from higher degree maybe worse compare to starting from low degree because of the high cost disadvantage.

In fact, if we sort out the fixation events according to the degree of the seed cooperator, as shown in Fig. 4.7, the "founder effect" clearly indicates the advantage of starting cooperation from a higher-degree node. This seemingly paradoxical result can be explained by considering the first evolutionary success of seed cooperator. If cooperation starts at the node 0 of degree k_0, the probability can be computed that this seed node spread the cooperation before death. Once a node, say the node i of degree k_i, from the seed's neighborhood, $\mathbf{N}_0$, is randomly picked for replacement with probability $1/N$, the seed node competes for reproduction with the other $k_i - 1$ nodes of $\mathbf{N}_i$. The odds for the seed cooperator to be selected for reproduction can be expressed as

$$\sum_{i \in \mathbf{N}_0} \frac{1}{N} \cdot \frac{(1-w) - wk_0}{(1-w)k_i + w(b/c\tau_i - k_0)} \equiv S_w \,, \tag{4.23}$$

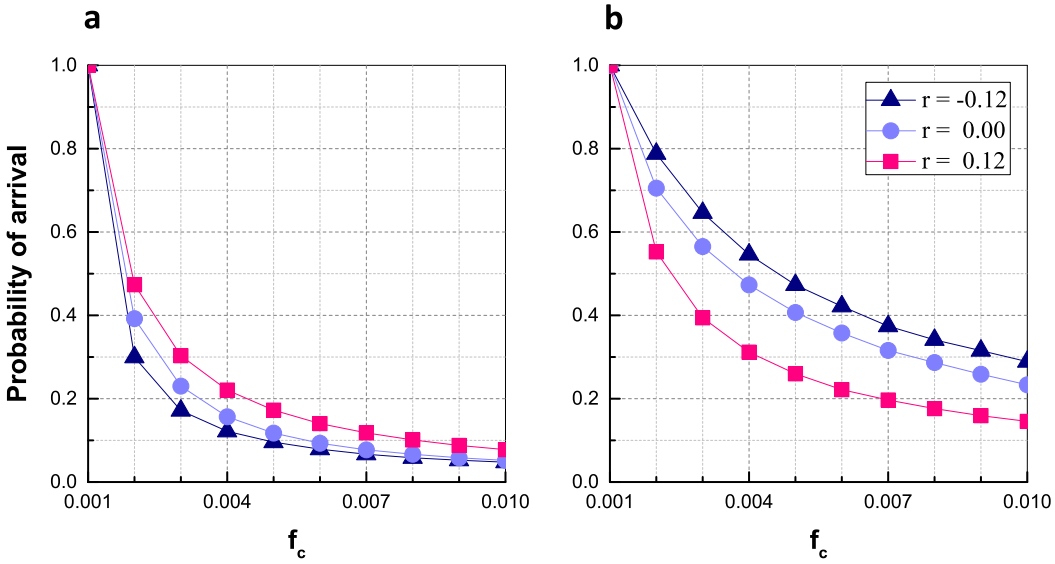

Fig. 4.8 Averaged probability of evolutionary success upto 10 cooperators started from (a) low degree seed, $k_{\text{seed}} < \bar{k}$ and (b) high degree seed, $k_{\text{seed}} > 5\bar{k}$. Figure shows the degree of seed effects on the evolutionary success when the cooperator try to invade the sea of defectors on structured populations. Starting at low degree nodes, which is the majority of the population in degree-heterogeneous structures, mostly failed. The probability to reach 10 cooperators starting from low degree nodes less than 0.1. However, if the seed initiated at hubs the chance of proliferation increased by structural benefit under the death-birth dynamics. The seed effect, however, amplified by the disassortative mixing and neutralized by the assortative mixing. Figure obtained on the configuration of $\gamma = 2.5$ at $b/c = 8.0$ and $w = 0.0095$.

where the cost of cooperation is set to 1 and τ_i is the number of triangles with the edge $(0,i)$ as a side, in which the number of common neighbors between 0 and i. Notice that S_w depends, through k_i and τ_i, on up to the second-order adjacency from the seed. The degree of success of the initial proliferation of cooperation is now determined based on by how much S_w is greater than $1/N$. By replacing $\tau_i \sim 0$ with its respective ensemble average of low clustering,

$$S_w \leq \frac{1}{N} \sum_{i \in \mathbf{N}_0} \frac{1 - w(k_0 + 1)}{k_i - w(k_0 + k_i)} \,. \tag{4.24}$$

Eq. 4.24 explains the benefit of starting the cooperation at a hub node. In the weak-selection limit, where fitness is insensitive to the payoff, the seed cooperator may overcompensate the apparent disadvantage of excessive exploitation. Note that Eq. 4.24 converges to the influence of node 0 in the limit of neutral selection, $w \sim 0$. As consequence, once taken by either C or D, hubs become the stronghold in proliferating the strategy.

Fig. 4.8 clearly shows the structural benefit starting from the high degree. Interesting point is the side effect of the degree-mixing. It is represented that the benefit starting from hub reduced in case of assortative mixing while enhanced in disassortative mixing compare to neutral Fig. 4.8 (b). Surprisingly,

we observed that the structural disadvantage initiated at low degree nodes get worse in negative mixing while enhanced in positive mixing. It can be understood from the feature of positive and negative degree-mixing that will be discussed in following sections. What the observation indicating is that even early evolutionary success achieved, it does not continued longer.

4.3.3 Effect of degree heterogeneity

The key spot: Hubs

Despite the apparent benefit of utilizing the most connected nodes as a seed cooperator, the fraction of those hubs is negligibly small even in scale-free networks. The greater majority of nodes have smaller degrees than the nominal average, rendering the existence of hubs is not desirable. Thus, it is important to take the control over hubs. Importance of taking control of hubs for the evolutionary success of cooperators appeared in their manifest advantage of spreading ability. Regardless what the strategy is, hubs have high accessibility to the competition for reproduction through the high connectivity. Whenever one of its neighbor dies hubs trying to spread their identity under the death-birth process. Influence captures the aspect quantitatively. Thus, if a hub turned into cooperator, cooperators achieves the stronghold that they can rely on. Further more in the evolutionary game the fitness of individual proportional to the number of cooperators in neighborhood, the influence of cooperating hub will be increased by its evolutionary success. On the contrary, if a hub is defector, it is big menace to cooperators. Defector hubs will try to break down cooperating clusters with its fitness that earned from exploitation. Unless cooperators take over the hub spot, cooperators exterminated by defector hubs with high probability.

Collecting discussions on the seed effect and influence of hubs we could summarize on the suppression of cooperation in the degree-heterogeneous population. It is because of the existence of hubs. With a fixed mean degree $\langle k \rangle$, as γ decreases, more and more nodes would have degrees lower than the nominal average, leaving just a few massively connected hubs. The more degree heterogeneous, the more high degree hubs appear. If hub become a cooperator, cooperators can rely on cooperator hubs as a stronghold based on its structural benefit of reproduction. However, before cooperators achieve evolutionary success on hub node, a defector hub in the role of exploiter against cooperators and with exploited payoff it has high chance to outcompete cooperators at birth competition. At the same time to take over hub spot cooperator have to face many of competitors due to the high connectivity that hub has. Even in the case that any of competiting defectors doesn't have source of exploitation, the probability that a single cooperator take over the spot inversely proportional to the degree of hub. Therefore, in more and more heterogeneous structure survival of seed cooperator become more and more difficult. As consequence the degree-heterogeneity suppresses the emergence of cooperation.

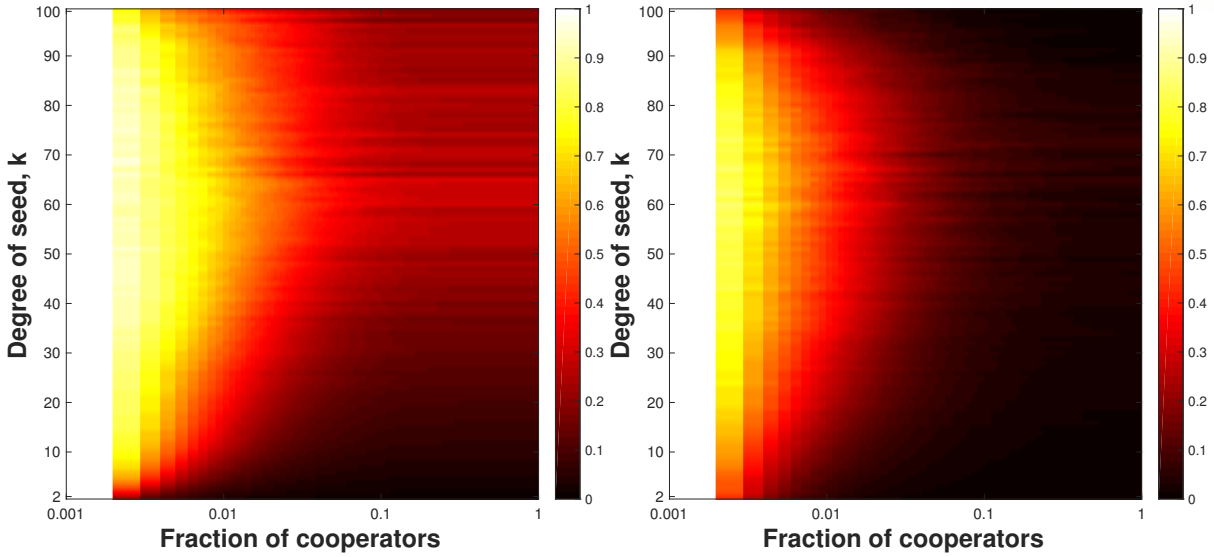

(a) $\gamma = 2.5, r = -0.12$ (b) $\gamma = 2.5, r = 0.12$

Fig. 4.9 The probability of arrival to f_C given that the degree of seed cooperator, k_{seed} is k, on disassortative (a) and assortative (b) structures. The evolutionary success in early stage depends on the degree of seed cooperator. The arrival probability is increasing as the degree of seed getting higher. However, the optimum degree of seed for the first few successful steps of spreading cooperators is not the highest degree, which represent the balance between the initial cost and the utilized structural benefit as a hub. Notice that the fraction of cooperators, f_C, expressed in logarithm scale. $b/c = 8.0$ and $w = 0.0095$.

4.3.4 Stages in evolutionary success of cooperation

Major previous studies focused on the fixation probability of cooperation. We were curious about how cooperators taking over the whole population starting from a single cooperator on complex population structure, since there is not only structural complexity but also configurational complexity that affects on the fitness of an individuals. For example, suppose we have a certain fraction of cooperators. The fixation probability from that fraction on degree-homogeneous structure verses degree-heterogeneous structure at the same benefit cost ratio will be different, because the relative fitness of an individual against its potential competitor on each structure depending on the combination of two complexities. To clarify, we quantified the arrival probability to a certain fraction of cooperators from randomly placed seed cooperator and the conditional fixation probability from a certain frequency of cooperators. Despite we obtained results using many structural and dynamic parameters, from now we focus on the results from the assortative ($r = 0.12$) and disassortative ($r = -0.12$) structures which obtained from the most degree-heterogeneous populations ($\gamma = 2.5$). More detailed results from selected structures are represented in Appendix B.

First we investigated how much does cooperation can be proliferated to the population starting from a single cooperator in average. Fig. 4.9 shows the arrival probability to a certain fraction of cooperators through the evolutionary success that started from a seed cooperator with degree k. As we expected from the understanding the seed effect, the evolutionary success in early stage depends on the degree of seed

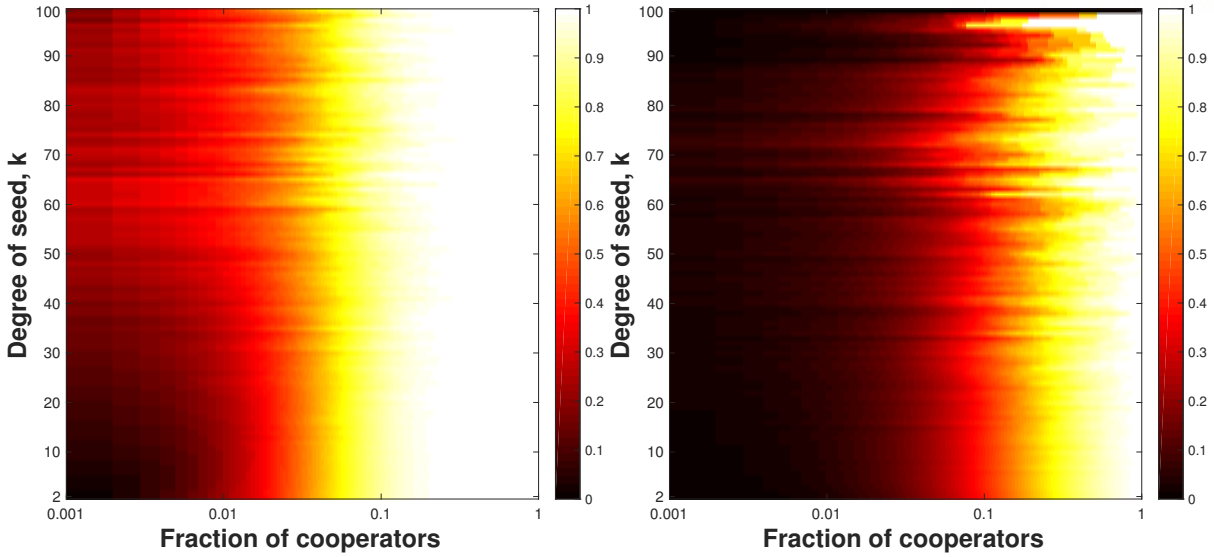

(a) $\gamma = 2.5, r = -0.12$ (b) $\gamma = 2.5, r = 0.12$

Fig. 4.10 The conditional fixation probability from a certain fraction of cooperators, f_C, given that the degree of seed cooperator, k_{seed} was k on disassortative (a) and assortative (b) structures. There is seed dependency of the fixation until certain fraction, $f_C < 0.01$ for the disassortative mixing and $f_C \sim 1$ for the assortative mixing. The edge between red and yellow domain around $f_C \sim 0.05$ in (a) clearly independent from the degree of seed which indicating that the seed dependency disappeared. In (b) the edge between color domain is noisy due to the rare fixation on assortative mixing. $b/c = 8.0$ and $w = 0.0095$.

cooperator. Regardless the level of degree-mixing, there is similar tendency that the arrival probability is increasing as the degree of seed getting higher. We can notice that the optimum degree of seed for the first few steps of successful spreading is not the highest degree, which represent the balance between the initial cost and the utilized structural benefit of reproduction as a hub. Furthermore, there is clear threshold that the proliferation of cooperation is strongly limited. The edge of limited expansion depends on the degree-mixing of given structure and the degree of seed but in both cases the threshold can be observed in range $0.01 < f_C < 0.1$. On the other hand, if the fraction of cooperator reached more than the threshold it seems remained as a constant. It means that if the fraction of cooperators is more than the threshold, evolutionary success of cooperators until the fixation event is ensured.

Fig. 4.10 shows the conditional fixation probability from certain fraction of cooperators, f_C, which arrived from a single cooperator initiated at the node of degree k. As we previously discussed from the arrival probability there is certain threshold fraction of cooperators that ensure the emergence of cooperation. However, in this case the threshold seems not really depends on the degree of seed, but the structural characteristics. We can observe there is seed dependency of the fixation until certain fraction, $f_C < 0.01$ for the disassortative mixing and $f_C \sim 0.1$ for the assortative mixing. However, the seed dependency disappeared at certain point. In Fig. 4.10 (a), in case of disassortative mixing the edge between red and yellow domain independent from the degree of seed. Above the edge the

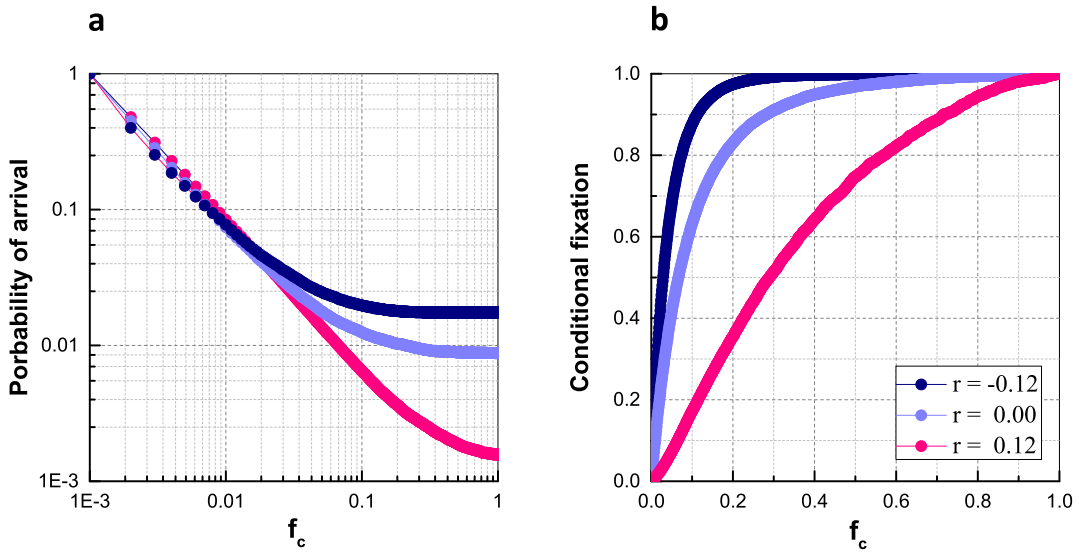

Fig. 4.11 (a) The arival probability to a certain fraction of cooperators from randomly placed single cooperator,(b) the conditional fixation probability from a certain fraction of cooperators on the structured population with $\gamma = 2.5$ at $b/c = 8.0$. The stages of evolutionary process of cooperators on structured populations divided into three, the survival, the expansion and the settle down. The survival stage is the fraction of cooperators in range of $0 < f_C < 3/N$. Denote by f_C^* the threshold fraction that guarantees the fixation, the expansion stage is in range of $2/N < f_C < f_C^*$. Above the threshold the stage is settle down. In this figure, the threshold fractions of each configuration, $f_C^*(G)$, strongly depend on the level of degree-mixing. For the disassortative structure, $f_C^* \sim 0.2$ while for the assortative mixing, $f_C^* \sim 1.0$, which represent the selection of cooperation is favoured more on the negatively degree-mixed populations.

conditional fixation probability dramatically increased and around $f_C \sim 0.1$, which is still the majority among the total population is defectors, the evolutionary success of cooperators almost guaranteed. It is strongly suggesting that when the number of cooperator reached at that certain fraction, the combination of configurational and structural complexity provide sufficient compensation to cooperators and that assortment is enough to outcompete defectors.

Based on observation we may divide the stages of evolutionary process of cooperation on the structured population into three, those are the survival, the expansion, and the settle down. In the stage of survival, a seed cooperator achieves the first evolutionary success or die out. Regardless the benefit cost ratio and structural characteristics, the first evoluionary success of randomly placed seed cooperator approximately proportional to the degree of itself over the harmonic mean of neighbors degree under the weak selection. The optimum seed degree depends on the balance between the initial cost and the structural benefit. If seed cooperator succeed survive, two cooperators try to expand cluster based on their reciprocal compensation. Expansion period strongly depends on the compensation for the mutual cooperation. Higher payoff for reciprocal altruism leads more evolutionary success for cooperators. The evolutionary success of cooperators for a hub in this stage decide whether continuing expansion of

cooperating cluster or shirked by robust proliferation of defector hubs. If cooperator cluster expanded successfully in this chaotic random drift across complex interactions, finally the evolutionary population system could reach to the point where the fraction of cooperators sufficiently outcompete defectors during further evolutionary processes. We call this stage as the settle down.

4.3.5 Effect of degree-mixing

Amplifying or neutralizing the seed effect

The effect of degree-mixing observed throughout stages of the evolutionary process. In this part we focus on the effect of degree-mixing on the emergence of cooperation. We already witnessed the degree-mixing amplifying or neutralizing the seed effect from the Fig. 4.8. The structural benefit or loss of reproduction starting at high degree or low degree, respectively, amplified by the negative degree-mixing and neutralized by the positive mixing. Since, in disassortative mixing, low degree nodes are mostly connected to high degree nodes, the first cooperator at low degree node under the high influence of D-hub in neighborhood. Despite of the low cost pressure to the seed, this configuration cause decreasing of potential evolutionary success and increases the probability of extinction. As the opposite situation, when a seed cooperator initiated at high degree spot, the cooperator have to pay more cost but the structural benefit of reproduction amplified by decreased size of the pool for competition, since its neighbors have poor connectivity. On the other hand, in case of assortative mixing the threat of extinction to low degree seed decreased by absence of the direct connection from hubs while the structural benefit of reproduction to hubs also decreased by many number of potential competitors, thus the seed effect is neutralized. As consequence due to the majority of low degrees among the population, the evolutionary success in the early stage is slightly better in assortative population as shown in Fig. 4.11 (a).

However, the amplified or neutralized seed effect by degree-mixing pattern conflict to the conditional fixation probability from the seed of degree, k_{seed}, as we observed in Fig. 4.7. The fixation probability given the degree of seed, k_{seed}, has tendency which is proportional to the degree of seed k_{seed}. Moreover, the tendency amplified or neutralized by disassortative or assortative mixing, respectively. The explanation for that can be found from the settle down threshold, f_C^*, which guarantees further evolutionary success of cooperators, if evolutionary population of cooperators reached above that number of cooperators. As shown in Fig. 4.11 (b), the settle down threshold in disassortative mixing much smaller compare to the assortative mixing. From this observation we can notice that the selection of cooperators during evolutionary process facilitated by disassortative mixing or suppressed by assortative mixing in the stage of expansion.

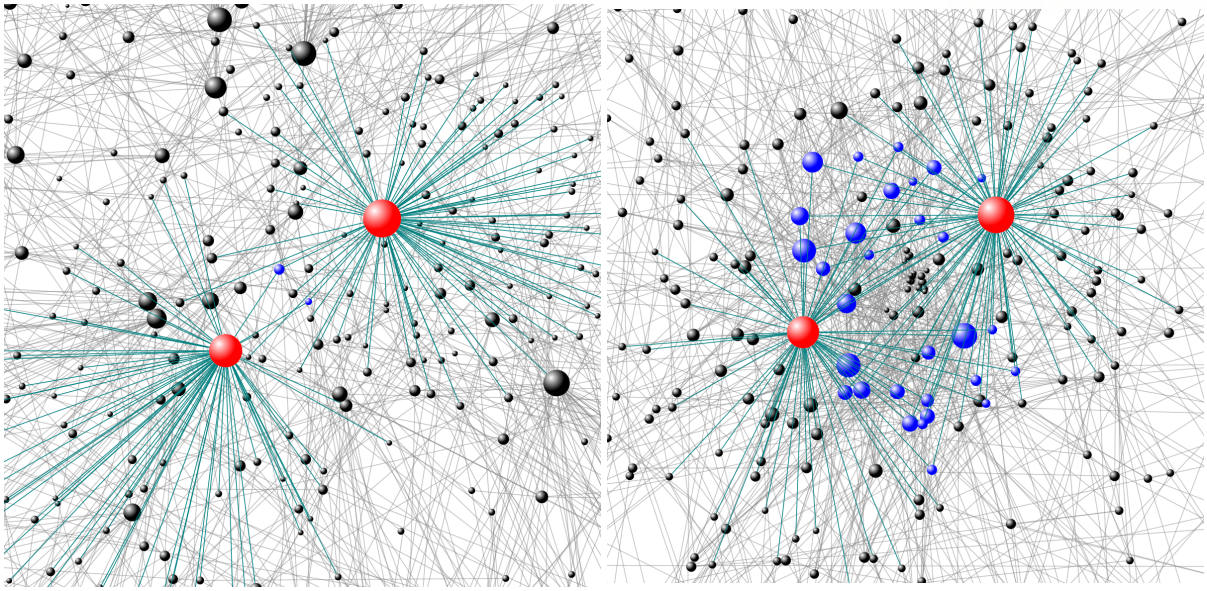

(a) $\gamma = 2.5, r = -0.12$ (b) $\gamma = 2.5, r = 0.12$

Fig. 4.12 Visualized example of structural equivalence between the highest degree hubs in (a) disassortative and (b) assortative mixing from the sample network with the degree exponent $\gamma = 2.5$. The size of nodes proportional to their degree. The most connected two hubs, degree of $k = 90$ and $k = 69$, are indicated as two red nodes and common neighbors between them are indicated as blue nodes. The green color links showing the connection between hubs and others. The number of common neighbors between two hubs in disassortative mixing is 2 and in assortative mixing is 30. Therefore, hubs in assortative mixing is much more structually equivalent than in disassortative mixing. The networks in figure share the degree sequence.

Interference via structural equivalence

The evidence of relative high pressure of suppression to the emergence of cooperation in assortative mixing can be addressed due to the high structural equivalence between a pair of nodes. In general, the level of structural equivalence between a pair of individuals in a structured population decide the similarity of local configuration of strategies for a pair of individuals during the evolutionary dynamics. As an example, the number of common neighbors between two highest degree hubs is much more in assortative mixing compare to disassortative one as shown in Fig. 4.12. In this example structure, the pair of highest degree hubs in the assortative mixing have many of common neighbors, they play the game with same partners and they also compete for reproduction of their identity toward same targets. If both of hubs have identical strategy, even they compete each other in individual level their trial for evolutionary success toward same direction of the selection. However, if they do have opposite strategy against each other, the direction of evolutionary success of each individual are out of joint and consequently, they do interfere reproduction against each other. Thus, the interference between a pair of individuals only has the meaning when the pair have different strategies.

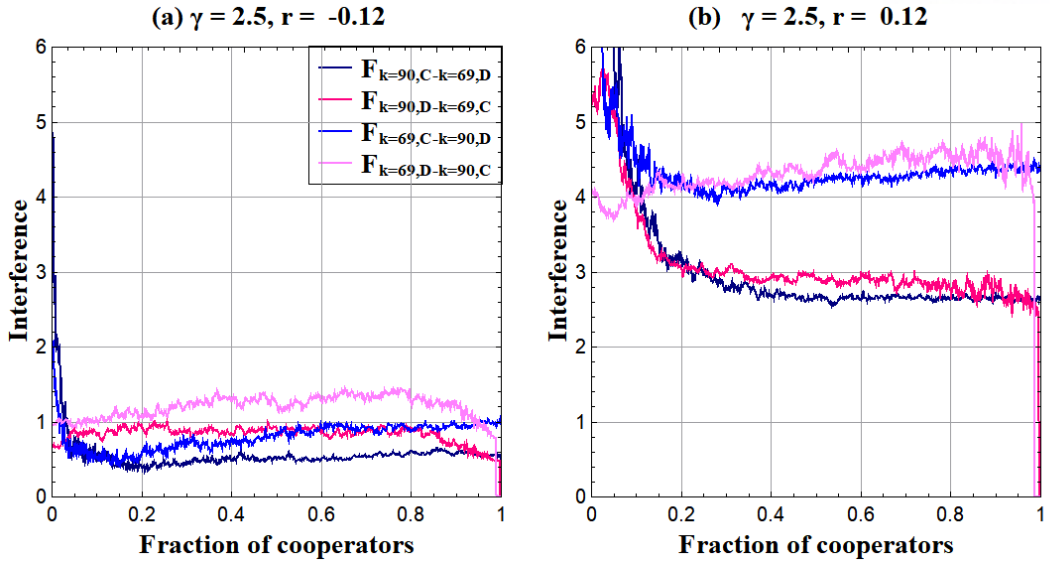

Fig. 4.13 Interference between pair of hubs, which represented in Fig. 4.12, as function of the total fraction of cooperators in the population. Navy and blue belong to interference from D-hub to C-hub and pink and light pink belong to interference from C-hub to D-hub. Interference between hubs in assortative mixing is much stronger than in disassortative mixing. The strong interference mainly cause the high barrier against cooperators for taking over hub community in assortative mixing. Figure obtained using $b/c = 8.0$ and $w = 0.01$.

Take account of the interference quantitatively we suggest the following logic. Let consider a pair of individuals say i and j. When one of common neighbor between them, say l, become a stage of competition for reproduction from the random death, the pair of individuals join to the competition. It is reasonable to quantify the strength of interference from j to i as the relative fitness of j compare to i, f_j/f_i. Because in competition for reproduction the interference to i from the competitor, j, meaning how much is j relatively fitter than i so that reduces the probability of evolutionary success of i. At the same time, if the competition pool is big, the actual interference from j to i may not big. Therefore, we rescale the relative fitness with the size of competition pool, that is the degree of common neighbor minus one, $k_l - 1$, since the minimum size of competition happens between two individuals. So we defined the interference from j to i, F_{ij}, as the total sum of potential rescaled relative fitness of j against i through their common neighbors when the two have different strategies,

$$F_{ij} = \sum_l A_{il} A_{lj} \frac{1}{k_l - 1} \frac{f_j}{f_i} (1 - \delta_{s_i s_j}). \tag{4.25}$$

where s_i and s_j indicate strategies of i and j, respectively.

The interference between two largest hubs in disassortative and assortative mixing during evolutionary process is shown in Fig. 4.13. As we expected the interference between two hubs is much stronger in assortative mixing compare to disassortative case. Interference between a pair of individuals proportional

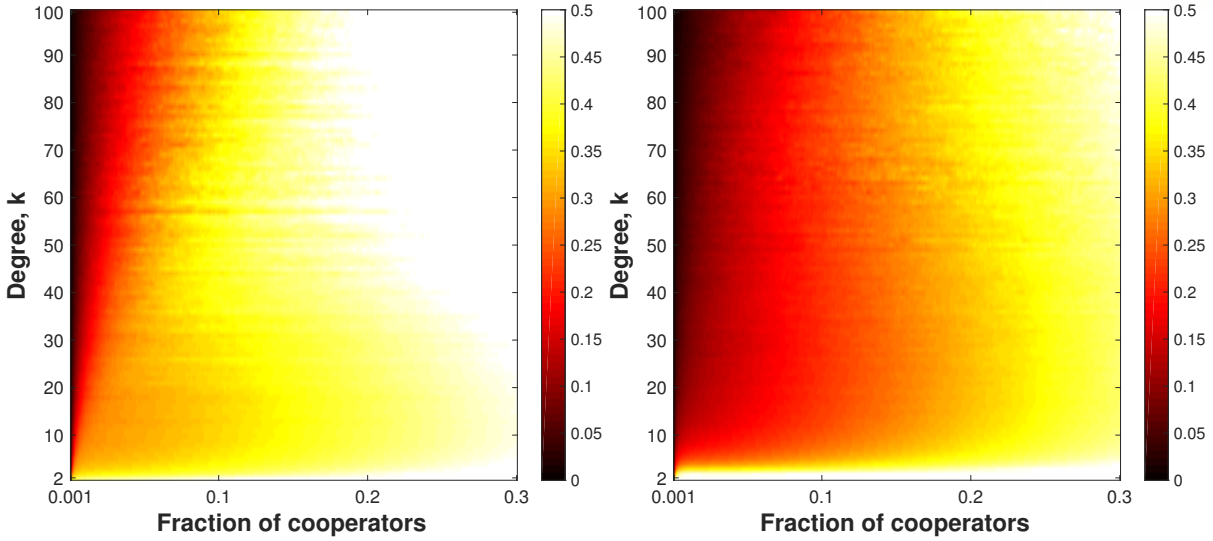

(a) $\gamma = 2.5, r = -0.12$ (b) $\gamma = 2.5, r = 0.12$

Fig. 4.14 The averaged local frequency of cooperators around the cooperator of degree k on (a) disassortative and (b) assortative structures when the total fraction of cooperators among the population in range of $1/N < f_C < 0.3$, which is early to expansion stage. (a) in disassortative population, cooperator hubs take over their neighbors at relatively lower fraction of cooperators in the population, since hubs in disassortative mixing are relatively isolated even cooperator hubs doesn't have enough compensation or reciprocity from their neighborhood structural advantage facilitate spreading the strategy. (b) in assortative mixing cooperator hubs have much less cooperating neighbors around compare to disassortative at the same level of total cooperators in the population. Rather than around hubs, cooperators are stick together in low degree spots, $k < \bar{k}$. Due to the structural equivalence without accordance of strategies among hubs as cooperation it requires stronger reciprocity as more cooperator in neighborhood or more compensation from reciprocal interactions. The average take over the data from 10^5 of simulations on 200 independently generated network ensemble of each assortativity. Notice that hubs of degree $k > 10$ are very rare in each network sample.$b/c = 8.0$ and $w = 0.0095$.

to the structural equivalence, or similarity between them. We confirmed in Ch.2 that similarity between a pair of nodes is much larger in assortative mixing compare to disassortative mixing as shown in Fig. 2.8. Expanding our observation of interference between hubs to any pair of nodes in competing position, we can notice that interference in assortative mixing between any pairs of cooperator and defector is much stronger than in disassortative mixing. Which mainly cause the higher barrier against cooperators for taking over population in assortative mixing compare to disassortative mixing.

Fig. 4.14 represent the averaged local frequency of cooperators around a cooperator degree k when the total fraction of cooperators in the whole population in range $1/N < f_C < 0.3$, which is early to expansion stage. As shown Fig. 4.14 (a) in disassortative population, cooperator hubs take over their neighbors at relatively lower fraction of cooperators in the population, since hubs in disassortative mixing are relatively isolated, even cooperator hubs doesn't have enough compensation or reciprocity from their neighborhood, the structural advantage facilitate spreading the strategy. In case of assortative mixing, cooperator hubs have much less cooperating neighbors compare to disassortative structure at the same

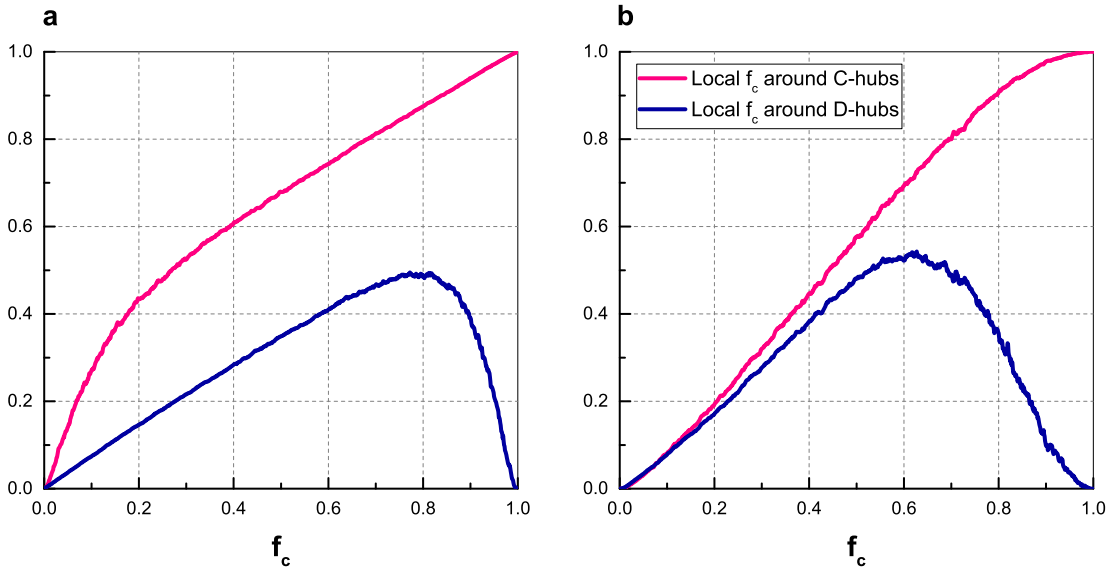

Fig. 4.15 Local fraction of coopertors around C-hubs (pink) and D-hubs (blue) in (a) disassortative structure and (b) assortative structure across the evolutionary process. The gap between local fraction around cooperating hubs and defecting hubs very small in assortative structure until the global fraction of cooperators reaches $f_C \sim 0.6$. In the disassortative mixing from the early stage to the final fixation the gap is huge. Figure obtained from the statistics of top 5 highest degree nodes of networks $\gamma = 2.5$, $r = -0.12$ for disassortative and $r = 0.12$ for assortative degree-mixing. Figure obtained using $b/c = 8.0$ and $w = 0.0095$.

level of total cooperators in the population. Rather than hub community cooperators are stick together in low degree community, $k < \bar{k}$ as shown in Fig. 4.14 (b). Expansion of cooperating cluster in hub community from cooperating hubs are obstructed by defector hubs due to the structural equivalence, and thus without accordance in strategy among hubs as cooperation it requires stronger reciprocity as more cooperator in neighborhood or more compensation from reciprocal interactions. Notice that the aligned increment of local cooperators around hubs in assortative mixing as increasing the total fraction of cooperators in whole population.

Role of hubs: stronghold or barrier

In addition to the interference through the structural equivalence, the exploitation of cooperators by defector hubs is also depends on the level of structural similarity. Suppose we have a cooperator and a defector hubs. The evolutionary success of cooperator hub toward one of its neighbors leads the compensation to cooperator hub in the next round of game. In case of defector hub, its reproduction leads to decreasing the source of exploitation. However, if the two hubs share common neighbors, the evolutionary success of cooperator will lead increasing of the absolute fitness not only itself but also to defector. Since a newly introduced cooperator neighbor is also a neighbor of defector hub, it is under the exploitation. As the opposite case, the evolutionary success of defector hub leads reducing not only the

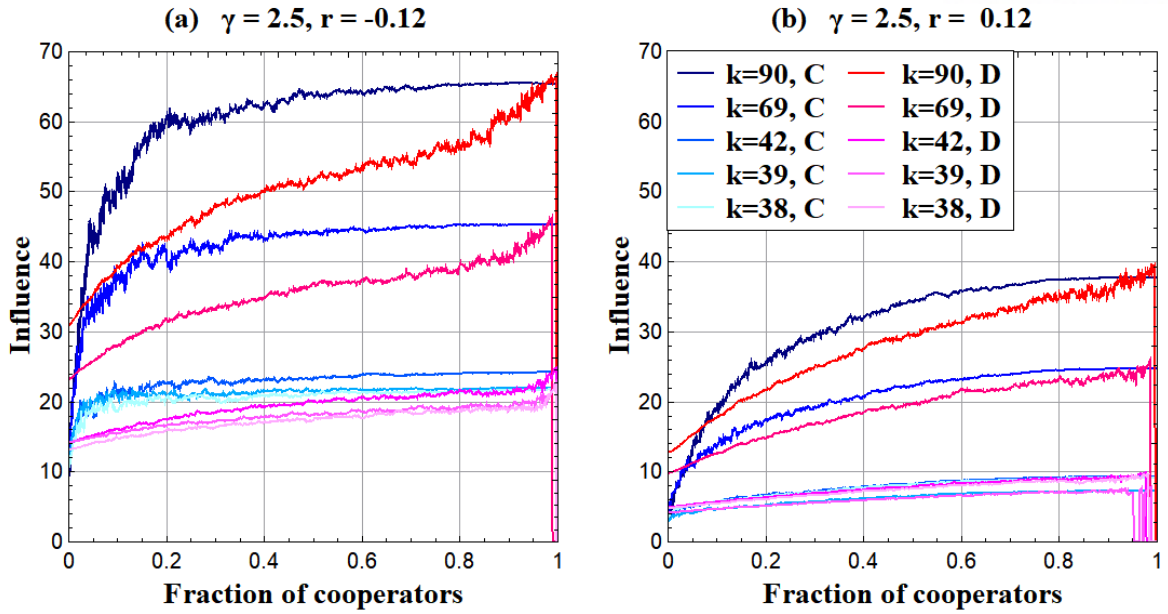

Fig. 4.16 The influence of top 5 hubs during the evolutionary process from network samples of disassortative and assortative mixing that share the degree sequence of $\gamma = 2.5$. Since the fitness of individuals in evolutionary game on structured population depends on the structural and strategic configurations among individuals, influence varies during dynamics. Regardless what is the strategy of hub, the potential evolutionary success of hubs in disassortative mixing (a) is much larger than in assortative mixing (b). Commonly in both cases the influence of C-hubs is smaller than D-hubs, however, above a certain fraction of cooperators C-hubs being more influential than D-hubs. That points in disassortative mixing is much lower than assortative mixing. We can also notice that influence of C-hubs in disassortative mixing explosively increases while in assortative mixing it is gradual. Consequently C-hubs in disassortative mixing lead the expansion of cooperator cluster.

source of exploitation but also the source of reciprocity for the cooperator hub. Fig. 4.15 showing the local fraction of cooperators around cooperating hubs and defecting hubs in disassortative and assortative mixing. As we can see clearly, in disassortative mixing the local fraction of cooperators around C-hub and D-hub totally separated with huge gap between them, since they have low similarity while in assortative mixing the gap between them is very small due to the high level of structural similarity. Consequently this different level of local fraction of cooperators around hubs leads to totally opposite effect on the selection of cooperation.

Extending discussion of the effect of degree-mixing on the seed effect, the structural advantage for reproduction of hubs amplified by disassortative mixing and neutralized by assortative mixing. As shown in Fig. 4.16 the influence of cooperating or defecting hubs is much greater in disassortative mixing than in assortative of the same degree throughout the level of cooperation in populations. Since the fitness of individuals in evolutionary game on structured population depends on the structural and strategic configurations among individuals, influence varies during dynamics. Therefore, the influence of an individual depends on the local fraction of cooperators.

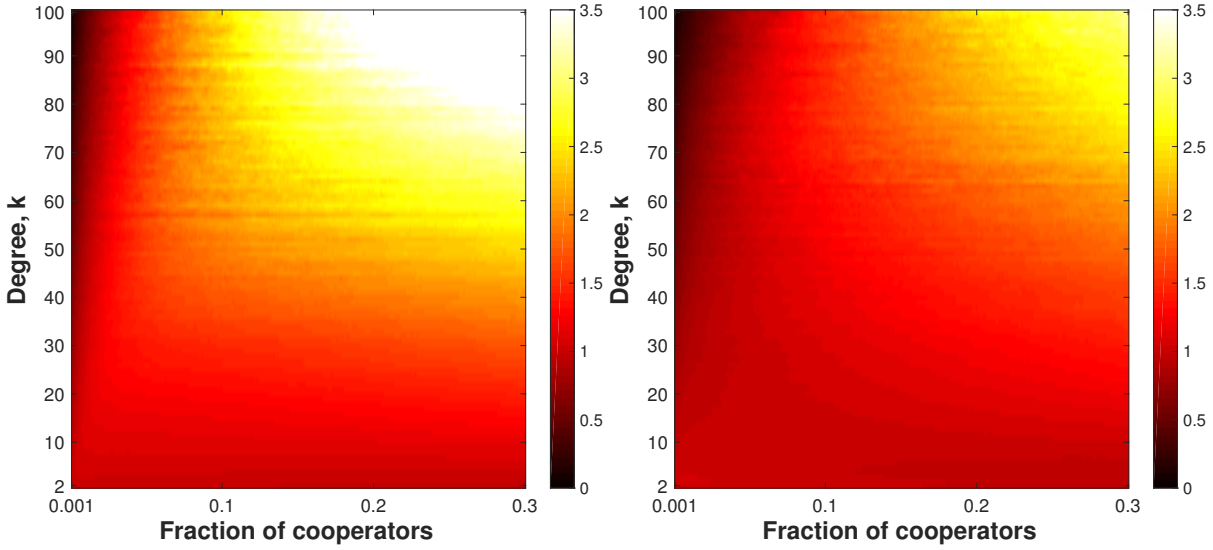

(a) $\gamma = 2.5, r = -0.12$ (b) $\gamma = 2.5, r = 0.12$

Fig. 4.17 The averaged relative fitness of cooperator of degree k against its potential defector competitors in (a) disassortative and (b) assortative structures when the total fraction of cooperators in the population is in range $1/N < f_C < 0.3$. Relative fitness of cooperator against competing defectors represent potential competitiveness for reproduction of cooperators during the dynamics. In disassortative mixing, the relative fitness of cooperator hubs against their potential competitors start outcompete in early stage and thus cooperating hubs take a role of stronghold. In assortative mixing, the relative fitness of cooperator hubs not significantly outcompete against their competitors. At the same time, neutralized structural advantage for reproduction, and strong interference between hubs due to the high structural similarity, take over hub community requires much higher compensation for mutual cooperation. Thus, massively interconnected hub community working as the barrier against proliferation of cooperators. Figure obtained using $b/c = 8.0$ and $w = 0.0095$.

In disassortative mixing and the high level of local fraction of cooperators around C-hub leads high influence of C-hub. As shown in Fig. 4.16, the potential evolutionary success of C-hubs in disassortative mixing is approximately double compare to same degree C-hubs in assortative mixing. Notice that the explosive increment of influence in early expansion stage when the total fraction of cooperators in range $1/N < f_C < 0.2$, Fig. 4.16 (a). It is indicating that if a hub become a cooperator it take a role of stronghold based on the overwhelming potential evolutionary success. In addition, the relative fitness of cooperator hubs against potential defecting competitors already outcompete in early stage of evolutionary process as shown in Fig. 4.17 (a). These multiple factors let the disassortative mixing reduce not only the settle down point, f_C^* but also the threshold benefit-cost ratio, b/c^*, and facilitate the emergence of cooperation.

On the contrary, in assortative mixing the relative fitness of cooperator hubs not significantly outcompete against their competitors. Because of the high structural equivalence, the absolute increment of fitness of cooperating hub as the results of its reproduction does not leads to increment relative fitness against defector hubs. Therefore, taking over the hub community in assortative mixed population by cooperators become more difficult. In addition, proliferation of cooperators, especially to hub community, is resisted

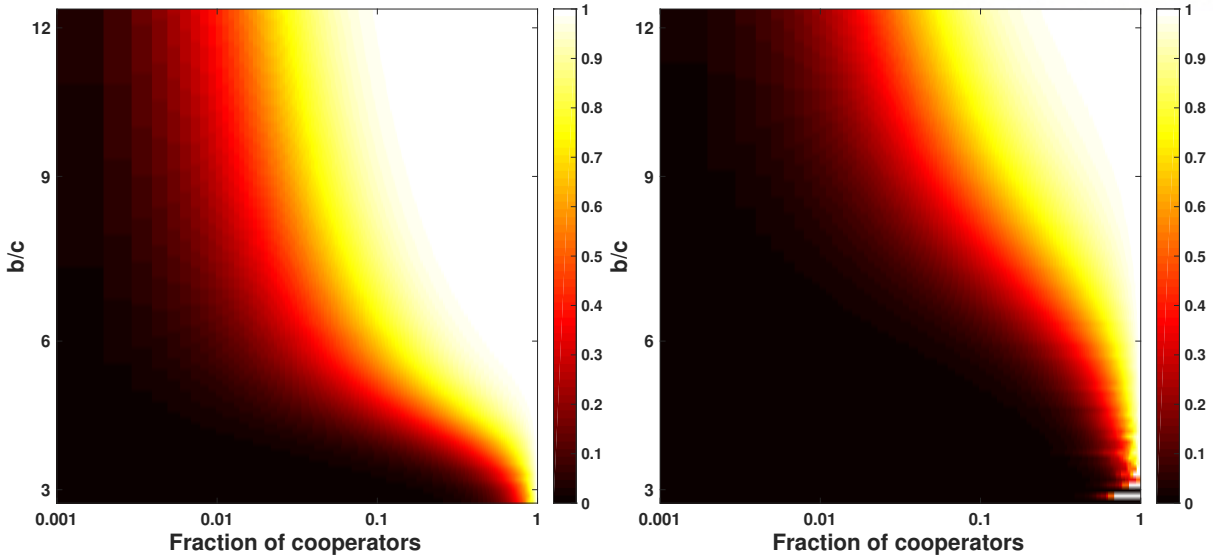

(a) $\gamma = 2.5, r = -0.12$ (b) $\gamma = 2.5, r = 0.12$

Fig. 4.18 The heatmap of the conditional fixation probability at b/c from a certain fraction of cooperators, f_C, in which arrived through evolutionary success of cooperators on (a) disassortative and (b) assortative populations. The required fraction of cooperators, f_C^* which guarantees the success of taking over the population depends on population structure and the benefit-cost ratio. We can notice that as the b/c increases the threshold of evolutionary success decreases in both structures. However, the selection of cooperators in disassortative mixing is much favoured. Above the general network reciprocity, $b/c > k = 4$, the threshold quickly decreased in the disassortative mixing (a) while in assortative mixing the threshold decreases slowly (b). Note that f_C axis is log-scaled.

by neutralized structural advantage for reproduction, and strong interference between hubs. These factors are cause of much higher compensation for mutual cooperation to take over hub community. Thus, massively interconnected hub community working as the barrier against proliferation of cooperators.

Fig. 4.18 shows the overall results of the conditional fixation probability as function of the fraction of cooperators, f_C, given the benefit-cost ratio, b/c, on disassortative and assortative populations. As increasing b/c, the threshold fraction ensures the evolutionary success of cooperation decreasing, which is the edge between yellow and white domain in Fig. 4.18. The tendency of decreasing depends on the level of degree-mixing due to the effect of degree-mixing during the evolutionary process in strategic populations as we discussed so far. The effect of degree-mixing, however, is amplified by the degree-heterogeneity as shown in Fig. 4.6. Since the more degree-heterogeneous, the more fat-tailed degree distribution, we conclude that behavior and interaction pattern of few massively connected individuals governing the population.

4.4 Summary

In summary, we have explored the emergence of cooperation on the structured population based on the evolutionary game dynamics. We investigated the synchronous update and asynchronous update on the characterized population in terms of the degree-heterogeneity and the degree-degree correlation. Under the synchronous update that imitate the best with comparison the payoff the effect of degree-heterogeneity turned out the level of cooperation maintained by cooperating hubs.

In case of selection dynamics we measured the fixation probability of cooperator which is the probability of evolutionary success starting from a single cooperator take over the whole population under the death-birth update. The interplay between dynamics and population structure utilized as the structural advantage to high-degree nodes that turned out high influence regardless what the strategy is. Suppression to the emergence of cooperation in degree-heterogeneous network could be addressed as the combination of founder effect and robust proliferation of defector hubs in early stage. Taking over defector hubs as a cooperator hub in early stage mostly decide further evolutionary outcome, however, without sufficient compensation for mutual cooperation the even occur very rarely.

On the stage of expanding cooperating cluster, the degree-mixing pattern enhance or inhibit the proliferation of cooperators. Main reason of the effect caused by the different level of structural equivalence between a pair of hubs, which very low in disassortative mixing and very high in assortative mixing. Structural simiarlity provide the path of interference between individuals with opposite strategies and also the chance of exploitation to defectors from the evolutionary success of cooperators. In addition the utilized structural advantage of reproduction for highly connected individuals is amplified by disassortative mixing but neutralized by assortative mixing. Consequently in disassortative mixing cooperator hubs take a role of stonghold which facilitate the expansion of cooperating cluster while in assortative mixing viscous interaction among hubs work as the barrier against invasion of cooperators into hub community.

Chapter 5

Conclusions

In this dissertation we have explored how structured population affect on the emergence phenomena from the evolutionary dynamics.

First we investigated evolutionary dynamics on the structured populations. Compare to the Moran process, that is the birth-death(BD), we observed different outcomes from the dynamics with flipped order to the death-birth(DB). Previous studies on BD process summerized that population structures classified into three catagories based on comparison with the Moran fixation, which are the isothermal structure, the selection suppressor and the selection amplifier. We found that the flipped Moran process changes the characteristics that defined previously. Significantly different outcome obtained from the star structure which was the selection amplifier based on BD, turned out it is selection suppressor under DB. Under the BD process, the temperature of node is defined by the sum of incoming flow of evolutionary success from its neighborhood. Contrastively for the DB process, we defined the influence of a node as the sum of outgoing flow of evolutionary success from itself under. It turned out that in case of BD, initiated low degree node has higher fixation while under the DB fixation proportional to the degree of seed. Interestingly in case of neutral selection, the temperature of a node is identical to the influence for unweighted structures as the degree times the harmonic mean of neighbor degrees.

Second we addressed structurally preferred population for the selection of cooperation based on the evolutionary game theory. From the numerical simulation on generated populations with desired level of degree-heterogeneity and degree-mixing, we have found that interplay between microscopic dynamics and the structure leads different macroscopic behavior of the system. From the synchronous update in which an individual imitate the strategy of the best payoff among neighbors including oneself, hubs were stronghold to maintain the high level of cooperation under the high temptation. Typically when degree-degree configuration were mixed, population in the negative and positive mixing showed different outcomes. From the positively mixed configuration sudden drop of cooperating population observed that

caused by collapse of cooperating hub cluster. In case of negative mixing, rare chance for imitation from hub leads sustain initially given strategy.

Comparison with synchronous imitation the selection dynamics based on the death-birth performed. In the selection dynamics the hubs were distinguished as the object of subjugation for the evolution of cooperation. Utilized structural benefit of hub for proliferating under the death-birth based on high connectivity, when hubs become cooperator it take a role of stronghold. However, until cooperator take over the spot defector hubs are menace for cooperators which is the main source of suppression of cooperation from the degree-heterogeneity.

Emergence of cooperation on the complex structured population that contain the degree-heterogeneity and the degree-degree correlation achieved throughout following stages. Survival: the survival of seed cooperator and its first evolutionary success depends on the degree of seed and the harmonic mean of its neighbors degree. Unless initiated at high degree node the chance is very low, thus, most of trial failed. Expansion: after the first evolutionary success, sufficiently enough compensation for mutual cooperation leads the growth of cooperating cluster. In this stage taking over hubs before extinction decide further evolution. Once a hub become a cooperator, as the results of evolutionary success fitness increased. Consequently hubs lead growing of cooperating cluster based on its high fitness. Settle down: Finally when the size of cooperating cluster arrived at certain fraction cooperation outcompete defection which depends on the benefit cost ratio and population structure.

Meanwhile, the robustness of cooperator hubs during the process depends on the degree-mixing. We have found that the structural equivalence between any of two nodes, especially between hubs, get higher in assortative mixing and lower in disassortative mixing. This structural differences leads different level of interference between a cooperator hub and a defector hub. In disassortative mixing, hubs are isolated from other hubs and also have low structural equivalence. From the isolation, a cooperator hub not exposed under the chance taken over by another defector hub and low structural equivalence allows negligible interference from a defector hub to a cooperator hub that disturbing evolutionary success. In case of assortative mixing, evolutionary success of a cooperator hub become a benefit not only to spreader but also to other defectors through high structural equivalence. Thus, even the absolute fitness of cooperator hub increased the relative fitness compare to potential competitors not enough to outcompete which leads to significant interference. Consequently the disassortative mixing facilitate the emergence of cooperation with relatively lower benefit-cost ratio while the assortative mixing requires higher compensation for mutual cooperation.

Appendix A

Selection Dynamics on Star Graph

Results of evolutionary dynamics on the star graph were extremely different under the birth-death (BD) and the death-birth (DB) update rules. The star is selection amplifier under the BD and it is the selection suppressor under the DB. These extreme difference caused by unbalanced transition probabilities as the consequence of interplay between update rule and the structure.

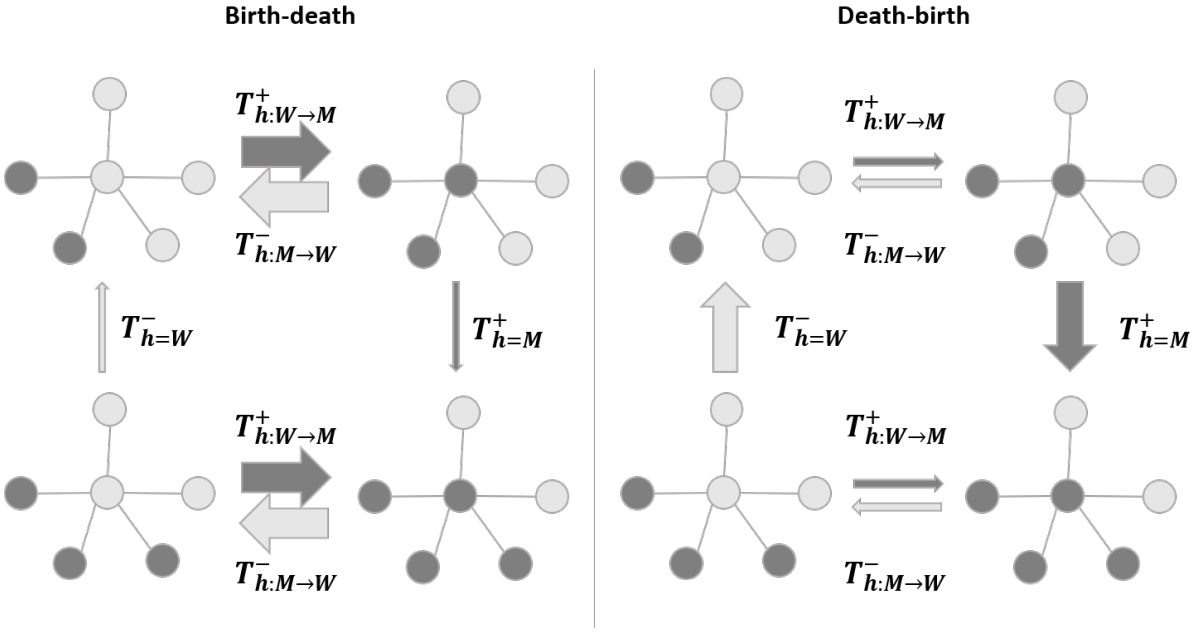

Fig. A.1 Schematic description of transition probabilities of evolutionary processes on the star structure. Light gray represent wild-type with fitness 1, and dark graph represent mutant with fitness r. Transitions corresponding to increasing and decreasing the number of mutant indicated with dark gray and light gray arrows respectively. The probabilities are unbalanced due to interplay between update rule and the structure, under the BD, updating the center is more likely occur rather than updating one of leafs, while under the DB, updating one of leafs is more likely happens. These unbalances represented as the thickness of arrows.

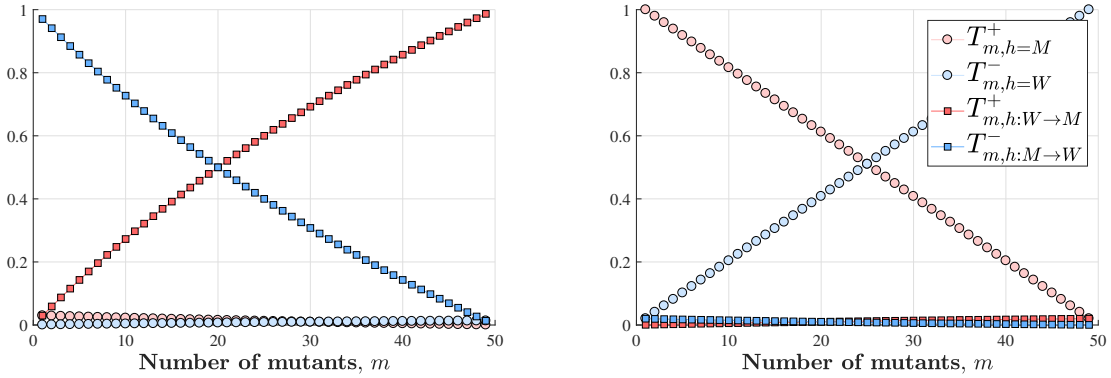

(a) Birth-death (b) Death-birth

Fig. A.2 Transition probabilities of (a) the birth-death and (b) the death-birth as function of the number of mutants on star graph size of $N = 50$, the relative fitness of mutant $r = 1.5$. Transition probabilities are unbalanced on star graph. Under the BD, transition of the center much more likely happens rather transitions of leafs. Under the DB, however, it is totally opposite. The interplay between limited interactions though the center and the sequence of dynamics leads this unbalanced transitions. Consequently the center is super "hot" spot under the BD and it is super influencer under the DB, which contributes for amplifying or suppressing the selection respectively.

The states of star, say m, with m mutant divided into two depends on the state of center node, h. In Fig. A.1 possible transitions are represented as arrows. Since leaf nodes interacting only with the center node, increasing or decreasing number of mutant among leafs depends on which type is occupying the center. There are four possible transitions as follows. $T^-_{m,h=W}$: the probability of decreasing one mutant when the center is wild-type, $T^+_{m,h=M}$: the probability of increasing one mutant when the center is mutant, $T^-_{m,h:M\to W}$: the probability of decreasing one mutant as the center updated from mutant to wild-type, and $T^+_{m,h:W\to M}$: the probability of increasing one mutant as the center updated from wild-type to mutant. Probabilities under each update rule are following. For the BD those are given by,

$$\begin{aligned} T^+_{m,h:W\to M} &= \frac{mr}{mr+N-m}\times 1, & T^+_{m,h=M} &= \frac{r}{mr+N-m}\frac{N-m}{N-1}, \\ T^-_{m,h:M\to W} &= \frac{N-m}{mr+N-m}\times 1, & T^-_{m,h=W} &= \frac{1}{mr+N-m}\frac{m}{N-1}, \end{aligned} \tag{A.1}$$

and for the DB we have,

$$\begin{aligned} T^+_{m,h:W\to M} &= \frac{1}{N}\frac{mr}{mr+(N-1)-m}, & T^+_{m,h=M} &= \frac{N-m}{N-1}\times 1, \\ T^-_{m,h:M\to W} &= \frac{1}{N}\frac{N-m}{(m-1)r+N-m}, & T^-_{m,h=W} &= \frac{m}{N-1}\times 1, \end{aligned} \tag{A.2}$$

As represented in Fig. A.2 the sequence of updating rule changes the unbalance transitions. Under the BD, transition of the center $(T^+_{m,h:W\to M}, T^-_{m,h:M\to W})$ much more likely happens rather transitions of leafs $(T^+_{m,h=M}, T^-_{m,h=W})$. Under the DB, however, it is totally opposite. The interplay between limited interactions

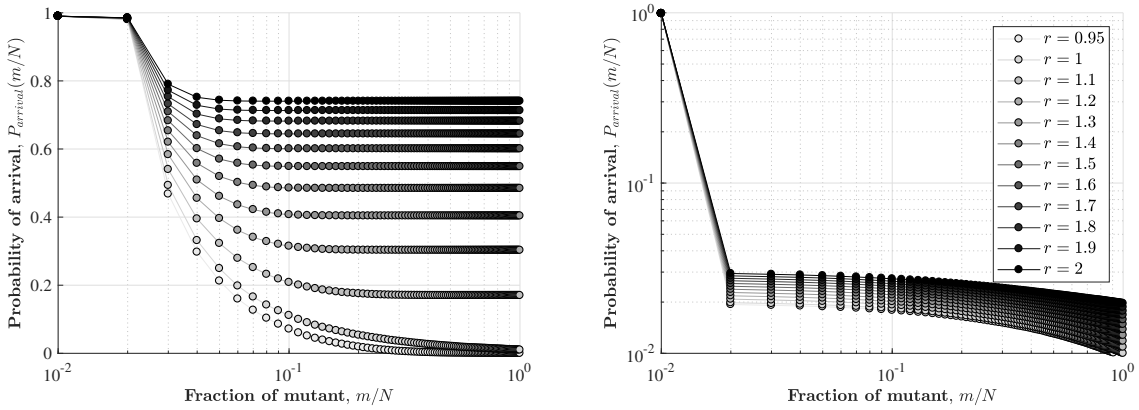

(a) Birth-death (b) Death-birth

Fig. A.3 Probability of arrival to state m from randomly placed a single mutant with relative fitness r under (a) the birth-death and (b) the death-birth as function of the number of mutants on star graph size of $N = 100$. Under the BD mutant survive and proliferate its identity to whole population while under the DB survival of a seed mutant is very difficult unless it placed at the center. Notice that y-axis of (b) is log-scaled.

though the center and the sequence of dynamics leads this unbalanced transitions. Consequently the center is super "hot" spot under the BD and it is super influencer under the DB, which contributes for amplifying or suppressing the selection respectively.

In Fig. A.3 the probability of arrival to state m from a randomly placed seed mutant with the relative fitness r is represented. Note that on star graph, most of seed mutant initiated at leaf node. Under the BD, the evolutionary success of seed to the center easily achieved ($m = 1 \rightarrow m = 2$), however, spread mutant from the center to other leaf depends on the relative fitness. In case of DB, most of the seed wiped out by the center at the beginning as shown in Fig. A.3 (b).

In Fig. A.4 the conditional fixation probability from the state m given the relative fitness of mutant r, $\rho_M(r, m/N)$, is represented. Under the BD, the fixation of mutant is guaranteed only with few mutants. Since, the probability that the center is mutant is proportional to the number of mutant among the leaf, as many of leaf is occupied by mutant, the fixation get easier Fig. A.4 (a). Meanwhile, under the DB, the evolutionary success of mutant extremely depends of on the center. Most of invasion from leafs failed as shown in Fig. A.3 (b), however, if the center taken over by mutant, proliferation of mutant get much easier as shown in Fig. A.4 (b). We can see the sudden increase of the conditional fixation probability at $\rho_M(r, 2/N)$.

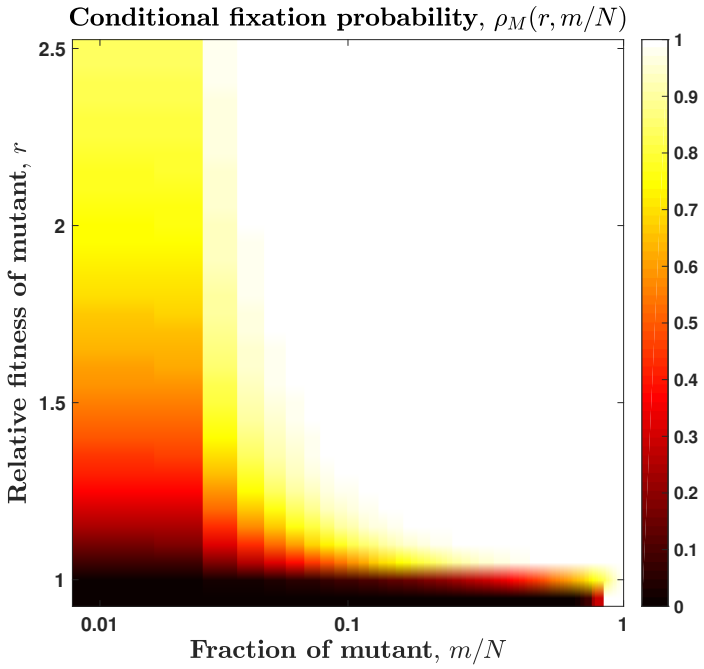

(a) Birth-death

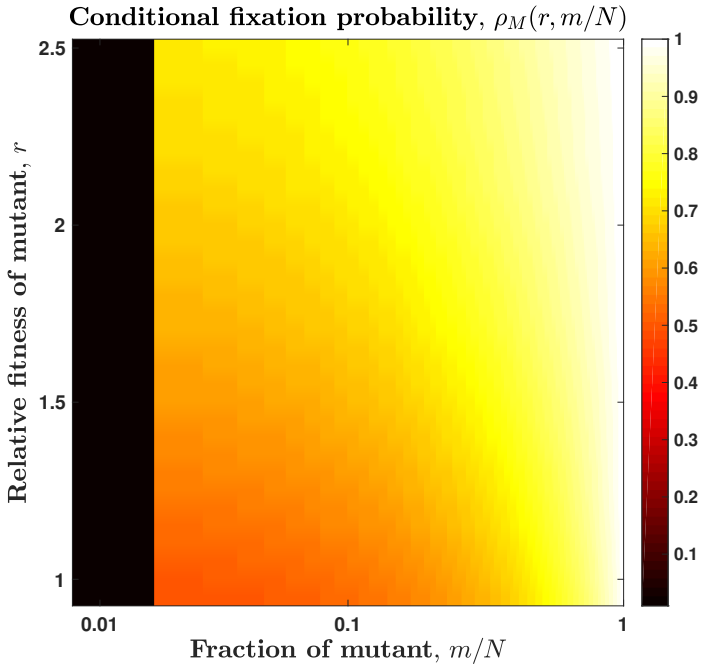

(b) Death-birth

Fig. A.4 Conditional fixation probability from the state m given the relative fitness of mutant r, $\rho_M(r, m/N)$ under (a) the birth-death and (b) the death-birth on star graph, size of $N = 100$. Under the BD the fixation probability gradually increased as the number of mutant increasing. Under the DB, the fixation extremely depends on the center. Once the center become a mutant type $(m = 1 \rightarrow m = 2)$, fixation probability suddenly increased as shown as the edge between black domain $(m = 1)$ and the yellow $(m = 2)$ in (b).

Appendix B

Various Quantification of Cooperativity in Prisoner's Dilemma Game

To investigate how the degree-heterogeneity and the degree-mixing affect to the emergence of cooperation we measured following list of quantities.

- **Conditional arrival probability:** the probability that the total fraction of cooperator arrived to f_C from a single cooperator initiated at node of degree k. The arrival probability measure the evolutionary success of cooperators on each characterized structured populations. We confirmed that the optimum degree of seed for most successful proliferation is not the most connected node, but balanced between the initial cost and the structural advantage for reproduction as highly connected spot, depending on the level of degree-heterogeneity.

- **Conditional fixation probability:** the probability of fixation from a certain fraction of cooperators that reached through the evolutionary success from a seed cooperator initiated at node degree k. From the conditional fixation probability we found that the threshold fraction of cooperators, f_C^*, which guarantees further evolutionary success upto the fixation depends on the level of degree-heterogeneity and the degree-mixing.

- **Probability of finding cooperators at node of degree k:** the probability that find a cooperator of degree k when the total fraction of cooperators in population is f_C. This probability indicating how cooperators taking over populations through the evolutionary success, and how cooperators are distributed in the population.

- **Local fraction of cooperators:** the probability that find a cooperator around a cooperator of degree k when the total fraction of cooperators in population is f_C. The local fraction of cooperators

around cooperator of degree k shows how the degree-mixing pattern effect on the influence of hubs. The disassortative mixing amplified the influence of hubs which leads hubs as the stronghold for cooperating clusters and the assortative mixing neutralized it which leads hub community working as barrier against invading cooperators.

- **Relative fitness of cooperators:** the averaged one-in-one relative fitness of cooperators against their potential competing defectors when the total fraction of cooperators in population is f_C. The relative fitness represent the potential evolutionary success of cooperators. Since the fitness of individuals under the evolutionary game dynamics depends on their payoffs, the relative fitness of cooperators increases as the local fraction increases.

- **Overall conditional fixation probability:** the probability of fixation from a certain fraction of cooperators given the benefit-cost ratio, $\rho_C(f_C, b/c)$. The overall conditional fixation probability summerize the effect of given structural characteristics of population on the evolution of cooperation. The critical threshold, $f_C(b/c)^*$, which is the settle down point, strongly depends on the level of degree-heterogeneity and the level of degree-mixing.

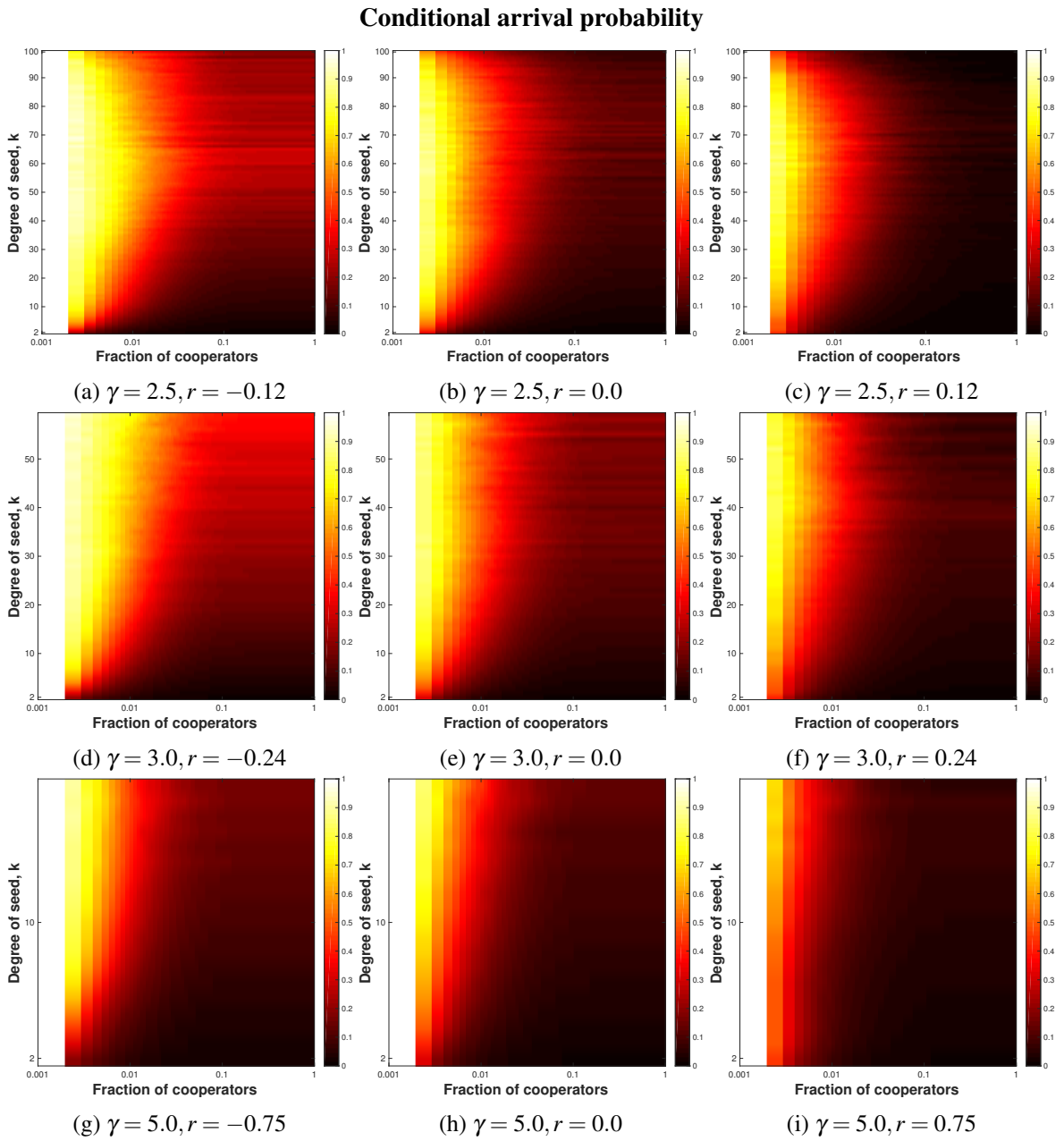

(a) $\gamma = 2.5, r = -0.12$ (b) $\gamma = 2.5, r = 0.0$ (c) $\gamma = 2.5, r = 0.12$

(d) $\gamma = 3.0, r = -0.24$ (e) $\gamma = 3.0, r = 0.0$ (f) $\gamma = 3.0, r = 0.24$

(g) $\gamma = 5.0, r = -0.75$ (h) $\gamma = 5.0, r = 0.0$ (i) $\gamma = 5.0, r = 0.75$

Fig. B.1 The probability of arrival to f_C at $b/c = 8.0$ that the degree of seed cooperator, k_{seed} was k on each characterized structure. Survival of seed cooperators and upto few evolutionary success depends on the degree of seed, k_{seed}. If the seed is placed at high degree spot it take advantage. However, most of trial invasion from seed cooperator into the sea of defectors wiped out in early stage since the majority of population is low degree. Notice that the total fraction of cooperators, f_C, in logarithm scale.

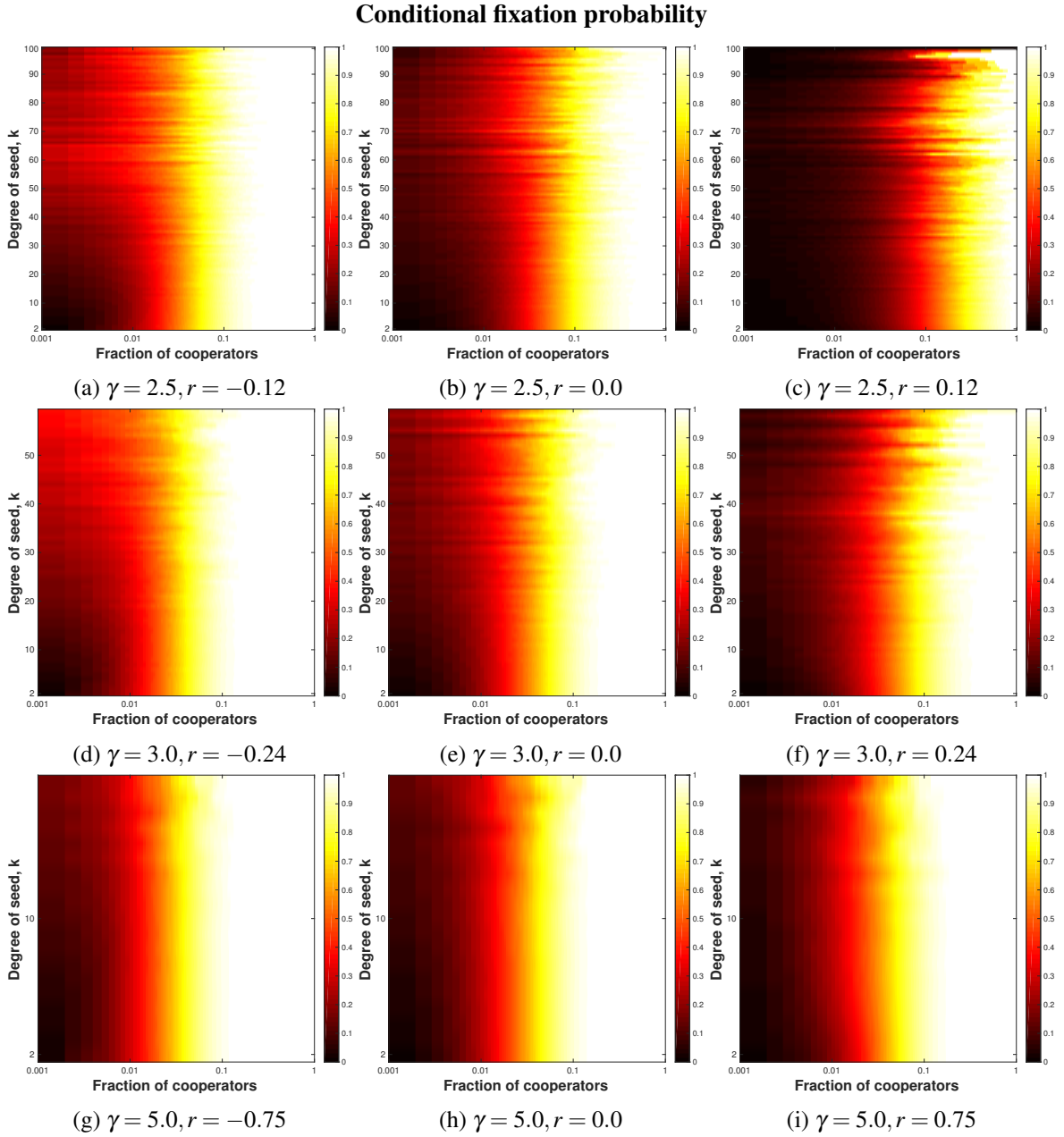

(a) $\gamma = 2.5, r = -0.12$ (b) $\gamma = 2.5, r = 0.0$ (c) $\gamma = 2.5, r = 0.12$

(d) $\gamma = 3.0, r = -0.24$ (e) $\gamma = 3.0, r = 0.0$ (f) $\gamma = 3.0, r = 0.24$

(g) $\gamma = 5.0, r = -0.75$ (h) $\gamma = 5.0, r = 0.0$ (i) $\gamma = 5.0, r = 0.75$

Fig. B.2 The conditional fixation probability at $b/c = 8.0$ from a certain fraction of cooperators, f_C, given the degree of seed cooperator, k_{seed} was k on each characterized structure. The threshold, f_C^*, depends on the level of degree-heterogeneity and the degree-mixing. The more heterogeneous, the higher threshold, and the more disassortative, the lower threshold.

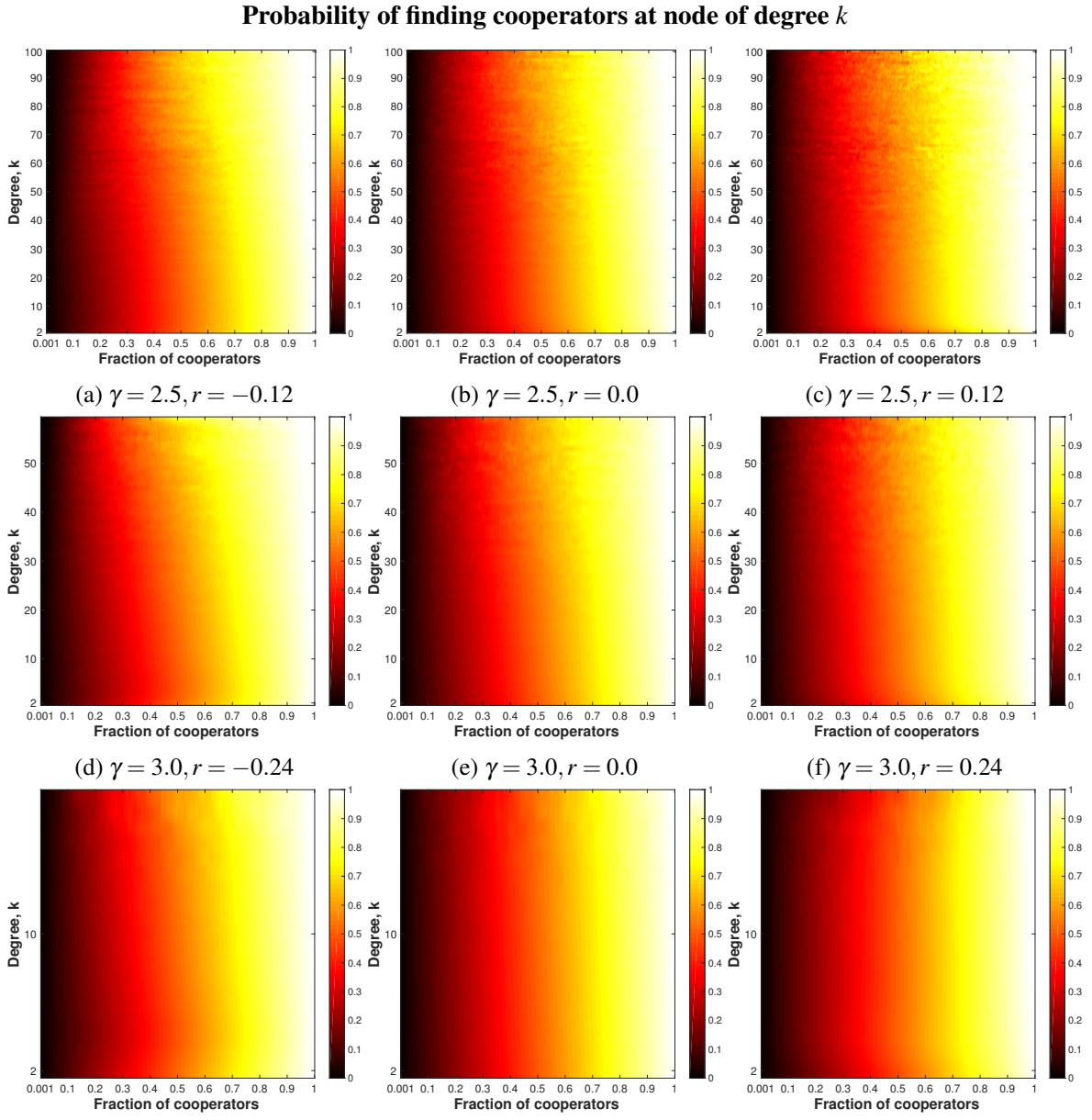

(a) $\gamma = 2.5, r = -0.12$ (b) $\gamma = 2.5, r = 0.0$ (c) $\gamma = 2.5, r = 0.12$

(d) $\gamma = 3.0, r = -0.24$ (e) $\gamma = 3.0, r = 0.0$ (f) $\gamma = 3.0, r = 0.24$

(g) $\gamma = 5.0, r = -0.75$ (h) $\gamma = 5.0, r = 0.0$ (i) $\gamma = 5.0, r = 0.75$

Fig. B.3 Probability of finding cooperators at node of degree k at $b/c = 8.0$ when the total fraction of cooperators in the population is f_C on each characterized structure. Figure is showing that the probability find cooperating hub is slightly higher in disassortative mixing compare to assortative mixing at the same level of total fraction.

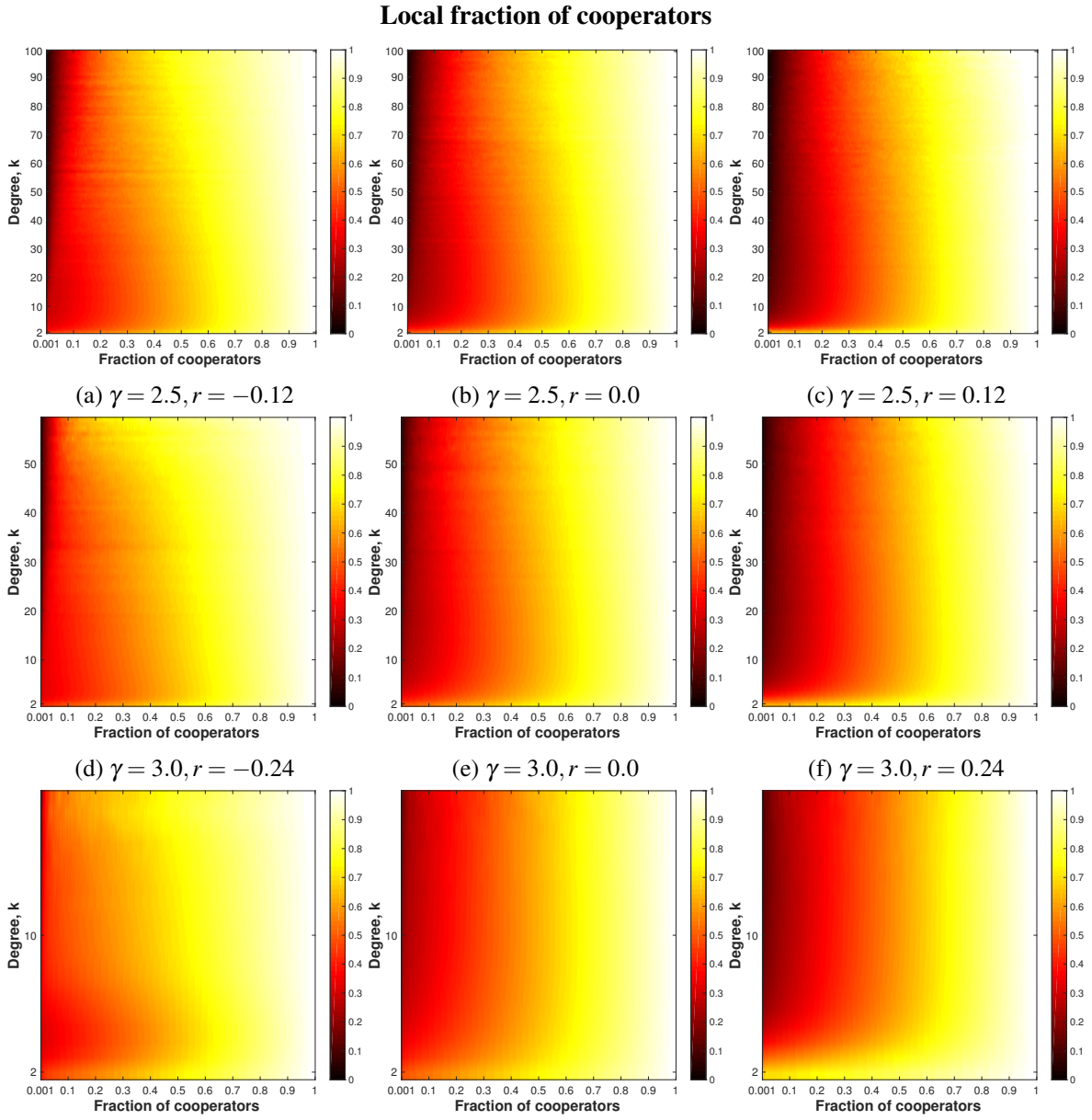

(a) $\gamma = 2.5, r = -0.12$ (b) $\gamma = 2.5, r = 0.0$ (c) $\gamma = 2.5, r = 0.12$

(d) $\gamma = 3.0, r = -0.24$ (e) $\gamma = 3.0, r = 0.0$ (f) $\gamma = 3.0, r = 0.24$

(g) $\gamma = 5.0, r = -0.75$ (h) $\gamma = 5.0, r = 0.0$ (i) $\gamma = 5.0, r = 0.75$

Fig. B.4 The local fraction of cooperators around the cooperator of degree k at $b/c = 8.0$ when the total fraction of cooperators in the population is f_C on each characterized structure. The local statistics showing how hubs in disassortative mixing governing its local neighborhoods based on the utilized structural benefit for reproduction and take a role of stronghold. The local fraction of cooperators around C-hub in disassortative mixing is much higher compare to the case of assortative mixing. Due to the high structural similarity among hubs cooperating hubs under the high interference which working as a barrier against cooperators.

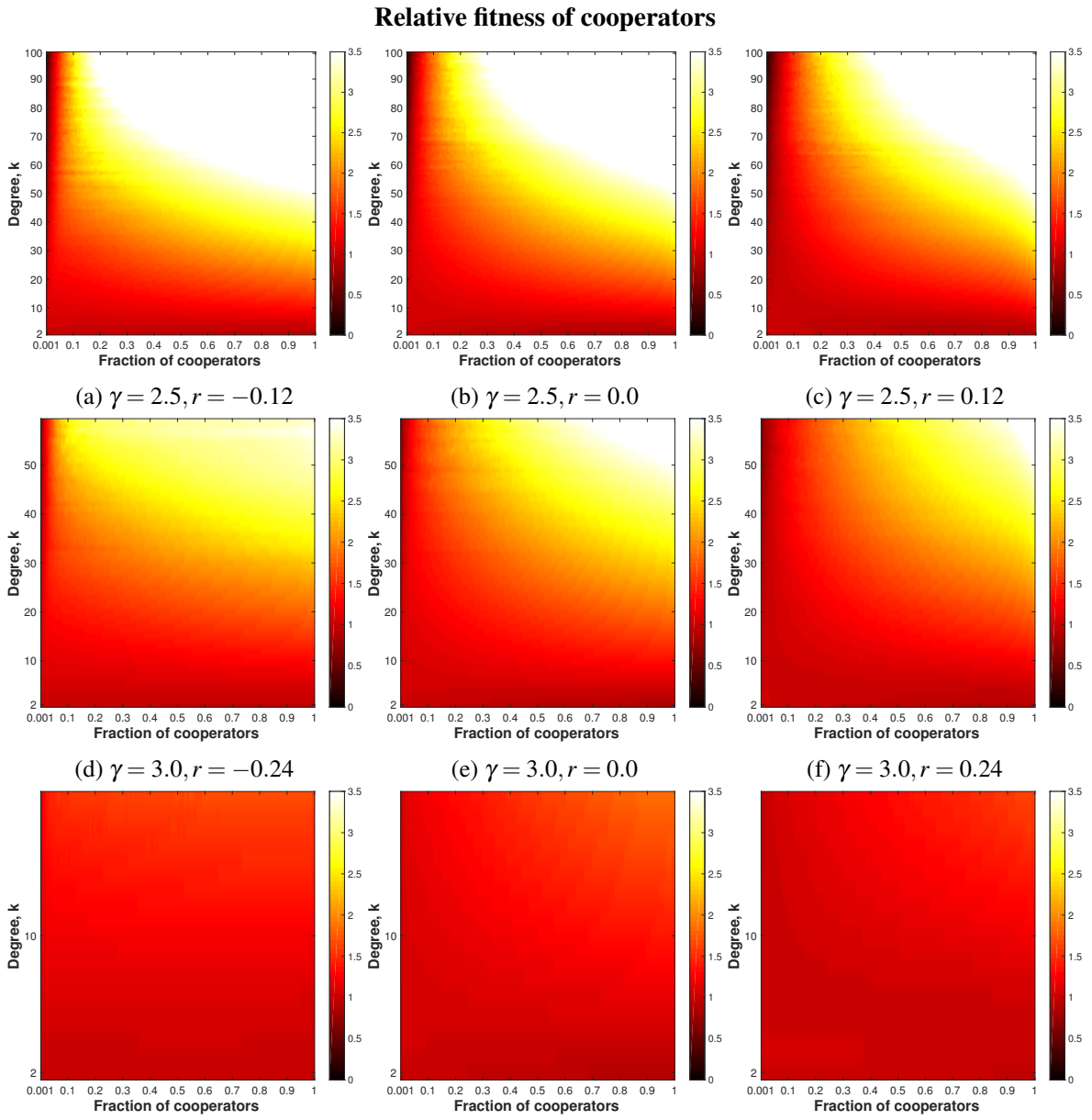

(a) $\gamma = 2.5, r = -0.12$ (b) $\gamma = 2.5, r = 0.0$ (c) $\gamma = 2.5, r = 0.12$

(d) $\gamma = 3.0, r = -0.24$ (e) $\gamma = 3.0, r = 0.0$ (f) $\gamma = 3.0, r = 0.24$

(g) $\gamma = 5.0, r = -0.75$ (h) $\gamma = 5.0, r = 0.0$ (i) $\gamma = 5.0, r = 0.75$

Fig. B.5 The averaged relative fitness of cooperator of degree k against its potential defector competitors at $b/c = 8.0$ when the total fraction of cooperators in the population is f_C on each characterized structure. Based on direct and strong reciprocity, C-hubs in disassortative structure take advantage in early stage. However, the effect of degree-mixing neutralized when the structure is degree-homogeneous since highly connected is absent.

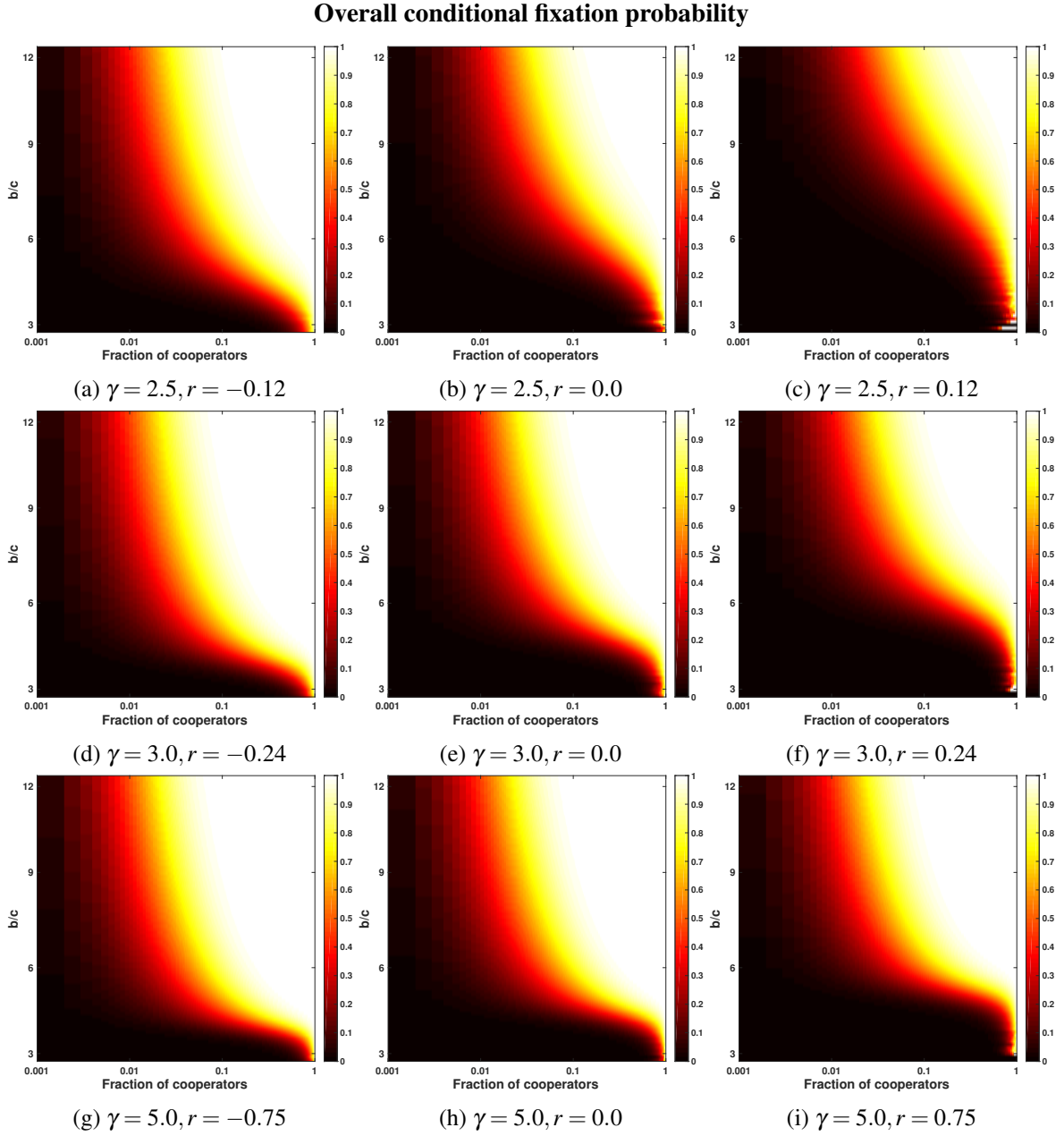

(a) $\gamma = 2.5, r = -0.12$ (b) $\gamma = 2.5, r = 0.0$ (c) $\gamma = 2.5, r = 0.12$

(d) $\gamma = 3.0, r = -0.24$ (e) $\gamma = 3.0, r = 0.0$ (f) $\gamma = 3.0, r = 0.24$

(g) $\gamma = 5.0, r = -0.75$ (h) $\gamma = 5.0, r = 0.0$ (i) $\gamma = 5.0, r = 0.75$

Fig. B.6 The conditional fixation probability from a certain fraction of cooperators in which arrived through evolutionary success of from a seed cooperator, f_C, given b/c. The required fraction of cooperators, f_C^* which guarantees the success of taking over the population depends on population structure. Note that f_C axis is log-scaled.

References

[1] Michael B Elowitz and Stanislas Leibler. A synthetic oscillatory network of transcriptional regulators. *Nature*, 403(6767):335, 2000.

[2] Martin Grandjean. La connaissance est un réseau. *Les Cahiers du Numérique*, 10(3):37–54, 2014.

[3] Alejandro F Villaverde and Julio R Banga. Reverse engineering and identification in systems biology: strategies, perspectives and challenges. *Journal of the Royal Society Interface*, 11(91):20130505, 2014.

[4] Alain Barrat, Marc Barthelemy, and Alessandro Vespignani. *Dynamical processes on complex networks*. Cambridge university press, 2008.

[5] Andrea Montanari and Amin Saberi. The spread of innovations in social networks. *Proc. Nat. Acad. Sci. USA*, 107(47):20196–20201, 2010.

[6] Fabrizio Altarelli, Alfredo Braunstein, Luca Dall'Asta, and Riccardo Zecchina. Optimizing spread dynamics on graphs by message passing. *Journal of Statistical Mechanics: Theory and Experiment*, 2013(09):P09011, 2013.

[7] Mark Newman. *Networks*. Oxford university press, 2018.

[8] Martin A Nowak. *Evolutionary dynamics*. Harvard University Press, 2006.

[9] R. E. Michod. *Darwinian Dynamics: Evolutionary Transitions in Fitness and Individuality*. Princeton University Press, 2000.

[10] J. Maynard Smith. *Evolution and the Theory of Games*. Cambridge University Press, 1982.

[11] J Maynard Smith and George R Price. The logic of animal conflict. *Nature*, 246(5427):15, 1973.

[12] Lawrence E Blume. The statistical mechanics of strategic interaction. *Games and economic behavior*, 5(3):387–424, 1993.

[13] B. Skyrms. *Evolution of the Social Contract*. Cambridge University Press, 2nd edition, 2014.

[14] Jeffrey A Fletcher and Michael Doebeli. A simple and general explanation for the evolution of altruism. *Proceedings of the Royal Society of London B: Biological Sciences*, 276(1654):13–19, 2009.

[15] Robert Axelrod. *The evolution of cooperation*. New York: Basic Books, 1984.

[16] Martin Nowak, Karl Sigmund, et al. A strategy of win-stay, lose-shift that outperforms tit-for-tat in the prisoner's dilemma game. *Nature*, 364(6432):56–58, 1993.

[17] Robert L Trivers. The evolution of reciprocal altruism. *The Quarterly review of biology*, 46(1):35–57, 1971.

[18] Martin A Nowak and Karl Sigmund. Evolution of indirect reciprocity by image scoring. *Nature*, 393(6685):573–577, 1998.

[19] Hisashi Ohtsuki and Yoh Iwasa. How should we define goodness?—reputation dynamics in indirect reciprocity. *J. Theor. Biol.*, 231(1):107–120, 2004.

[20] William D Hamilton. The genetical evolution of social behaviour. ii. *Journal of theoretical biology*, 7(1):17–52, 1964.

[21] J Maynard Smith. Group selection and kin selection. *Nature*, 201:1145–1147, 1964.

[22] Ilan Eshel and Luigi Luca Cavalli-Sforza. Assortment of encounters and evolution of cooperativeness. *Proc. Nat. Acad. Sci. USA*, 79(4):1331–1335, 1982.

[23] David C Queller. A general model for kin selection. *Evolution*, pages 376–380, 1992.

[24] Laurent Lehmann and Laurent Keller. The evolution of cooperation and altruism–a general framework and a classification of models. *J. Evol. Biol.*, 19(5):1365–1376, 2006.

[25] David Sloan Wilson. A theory of group selection. *Proc. Nat. Acad. Sci. USA*, 72(1):143–146, 1975.

[26] Arne Traulsen and Martin A Nowak. Evolution of cooperation by multilevel selection. *Proc. Nat. Acad. Sci. USA*, 103(29):10952–10955, 2006.

[27] John S Chuang, Olivier Rivoire, and Stanislas Leibler. Simpson's paradox in a synthetic microbial system. *Science*, 323(5911):272–275, 2009.

[28] Bruce R Levin and William L Kilmer. Interdemic selection and the evolution of altruism: a computer simulation study. *Evolution*, 28(4):527–545, 1974.

[29] John MAYNARD-SMITH. Group selection. *Q Rev Biol*, 51:277–283, 1976.

[30] Montgomery Slatkin and Michael J Wade. Group selection on a quantitative character. *Proceedings of the national academy of sciences*, 75(7):3531–3534, 1978.

[31] Marcy Uyenoyama and Marcus W Feldman. Theories of kin and group selection: a population genetics perspective. *Theoretical population biology*, 17(3):380–414, 1980.

[32] James F Crow and Kenichi Aoki. Group selection for a polygenic behavioral trait: estimating the degree of population subdivision. *Proceedings of the National Academy of Sciences*, 81(19):6073–6077, 1984.

[33] Len Nunney. Group selection, altruism, and structured-deme models. *The American Naturalist*, 126(2):212–230, 1985.

[34] Henry Harpending and Alan Rogers. On wright's mechanism for intergroup selection. *Journal of Theoretical Biology*, 127(1):51–61, 1987.

[35] Eörs Szathmáry and László Demeter. Group selection of early replicators and the origin of life. *Journal of theoretical biology*, 128(4):463–486, 1987.

[36] Robert Boyd and Peter J Richerson. Group beneficial norms can spread rapidly in a structured population. *Journal of theoretical biology*, 215(3):287–296, 2002.

[37] Benjamin Kerr and Peter Godfrey-Smith. Individualist and multi-level perspectives on selection in structured populations. *Biology and Philosophy*, 17(4):477–517, 2002.

[38] Jeffrey A Fletcher and Martin Zwick. Strong altruism can evolve in randomly formed groups. *Journal of theoretical biology*, 228(3):303–313, 2004.

[39] Martin A Nowak, Corina E Tarnita, and Edward O Wilson. The evolution of eusociality. *Nature*, 466(7310):1057–1062, 2010.

[40] Patrick Abbot, Jun Abe, John Alcock, Samuel Alizon, Joao AC Alpedrinha, Malte Andersson, Jean-Baptiste Andre, Minus Van Baalen, Francois Balloux, Sigal Balshine, et al. Inclusive fitness theory and eusociality. *Nature*, 471(7339):E1–E4, 2011.

[41] György Szabó and Christoph Hauert. Phase transitions and volunteering in spatial public goods games. *Physical Review Letters*, 89(11):118101, 2002.

[42] Zhaojin Xu, Zhen Wang, and Lianzhong Zhang. Bounded rationality in volunteering public goods games. *Journal of theoretical biology*, 264(1):19–23, 2010.

[43] Alberto Antonioni, Marco Tomassini, and Angel Sánchez. Short-range mobility and the evolution of cooperation: an experimental study. *Scientific reports*, 5, 2015.

[44] Dirk Helbing and Wenjian Yu. The outbreak of cooperation among success-driven individuals under noisy conditions. *Proc. Nat. Acad. Sci. USA*, 106(10):3680–3685, 2009.

[45] Martin A Nowak and Robert M May. Evolutionary games and spatial chaos. *Nature*, 359(6398):826, 1992.

[46] Carlos P Roca, José A Cuesta, and Angel Sánchez. Evolutionary game theory: Temporal and spatial effects beyond replicator dynamics. *Physics of life reviews*, 6(4):208–249, 2009.

[47] Zhen Wang, Satoshi Kokubo, Jun Tanimoto, Eriko Fukuda, and Keizo Shigaki. Insight into the so-called spatial reciprocity. *Physical Review E*, 88(4):042145, 2013.

[48] Benjamin Allen, Gabor Lippner, Yu-Ting Chen, Babak Fotouhi, Naghmeh Momeni, Shing-Tung Yau, and Martin A Nowak. Evolutionary dynamics on any population structure. *Nature*, 544(7649):227, 2017.

[49] Hisashi Ohtsuki, Christoph Hauert, Erez Lieberman, and Martin A Nowak. A simple rule for the evolution of cooperation on graphs and social networks. *Nature*, 441(7092):502, 2006.

[50] Francisco C Santos and Jorge M Pacheco. Scale-free networks provide a unifying framework for the emergence of cooperation. *Physical Review Letters*, 95(9):098104, 2005.

[51] Francisco C Santos, Jorge M Pacheco, and Tom Lenaerts. Evolutionary dynamics of social dilemmas in structured heterogeneous populations. *Proceedings of the National Academy of Sciences*, 103(9):3490–3494, 2006.

[52] Jesús Gómez-Gardenes, M Campillo, LM Floría, and Yamir Moreno. Dynamical organization of cooperation in complex topologies. *Physical Review Letters*, 98(10):108103, 2007.

[53] Francisco C Santos, Marta D Santos, and Jorge M Pacheco. Social diversity promotes the emergence of cooperation in public goods games. *Nature*, 454(7201):213, 2008.

[54] Christoph Hauert and Michael Doebeli. Spatial structure often inhibits the evolution of cooperation in the snowdrift game. *Nature*, 428(6983):643, 2004.

[55] Feng Fu, Long Wang, Martin A Nowak, and Christoph Hauert. Evolutionary dynamics on graphs: Efficient method for weak selection. *Physical Review E*, 79(4):046707, 2009.

[56] Carlos Gracia-Lázaro, Alfredo Ferrer, Gonzalo Ruiz, Alfonso Tarancón, José A Cuesta, Angel Sánchez, and Yamir Moreno. Heterogeneous networks do not promote cooperation when humans play a prisoner's dilemma. *Proceedings of the National Academy of Sciences*, 109(32):12922–12926, 2012.

[57] Martin A Nowak, Corina E Tarnita, and Tibor Antal. Evolutionary dynamics in structured populations. *Philosophical Transactions of the Royal Society B: Biological Sciences*, 2010.

[58] Erez Lieberman, Christoph Hauert, and Martin A Nowak. Evolutionary dynamics on graphs. *Nature*, 433(7023):312, 2005.

[59] Jeffrey Travers and Stanley Milgram. The small world problem. *Phychology Today*, 1(1):61–67, 1967.

[60] Mark EJ Newman. Coauthorship networks and patterns of scientific collaboration. *Proceedings of the national academy of sciences*, 101(suppl 1):5200–5205, 2004.

[61] Albert-László Barabási. Scale-free networks: a decade and beyond. *science*, 325(5939):412–413, 2009.

[62] Holger Ebel, Lutz-Ingo Mielsch, and Stefan Bornholdt. Scale-free topology of e-mail networks. *Physical review E*, 66(3):035103, 2002.

[63] Fredrik Liljeros, Christofer R Edling, Luis A Nunes Amaral, H Eugene Stanley, and Yvonne Åberg. The web of human sexual contacts. *Nature*, 411(6840):907, 2001.

[64] Hawoong Jeong, Sean P Mason, A-L Barabási, and Zoltan N Oltvai. Lethality and centrality in protein networks. *Nature*, 411(6833):41, 2001.

[65] Albert-László Barabási, Réka Albert, and Hawoong Jeong. Scale-free characteristics of random networks: the topology of the world-wide web. *Physica A: statistical mechanics and its applications*, 281(1-4):69–77, 2000.

[66] Réka Albert, Hawoong Jeong, and Albert-László Barabási. Internet: Diameter of the world-wide web. *nature*, 401(6749):130, 1999.

[67] Hawoong Jeong, Bálint Tombor, Réka Albert, Zoltan N Oltvai, and A-L Barabási. The large-scale organization of metabolic networks. *Nature*, 407(6804):651, 2000.

[68] Victor M Eguiluz, Dante R Chialvo, Guillermo A Cecchi, Marwan Baliki, and A Vania Apkarian. Scale-free brain functional networks. *Physical review letters*, 94(1):018102, 2005.

[69] Mark EJ Newman. Assortative mixing in networks. *Physical review letters*, 89(20):208701, 2002.

[70] Mark EJ Newman. Mixing patterns in networks. *Physical Review E*, 67(2):026126, 2003.

[71] Gerard Salton and M. J. McGill. *Introduction to Modern Information Retrieval*. McGraw Hill Book Co., New York, 1983.

[72] Albert-László Barabási and Réka Albert. Emergence of scaling in random networks. *science*, 286(5439):509–512, 1999.

[73] Réka Albert and Albert-László Barabási. Statistical mechanics of complex networks. *Rev. Mod. Phys.*, 74(1):47, 2002.

[74] Paul L Krapivsky and Sidney Redner. Organization of growing random networks. *Physical Review E*, 63(6):066123, 2001.

[75] Romualdo Pastor-Satorras, Alexei Vázquez, and Alessandro Vespignani. Dynamical and correlation properties of the internet. *Physical review letters*, 87(25):258701, 2001.

[76] Sergei Maslov and Kim Sneppen. Specificity and stability in topology of protein networks. *Science*, 296(5569):910–913, 2002.

[77] Duncan J Watts and Steven H Strogatz. Collective dynamics of 'small-world'networks. *nature*, 393(6684):440, 1998.

[78] Petter Holme and Beom Jun Kim. Growing scale-free networks with tunable clustering. *Physical review E*, 65(2):026107, 2002.

[79] Emily M Jin, Michelle Girvan, and Mark EJ Newman. Structure of growing social networks. *Physical review E*, 64(4):046132, 2001.

[80] Alexei Vázquez, Romualdo Pastor-Satorras, and Alessandro Vespignani. Large-scale topological and dynamical properties of the internet. *Physical Review E*, 65(6):066130, 2002.

[81] Erzsébet Ravasz, Anna Lisa Somera, Dale A Mongru, Zoltán N Oltvai, and A-L Barabási. Hierarchical organization of modularity in metabolic networks. *science*, 297(5586):1551–1555, 2002.

[82] Jean-Pierre Eckmann and Elisha Moses. Curvature of co-links uncovers hidden thematic layers in the world wide web. *Proceedings of the national academy of sciences*, 99(9):5825–5829, 2002.

[83] Erzsébet Ravasz and Albert-László Barabási. Hierarchical organization in complex networks. *Physical Review E*, 67(2):026112, 2003.

[84] David V Foster, Jacob G Foster, Peter Grassberger, and Maya Paczuski. Clustering drives assortativity and community structure in ensembles of networks. *Physical Review E*, 84(6):066117, 2011.

[85] Paul Erdos and Alfréd Rényi. In *On random graphs*, volume 6, pages 290–297. Publicationrs Mathematicae, 1959.

[86] Paul Erdos and Alfréd Rényi. On the evolution of random graphs. *Publ. Math. Inst. Hung. Acad. Sci*, 5(1):17–60, 1960.

[87] K-I Goh, B Kahng, and D Kim. Universal behavior of load distribution in scale-free networks. *Phys. Rev. Lett.*, 87(27):278701, 2001.

[88] Juyong Park and Mark EJ Newman. Statistical mechanics of networks. *Phys. Rev. E*, 70(6):066117, 2004.

[89] Jae Dong Noh. Percolation transition in networks with degree-degree correlation. *Physical Review E*, 76(2):026116, 2007.

[90] Martin A Nowak. Five rules for the evolution of cooperation. *science*, 314(5805):1560–1563, 2006.

[91] Patrick Alfred Pierce Moran. Random processes in genetics. In *Mathematical Proceedings of the Cambridge Philosophical Society*, volume 54, pages 60–71. Cambridge University Press, 1958.

[92] Harold C Neu. The crisis in antibiotic resistance. *Science*, 257(5073):1064–1073, 1992.

[93] Tibor Antal and Istvan Scheuring. Fixation of strategies for an evolutionary game in finite populations. *Bulletin of mathematical biology*, 68(8):1923–1944, 2006.

[94] Motoo Kimura. Preponderance of synonymous changes as evidence for the neutral theory of molecular evolution. *Nature*, 267(5608):275, 1977.

[95] Motoo Kimura. *The neutral theory of molecular evolution*. Cambridge University Press, 1983.

[96] Oskar Morgenstern and John Von Neumann. *Theory of games and economic behavior*. Princeton university press, 1953.

[97] Edward O Wilson and Bert Hölldobler. Eusociality: origin and consequences. *Proceedings of the National Academy of Sciences*, 102(38):13367–13371, 2005.

[98] Martin A Nowak, Corina E Tarnita, and Edward O Wilson. The evolution of eusociality. *Nature*, 466(7310):1057, 2010.

[99] Ashleigh S Griffin, Stuart A West, and Angus Buckling. Cooperation and competition in pathogenic bacteria. *Nature*, 430(7003):1024, 2004.

[100] David G Rand and Martin A Nowak. Human cooperation. *Trends in cognitive sciences*, 17(8):413–425, 2013.

[101] Peter D Taylor and Leo B Jonker. Evolutionary stable strategies and game dynamics. *Mathematical biosciences*, 40(1-2):145–156, 1978.

[102] E Christopher Zeeman. Population dynamics from game theory. In *Global theory of dynamical systems*, pages 471–497. Springer, 1980.

[103] Peter Schuster and Karl Sigmund. Replicator dynamics. *Journal of theoretical biology*, 100(3):533–538, 1983.

[104] John F Nash et al. Equilibrium points in n-person games. *Proceedings of the national academy of sciences*, 36(1):48–49, 1950.

[105] Reinhard Selten and Peter Hammerstein. Gaps in harley's argument on evolutionarily stable learning rules and in the logic of "tit for tat". *Behavioral and Brain Sciences*, 7(1):115–116, 1984.

[106] Martin Nowak and Karl Sigmund. A strategy of win-stay, lose-shift that outperforms tit-for-tat in the prisoner's dilemma game. *Nature*, 364(6432):56, 1993.

[107] Drew Fundenberg and Eric Maskin. Evolution and cooperation in noisy repeated games. *The American Economic Review*, 80(2):274–279, 1990.

[108] Tomohiko Konno. A condition for cooperation in a game on complex networks. *Journal of Theoretical Biology*, 269(1):224–233, 2011.

[109] Zhihai Rong, Xiang Li, and Xiaofan Wang. Roles of mixing patterns in cooperation on a scale-free networked game. *Physical Review E*, 76(2):027101, 2007.

[110] Salvatore Assenza, Jesús Gómez-Gardeñes, and Vito Latora. Enhancement of cooperation in highly clustered scale-free networks. *Physical Review E*, 78(1):017101, 2008.

Acknowledgements

First and foremost, I would like to extend my deep gratitude to my advisor Prof. Cheol-Min Ghim for his continuous support for my Ph.D. research. His patience, motivation, and enthusiasm, let alone his deep and far-reaching knowledge, made it possible for me to complete this thesis. At the same time, his advises with careful concern not only for academic improvement but also for the path of life were every time helpful to overcome difficulties that I had faced. I hold him in high esteem for his deep thoughtfulness and I'm honored to be his the first student.

I would like to express my sincere thanks to the members of my thesis committee—Profs. Jaeup Kim, Pilwon Kim, Pan-Jun Kim, and Junhyo Jo for their insightful comments, hard but constructive criticism, and, for the most part, heart-warming encouragement. Especially, I was fortunate to have Prof. Pan-Jun Kim as my co-advisor, who used to remotely join the semiweekly conference calls from Hong Kong Baptist University. His passion as well as his sincere way of looking into the world and science guided me through my Ph.D. studies.

My sincere thanks also goes to the current and former fellow members from Physical Biology Biological Physics (PBBP) group in UNIST—Juneil Jang, Soohyun Kim, Haneul Kim, Woochul Jeong, Giju Jung, Chanhee Lee, and Jaehong Park for the stimulating discussions, heated debates, and numerous sleepless nights we were working together and for all the memories we have had since I joined the lab as a founding member. I wish their excellent academic achievement in the future and wish them all the best.

Last but not the least, I owe a great deal to my family. I would like to thank my parents Seong-In Yang and Eun-Sun Jung for begetting me at the very first place and for sacrificing many things for my own success. My grandmother Da-Ya Kim is a guardian angel who always wish me the best. My aunt Seong-Lim Yang is the one who has been caring for my well-being since I started my graduate study in Ulsan. To those family members I could not name, I am so grateful to all of you for supporting me.